MAC and Physical Layer Design for Ultra-Wideband Communications

By
Nishant Kumar

Thesis submitted to the Faculty of the
Virginia Polytechnic Institute and State University
in partial fulfillment of the requirements of the degree of

MASTER OF SCIENCE
in
Electrical Engineering

Dr. R. M. Buehrer (Chair)
Dr. Dennis G. Sweeney
Dr. Luiz A. DaSilva

May 3rd, 2004
Blacksburg, VA

Keywords: Ultra-Wideband, Impulse Radio, Multiband-OFDM, Medium Access Control, CSMA, CDMA

MAC and Physical Layer Design for Ultra-Wideband Communications

Nishant Kumar

Abstract

Ultra-Wideband has recently gained great interest for high-speed short-range communications (e.g. home networking applications) as well as low-speed long-range communications (e.g. sensor network applications). Two flavors of UWB have recently emerged as strong contenders for the technology. One is based on Impulse Radio techniques extended to direct sequence spread spectrum. The other technique is based on Orthogonal Frequency Division Multiplexing. Both schemes are analyzed in this thesis and modifications are proposed to increase the performance of each system. For both schemes, the issue of simultaneously operating users has been investigated.

Current MAC design for UWB has relied heavily on existing MAC architectures in order to maintain backward compatibility. It remains to be seen if the existing MACs adequately support the UWB PHY (Physical) layer for the applications envisioned for UWB. Thus, in this work we propose a new MAC scheme for an Impulse Radio based UWB PHY, which is based on a CDMA approach using a code-broker in a piconet architecture. The performance of the proposed scheme is compared with the traditional CSMA scheme as well as the receiver-based code assignment scheme.

A new scheme is proposed to increase the overall performance of the Multiband-OFDM system. Two schemes proposed to increase the performance of the system in the presence of simultaneously operating piconets (namely Half Pulse Repetition Frequency and Time spreading) are studied. The advantages/disadvantages of both of the schemes are discussed.

Acknowledgements

First and foremost, I would like to thank God for all that he has given to me. Without his grace, mercy and blessing I would not have been able to start and complete this work.

I would like to thank Dr. R. Michael Buehrer for his guidance and tremendous support which was lead to the successful completion of this thesis. His guidance and the knowledge he has given me has prepared me very well to undertake any challenge in the field of wireless communications. I am grateful to my committee members Dr. Dennis Sweeney and Dr. Luiz DaSilva for their help and suggestions.

I learned a tremendous amount in the course work that I undertook and would like to thank the faculty members of Virginia Tech. I would also like to thank the staff and fellow researchers at MPRG for giving me such an enriching experience and making the work environment so enjoyable. I am very grateful to my fellow workers and superiors at Staccato Communications from which I learned a tremendous amount. Their continued support was very instrumental in the completion of this work.

I would like to thank my parents for their love and affection and would never forget the values they have instilled in me and would always strive to make them proud. I would like to thank my brother Kushagra for his love and Devyani for her continued support, love and affection.

Contents

List of Figures

List of Tables

List of Equations

Chapter 1

1 Introduction

1.1 Overview of Ultra-Wideband

Ultra-Wideband (UWB) has recently gained great interest for high speed short range communication (e.g. home networking applications) as well as low speed long range communication (e.g. sensor network applications). The FCC defines a signal to be ultra-wideband if its fractional bandwidth is greater than 0.20 or the bandwidth (as defined by the -10dB points) occupies 500 MHz or more of the spectrum. The fractional bandwidth is defined as

$$B_f = 2\frac{f_H - f_L}{f_H + f_L}$$

where f_H and f_L are the upper and lower -10 dB emission points of the signal spectrum, respectively [29]. The center frequency of the transmission is defined as the average of the upper and lower –10 dB points i.e. $(f_H + f_L)/2$. UWB signals are of very short duration, typically on the order of a few nanoseconds and occupy the spectrum from near DC to tens of GHz. They are also known as "base-band carrier-less short pulse". The FCC recently allocated a band for UWB from 3.1 GHz – 10.7 GHz and provided two different spectral masks for UWB systems for indoor handheld devices and outdoor devices, as shown in Figure 1.1 and Figure 1.2 respectively. Although the frequencies allocated by the FCC do not qualify as base-band, the pulses are generated at base-band frequencies and are then up-converted in order to occupy the spectrum specified.

Since UWB signals occupy several octaves of frequency spectrum they are likely to interfere with other narrow band systems. Hence, UWB signals have to operate with very low transmit power (on the order of a few microwatts). Some of the potential advantages of using UWB signals are:

1) Extremely Low Probability of Intercept and Detection (LPI / D);
2) High data rate for short ranges;
3) Fine time resolution (used in radars and other position location applications);
4) Multipath immunity (can actually exploit multipath);
5) Capability of co-existence with other narrowband and UWB systems which greatly increasing overall spectral efficiency.

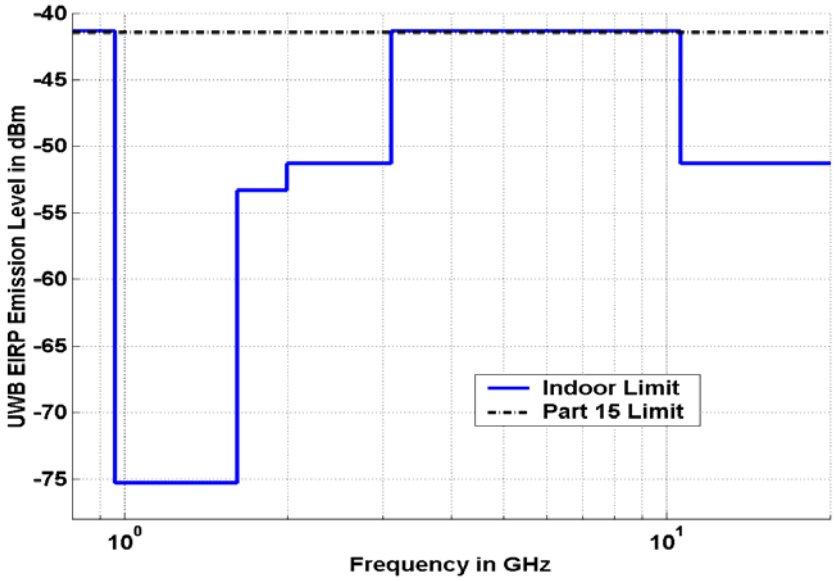

Figure 1.1 UWB Spectrum (Indoor limit)

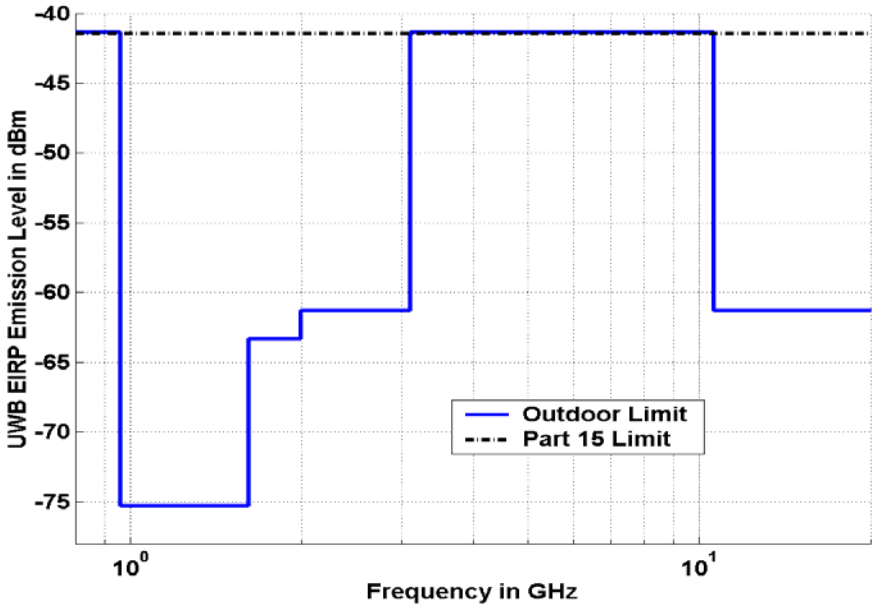

Figure 1.2 UWB Spectrum (Outdoor limit)

1.2 Flavors of UWB

UWB as a technology has been around since 1970s but was primarily used in the military for radar based applications. UWB communication has been synonymous with "impulse radio" for a long time. Although any communication system which complies with the FCC ruling can be termed UWB, two basic flavors of UWB have emerged in recent years:

1) Systems based on single carrier transmission or carrier-less transmission (e.g. impulse radio) [57]
2) Systems based on multi-carrier transmission (e.g. Multiband OFDM (Orthogonal Frequency Division Multiplexing) [30]).

Figure 1.3 shows an example of a single band and a multiband system in terms of their frequency and time properties.

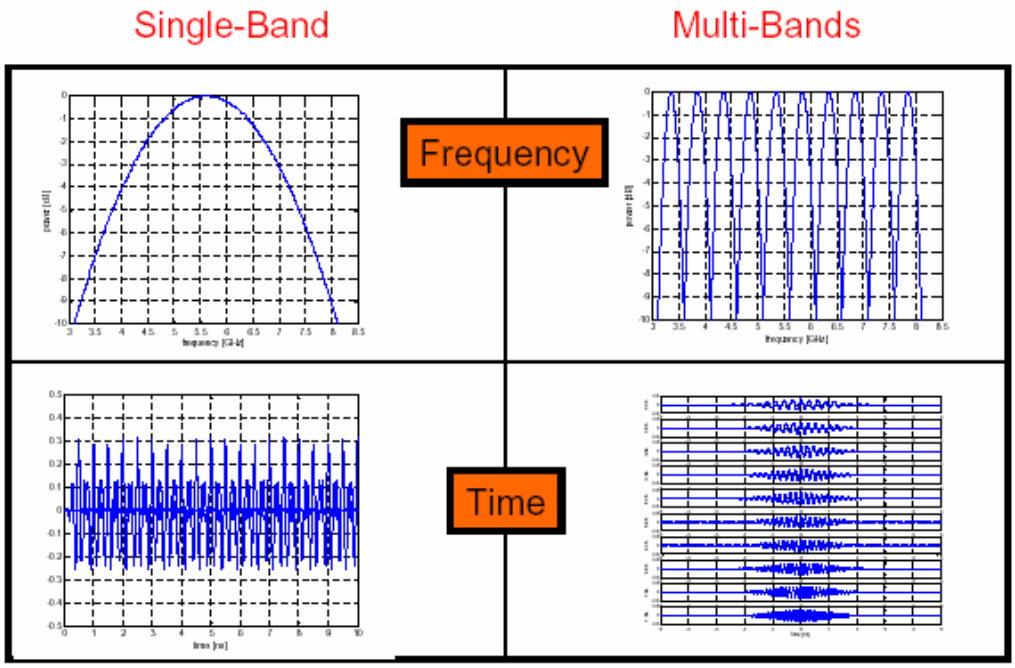

Figure 1.3 Single Band vs Multi-band approach

1.2.1 Impulse Radio

Impulse radio is different from traditional wireless communication systems in the sense that very short duration pulses are used to transmit information. It is also known as "carrier-less" transmission, since, in one method of transmitting data, the information signal is not modulated on to a carrier. Information is transmitted by modulating base-band pulses as opposed to traditional sinusoidal carrier modulation schemes such as QPSK, QAM, etc. Pulse position modulation (PPM) is a commonly proposed modulation technique for impulse radio systems. A general form of a PPM transmitted signal is given by

$$s(t) = \sum_{j=-\infty}^{\infty} Aw(t - jT_f - \delta d_{\lfloor j/N_s \rfloor}),$$

Equation 1.1 General form of a PPM transmitted signal

where

- A is the amplitude of the pulse,
- $w(t)$ is the transmitted pulse shape,
- T_f is the pulse repetition interval,
- δ is the time delay used for PPM modulation,
- N_s is the number of times the pulse is repeated
- d is the data bit to be transmitted in that particular transmission and
- $\lfloor X \rfloor$ is the floor function

If the system uses Binary PPM, d would take the values of either 0 or 1 and the pulse is sent at a different time instant depending on the data bit to be transmitted. For Quaternary PPM, d takes values from 0 – 3. An example of Quaternary PPM is shown in Figure 1.4. In the figure, δ is assumed such that the pulses are orthogonal in time. In general, other values of δ could be used.

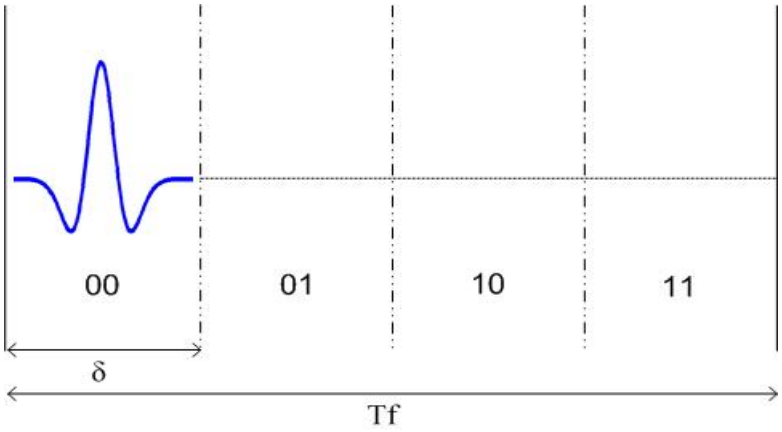

Figure 1.4 Quaternary Pulse Position Modulation

Some other possible modulation schemes with impulse radio are

1) On-off Keying (OOK), depicted in Figure 1.5. In this modulation scheme, the presence or absence of a pulse at a particular time is used to represent a bit 0 or 1. Such a transmitted signal can be represented by

$$s^{(k)}(t) = \sum_{j=-\infty}^{\infty} p_j A w(t - jT_f)$$

Equation 1.2 Transmitted signal using OOK modulation

where p_j is either 0 or 1. Superscript k represents the signal of the k^{th} user. The rest of the parameters are as defined above.

2) Bi-phase Modulation, depicted in Figure 1.6. In this modulation scheme, a pulse and its inverted counterpart are used to transmit the desired information. Such a transmitted signal can be represented by

$$s^{(k)}(t) = \sum_{j=-\infty}^{\infty} p_j Aw(t - jT_f)$$

Equation 1.3 Transmitted signal using bi-phase modulation

where p_j is either -1 or 1. The rest of the parameters are as defined above.

3) Pulse amplitude modulation depicted in Figure 1.7 is shown as an example of Quaternary amplitude modulation. In this modulation scheme, pulse of different amplitudes is used to transmit the desired information. Such a transmitted signal can be represented by

$$s^{(k)}(t) = \sum_{j=-\infty}^{\infty} p_j Aw(t - jT_f)$$

Equation 1.4 Transmitted signal using pulse amplitude modulation

where p_j is a different scaling factor {0, 1, …M-1} depending on the order of the modulation scheme. The rest of the parameters are as defined above. For example, as shown in the figure, to transmit bits "00" a pulse of the smallest amplitude is sent. If bits "11" are to be transmitted the pulse with the largest amplitude is sent. The mapping between the bits and the amplitude used can be changed by the designer and does not have any impact on the performance of the system unless the adjacent amplitudes do not differ by two bits. If the adjacent amplitudes differ by more than two bits, the performance of the system degrades.

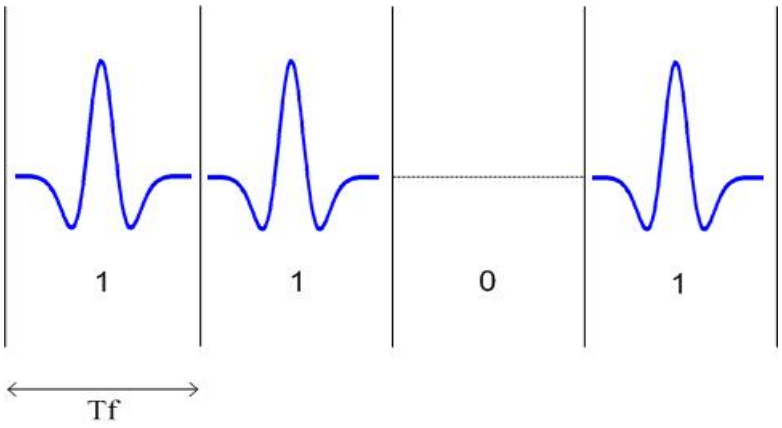

Figure 1.5 On-off Keying (OOK) modulation scheme

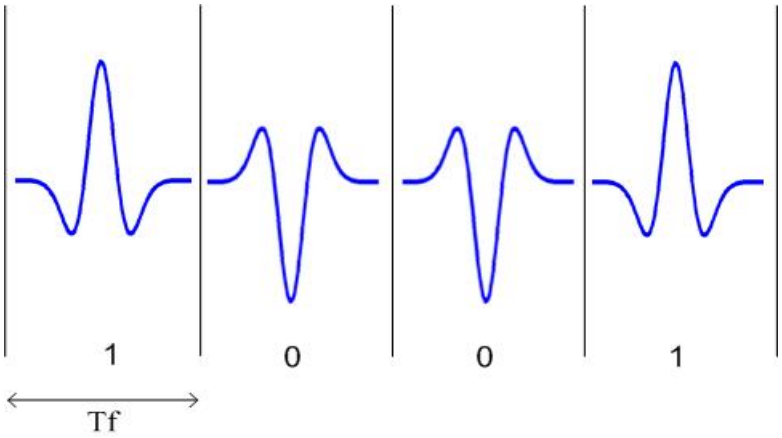

Figure 1.6 Bi-phase modulation scheme

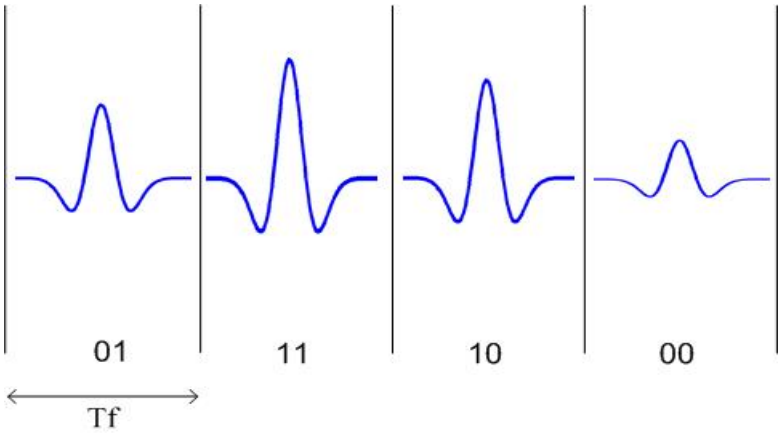

Figure 1.7 Pulse Amplitude modulation scheme

Any of the above stated schemes can be combined to form new modulation schemes. For example, bi-phase modulation can be combined with binary PPM to make bi-orthogonal modulation. Figure 1.8 below shows an example of such a scheme. Depending on the position as well as the polarity of the pulse transmitted (*i.e.,* actual pulse or its inverted version), the data bits transmitted are determined. In the figure below, data can be transmitted in either slot A or slot B and either the pulse or its inverted version could be transmitted, which gives 4 possible combinations (*i.e.,* 2 bits/pulse transmission).

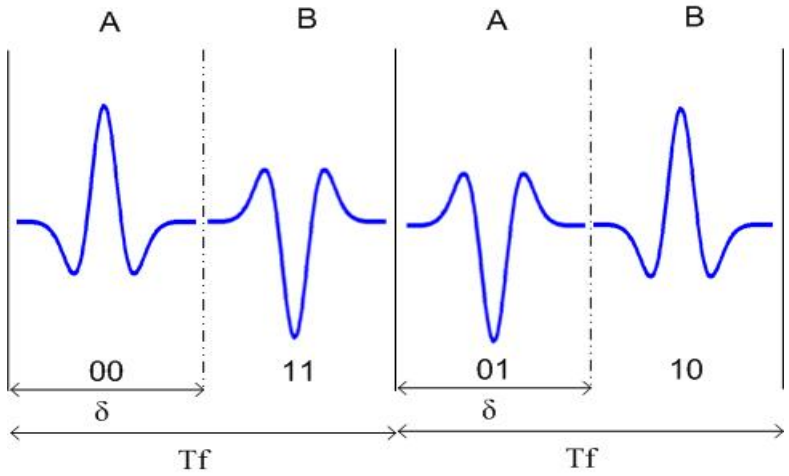

Figure 1.8 Bi-phase binary PPM

In order to accommodate multiple users in the system, a time hopped or CDMA based system is commonly used in UWB research. A time hopped pulse position modulated impulse radio system can be represented with the following equation, which is similar to the one presented in Equation 1.1 above. A similar equation was first presented in [31].

$$s(t) = \sum_{j=-\infty}^{\infty} w(t - jT_f - c_j T_c - \delta d_{\lfloor j/N_s \rfloor}),$$

Equation 1.5 Transmitted signal using time hopped pulse position modulation

where

- c_j is the time hopping code for a particular user,

- T_c is the time shift defined for the hopping code.

The rest of the parameters are as defined above. The hoping code value $c^{(k)}_j$ has to be less than a maximum c_{max}. The code set c_j could be Gold codes, etc. The codes are chosen such that they have good cross correlation and autocorrelation properties (i.e., the cross correlation of a code with other codes is very low for all possible alignments and the auto correlation of the code with itself is very high when the codes are perfectly aligned). Normally, $T_f >= c_{max}T_c$. Each user is given a unique code, which is used to identify transmission from that particular user.

As stated above, impulse radio uses pulses for communications. For such systems, the design of the pulse shape becomes a crucial factor as it determines the spectrum occupied by the signal. Moreover, ultra-wideband pulses typically get distorted by the transmit and receive antennas. For near perfect correlation, it is highly desirable to correlate the received pulse with a pulse shape which has taken into account the distortions due to transmit and receive antenna, *i.e.,* matched filtering which maximizes SNR. Gaussian modulated sinusoidal pulses are a class of pulses widely used for UWB system design, as they are easy to generate. These pulses are sinusoids multiplied by Gaussian pulses. A typical pulse shape and its spectrum are shown in Figure 1.9. The in-phase and quadrature components of the carrier can be simultaneously transmitted and carry the information of the signal. Note that such a pulse can either be generated through modulating a base-band pulse, or by using a band-pass filter with the desired pulse shape.

Traditional narrowband systems have a relatively narrow bandwidth as compared to UWB (impulse radio) systems, which leads to a longer symbol duration. Hence, in multipath channels multiple copies of the transmitted sinusoids are received in the duration of a symbol, which leads to severe fading effects. Due to the small duration of the pulses, UWB systems potentially have a large number of resolvable multipath components. Also fewer pulses arrive during each symbol as compared to narrowband signals and hence UWB signals are not characterized by

such severe fading effects. As in DSSS (Direct Sequence Spread Spectrum) systems, the resolvable multipath can be captured using Rake receivers, which improves the performance of the system [32]. Rake receivers having up to 100 fingers have been proposed for impulse radio systems.

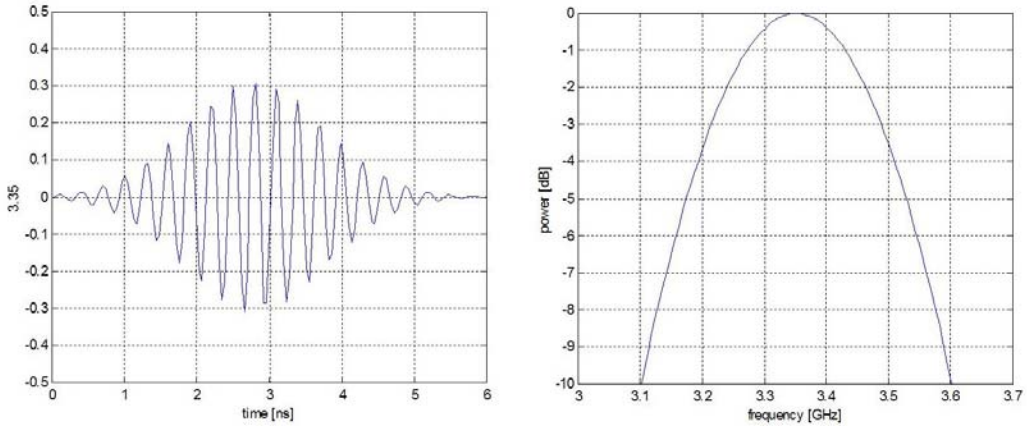

Figure 1.9 Gaussian Pulse and its spectrum

1.2.2 Multiband Systems

Due to the large bandwidth provided by the FCC (on the order of several GHz), it is possible to partition the spectrum into multiple 500 MHz bands that may be used to transmit data. This leads to several interesting system architecture band plan options, primarily centered on frequency hopping based techniques for the transmission of data.

With the ongoing process of standardization of UWB, various flavors of the multiband technique have evolved. Two of the most widely supported techniques are namely:

1) Multiband UWB and
2) Multiband-OFDM (Orthogonal Frequency Division Multiplexing).

In either of these schemes, the transmitted signal hops among multiple frequency bands. The kind of signal transmitted on each band in the former technique is pulse-based and in the latter is an OFDM signal. For the former scheme, either of

the modulation techniques explained in the previous section could be used. For an OFDM signal any of the traditional modulation schemes (i.e., QPSK, 16 QAM, etc.) could be used for modulation on each carrier. Multiple users are supported by providing them with different hopping patterns. An example of a frequency hopping multiband system is shown in Figure 1.10.

In both the Multiband UWB/Multiband OFDM scheme, a pulse spanning 500 MHz is transmitted in a hop band and then the center frequency is switched to the next hop band corresponding to the hop pattern for that particular user.

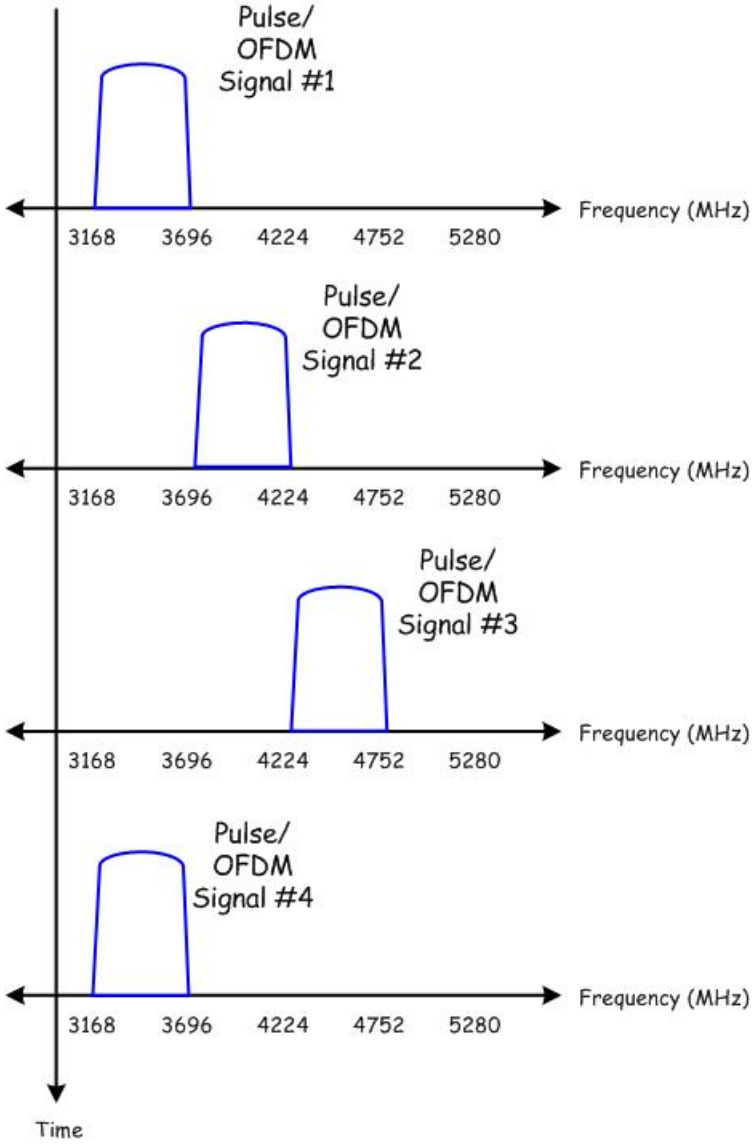

Figure 1.10 Multiband System

As UWB spans a very broad spectrum, it overlaps with some frequency bands that have already been allocated, e.g. the U-NII (Unlicensed National Information Infrastructure) band. Hence, UWB signals have to operate at very low transmit powers in order to avoid interference to the existing systems. From Shannon's theory of capacity, we know that

$$C = W \log_2(1 + P/N)$$

where

- C is the channel capacity (bits/sec),
- W is the channel bandwidth (Hz),
- P is the power spectral density (W/Hz) and
- N is the noise spectral density (W/Hz).

Since the UWB signal bandwidth is orders of magnitude greater than the data rate, UWB systems can operate at very low SNR and yet achieve high data rates. Also at low SNR, the system capacity increases linearly with power. To a narrowband system, such a low PSD (power spectral density) signal would ideally appear as noise.

UWB interference generated to the existing services due to the overlapping bands can also be mitigated by not transmitting a UWB signal in particular bands. This would ensure that UWB signals would not interfere with some existing services. An example of such a system is shown in Figure 1.11. Note that the U-NII band is from 5.15 GHz to 5.825 GHz. The figure below shows the highest frequency used for the lower band group to be 4.8 GHz and the lowest frequency used for the higher band group to be 5.9 GHz to provide UWB devices adequate protection from the U-NII band devices.

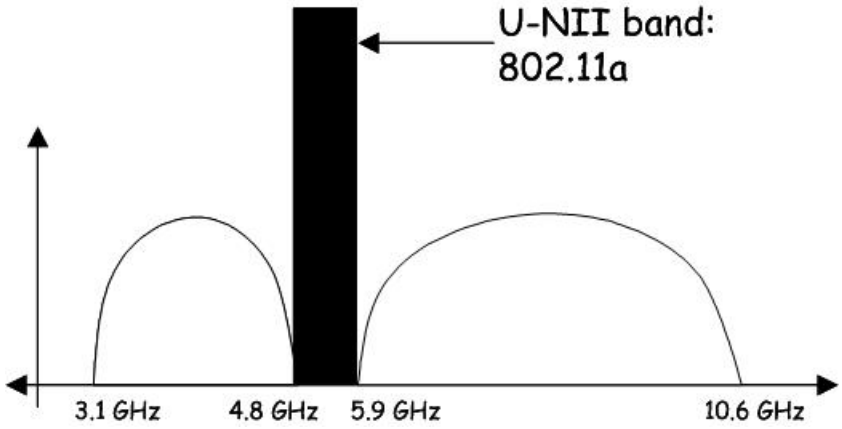

Figure 1.11 UWB Frequency Spectrum planning to avoid interference to/from 802.11a

1.2.3 Applications

UWB has been envisioned to serve two basic spheres of wireless communication:

1) High data rate, low range communication (e.g., home networking etc.);
2) Low data rate, long range communication (e.g., tactical communication, sensor networks, etc.).

From a commercial point of view UWB has been envisioned as a replacement to the Bluetooth technology and as being able to provide data speeds close to 100 Mbps for indoor applications (e.g., streaming video). The IEEE 802.15.3a working group is in the process of defining an Ultra wideband (UWB) based physical layer (PHY). The target applications focus on WPANs (Wireless Personal Area Networks) which have a range of approximately 10 meters. Standardization of a high speed PHY might also provide a basis for Wireless USB and Wireless 1394, which also demand such high speeds [33].

Due to the low probability of interception and the high speeds provided at short distances, the military is visualizing this technology in battlefield communication to provide high speed, reliable and secure data communications. The low SNR operation regime of UWB and the extremely high bandwidth used makes it ideal for tactical communication for LPI/D radios. Due to the large bandwidth used,

UWB also has the capability to give very precise position location and can be used in obstacle avoidance radars, precision geolocation systems, intrusion detection radars and device tags (used for locating specific devices). UWB has also been envisioned to be applied to sensor networks due to its low transmit power requirements.

1.3 Thesis Organization

In this thesis both the single band (impulse radio) and multiband flavors of UWB are being studied. This thesis proposes a new MAC layer for UWB (impulse radio) based communication and compares it with some existing MAC layers. Conceptual simulations have been performed which compare the proposed MAC with other MACs. Also, simulations related to multiband UWB (specifically multiband OFDM, the standard proposed by the 802.15.3a task group) are been carried out and the problem of simultaneously operating piconets (SOP) has been examined.

Chapter 2 explains the concepts of some of the existing MACs used in wireless communication (especially WLANs) and outlines their respective advantages and disadvantages. It reviews the existing work that has been done on UWB MACs and the motivation for the work described in this thesis.

Chapter 3 gives an overview of the simulation setup used for the simulations carried out for the proposed MAC scheme. This scheme is compared against a CSMA-based MAC and the simulation setup for this scheme is also presented. It discusses in detail the methodology and assumptions of the simulated MAC and PHY layers. In addition, some basic numerical system analysis is also presented. This chapter also describes the simulation setup of the receiver code assignment based MAC which is also compared with the proposed MAC in the following chapter.

An extensive analysis of the results obtained from the MAC simulations is presented in chapter 4. Various important parameters are defined and the systems are compared on the basis of those parameters. Results incorporating imperfect CSMA and hidden nodes are also discussed. Conclusions derived from the discussions in this chapter are also presented.

Chapter 5 outlines an alternative flavor of UWB, (MB-OFDM) and gives a detailed description of the simulated system. It also gives a brief overview of the 802.15.3 MAC.

Chapter 6 discusses the SOP (simultaneously operating piconets) problem and performs a simulation study of the various proposed approaches to solve the SOP problem under MB-OFDM. The effect of time-interleaving on the system is studied. Also, a novel idea called “bit-order reversal” is introduced exploiting the inherent frequency diversity of the system and improving performance.

Finally, Chapter 7 presents our overall conclusions. Potential interesting research issues for future are identified. The original contributions of the thesis are also summarized.

Chapter 2

2 MAC Layer Background and Motivation

Wireless spectrum is a scarce resource and each set of applications is allocated a fixed band of spectrum for its operation. Due to the high number of users in a typical application, contention is unavoidable and thus some sort of mechanism is required in order to allocate the resources (i.e. time, frequency band) fairly amongst all users. The MAC layer is responsible for allocating channels to users in the system. MAC protocols are typically defined as contention free or scheduled MAC protocols (e.g. TDMA, FDMA), contention based MAC protocols (e.g. CSMA/CA) or a combination of the two. Each of the access mechanisms has its own advantages and disadvantages, which have been described in detail in [2]. Random access protocols are useful in bursty traffic scenarios where the number of users is more than the total number of available channels. When a user wants to send a long packet or a continuous stream of data, we need to employ some sort of scheduling algorithm to provide the user continuous access to the channel.

This thesis initially concentrates on contention based MAC layer protocols, as they are deemed more suitable for Wireless LANs due to the intermittent/bursty nature of traffic. Typically employing channelized access techniques (i.e. TDMA, FDMA) would either lead to a waste of resources or significant overhead, both of which are undesirable. However, this thesis also analyzes spread spectrum based MAC layer protocols which have been actively considered for wireless LAN applications. A MAC layer based on a piconet architecture is proposed and the performance of various schemes under the framework is analyzed.

2.1 Overview of contention based MAC layer protocols

2.1.1 CSMA and CSMA/CA

CSMA (Carrier Sense Multiple Access) and CSMA/CA (Carrier Sense Multiple Access/Collision avoidance) are both contention based MAC protocols. A node with a packet to transmit senses the channel to check whether there is an ongoing transmission (hence the term "carrier sense (CS)"). The node proceeds with its transmission if it senses the channel as idle for a particular amount of time or else it defers its transmission until the end of the ongoing transmission. The node also initializes its back-off timer with a randomly selected time interval. The timer has a granularity of a back-off slot and is decremented every time the channel is sensed idle. The node is allowed to transmit when the timer reaches 0. This protocol takes advantage of the bursty nature of the traffic and allows multiple users to share the channel.

All contention based wireless networks suffer from the hidden node/exposed node problem, the hidden node problem being more severe as compared to the exposed node problem in most scenarios. These scenarios are clearly explained in Figure 2.1.

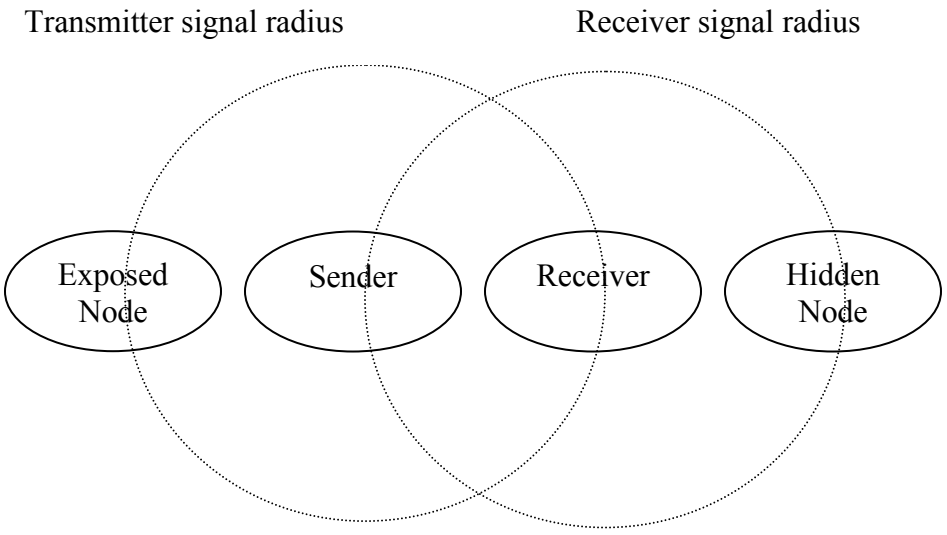

Figure 2.1 Hidden node/exposed node problem

The hidden node problem arises because the hidden node (see Figure 2.1) cannot sense the ongoing communication between the sender and the receiver. The hidden node senses the channel as idle and proceeds with transmission of its packet to the receiver. This causes interference at the receiver. The exposed node problem arises because the exposed node senses the channel as busy as it can listen to the sender's ongoing communication with the receiver. The exposed node can still communicate with its intended receiver if it is far away from the sender and hence would not cause interference to it. Both the hidden/exposed node problems lead to reduction in aggregate throughput. The CSMA protocol has no means to avoid the hidden node/exposed node problem.

The CSMA/CA protocol solves the hidden node problem by using the RTS (Request to send)/CTS (Clear to send) mechanism. An RTS packet is sent by the intended transmitter to the receiver in order to acquire the "floor" before beginning transmission. If the receiver is idle, it sends a CTS packet to the transmitter indicating that it is ready to receive data. All the nodes are always listening to the channel. When a node hears either an RTS or CTS packet, it knows that two nodes in its vicinity want to communicate with each other. The node then sets up its back-off counter equal to either the length of the transmission or any other value depending on the protocol used. Thus both the RTS and CTS packets inform the nearby neighbors of the transmitter and receiver, respectively, about the transmission, which inhibits others from sending packets and hence corrupting the data in the ongoing transmission. Before making an attempt to send any data after the back-off interval has elapsed, the node again senses the channel. This technique helps resolve contention and reduces collision probability under high load conditions.

2.1.2 MACA / MACAW / MACA-BI / FAMA / DBTMA

The protocols discussed in Section 2.1.1 require a particular node to listen for the carrier. It should be noted that carrier sense avoids collisions from happening at the transmitter but most of the collisions occur at the receiver (the hidden node/exposed node problem as stated above). A lack of carrier does not always indicate that it is safe to transmit (hidden node problem) and the presence of a carrier does not always mean that the node should not transmit (exposed node problem). So channel/carrier sense is not always an appropriate indication of the current channel utilization.

To overcome these limitations, a MACA (Multiple Access Collision Avoidance) protocol was proposed in [3]. This protocol gets rid of the carrier sense in the CSMA/CA protocol but retains the algorithms for collision avoidance, hence the name MACA. It relies on the RTS and CTS handshake to avoid collisions at the receiver. In [4], the MACA protocol proposed by [3] was slightly modified and a new multiple access protocol called MACAW (Multiple Access Collision Avoidance Protocol for Wireless LANs) was proposed. This protocol proposed the addition of an ACK for every DATA packet sent (this is now used in the 802.11 standards). The exchange sequence between the transmitter and the receiver looks like RTS-CTS-DATA-ACK and an additional step was added to it to make it look like RTS-CTS-DS-DATA-ACK where the DS stands for the Data Sending frame which tells the nodes that a successful exchange of RTS-CTS happened. This prevents an exposed node from trying to transmit an RTS to a sender which is near to it. This would lead to large back-offs because the sender is already transmitting data to another node and would not respond to the exposed nodes' requests. For a more complete explanation the reader should refer to [4]. The paper also proposed a new back-off mechanism, multiple increase and linear decrease (MILD).

In [5], the MACA-BI (MACA – By Invitation) protocol was proposed, in which an RTS frame is not sent from an intended transmitter to the receiver. This is a

receiver initiated protocol in which the receiver determines when the sender is likely to send a packet (either by relying on the packet arrival rate or by the sender telling the receiver in the previous packet about backlog of packets). The receiver then initiates (prepares the floor for transmission) a call by sending a CTS to the sender. The sender upon reception of the CTS, starts transmitting data to the receiver.

It should be noted that although an exposed terminal would be permitted to send because of the RTS-CTS mechanism, it would not receive the CTS while the other node is transmitting on the channel. Also as the hidden node is forbidden to access the channel, it cannot receive any packets and also cannot reply to any RTS sent to it. As seen above, both of these problems reduce system throughput.

The hidden node problem was also addressed in [6] by using a busy tone to indicate the ongoing transmission and thus preventing any other node from initiating another transmission. All the nodes monitor the busy tone to determine the availability of the channel. The proposed protocol did not use RTS and CTS for collision avoidance and depended on centralized access to avoid collisions (by using a centralized access topology, channel access time is allocated to each user such that two nodes do not contend for the same channel time). Attempts along similar lines were made by [7] and [8] to avoid the hidden node problem. They also used the busy tone technique to avoid collisions.

The FAMA (Floor Acquisition Multiple Access) scheme was proposed in which each node is required to acquire the channel ("floor") before it may initiate the transmission [9]. The node used both carrier sensing and RTS-CTS to acquire the floor. Once the floor was acquired the node could successfully transmit data. In [10], FAMA-NPS (FAMA Non-Persistent Packet Sensing) was studied and it was shown that packet sensing schemes alone could not solve the hidden node/exposed node problem. FAMA was extended to FAMA-NCS, which uses a CTS dominance mechanism (longer CTS packets). If the node had begun

transmission of the CTS packet and at the same time an RTS packet is sent, the node transmitting the RTS packet would hear the CTS packet and would refrain from accessing the channel. In [11], Wireless Collision Detection (WCD) scheme was proposed, which requires network wide synchronization and would be difficult to implement in a wireless local area network.

Dual Busy Tone Multiple Access (DBTMA) was proposed in [12]. The protocol uses two out of band tones along with the RTS-CTS handshake for informing neighbors about an on-going transmission. The protocol resolved the hidden node/exposed node problem completely. A brief description of the algorithm is as follows. Once an RTS packet is transmitted, the BT_t (Busy Tone – Transmitter) signal is set to prevent the RTS from getting corrupted. On hearing the BT_t tone, the other transmitters would refrain from sending an RTS packet and back-off. At the end of the RTS transmission, the transmitter turns off the BT_t tone and waits for the CTS packet from the receiver. Once the RTS packet is received, the receiver responds with the CTS packet and sets the BT_r (Busy Tone – Receiver) signal. Any transmitter in the vicinity of the receiver would hear the tone and would not transmit while the tone is set. It might happen that two simultaneous RTS are sent, which would corrupt the RTS signal. In this case the receiver would not understand the command and would not respond. Both the transmitters would individually time out and repeat the above procedure before sending the RTS packet. This prevents corruption of the data. This algorithm also solves the hidden terminal/exposed terminal problem, as the hidden nodes can reply to RTS requests by setting their busy tones and the exposed node can initiate a transmission because it no longer need to listen to the shared medium. The paper also states that the exposed terminal could initiate a request during an ongoing transmission. Although the DBTMA scheme solves the hidden/exposed node problem, it requires two additional channels for setting the BT_r and the BT_t signals. This is a significant overhead in the already crowded spectrum allocated for wireless LANs.

The 802.11 MAC layer [13] is based on the CSMA/CA + ACK protocol for unicast frames and the CSMA/CD (Carrier Sense Multiple Access/Collision Detection) protocol for broadcast frames. It also deploys a virtual carrier sense mechanism to avoid a station from transmitting when two nodes are already communicating.

Another class of MAC layer protocols based on the slotted ALOHA approach was introduced in [14] and [15]. Schemes were proposed in [14] to prioritize voice services and allot them a slot in each frame once they have acquired it following a regular contention algorithm. In the simulations bursty traffic was assumed and it was shown that this would increase the throughput of the system. The idea was improved upon in [15] and applied to MANETs with slight modifications. Both of the schemes used network wide synchronization to avoid slot misalignments due to clock drifts between nodes.

2.2 CDMA Based MAC Layer Protocols

The use of s spread spectrum based protocol was first illustrated in [16]. It was proposed to be used because of its inherent capability to work against jamming and multipath interference. Two protocols were proposed, namely the Common Transmitter (C-T) Based Protocol and the Receiver-Transmitter (R-T) Based Protocol. In the first method, a unique transmitting code is assigned to each user. There is also a common code used for addressing purposes. The destination and the source addresses are transmitted on the common code whereas the data is sent on the transmitter's code. All of the idle receivers are initially listening to the common code and once they recognize their address, they shift to the transmitting stations code. The only collisions that can happen in this scheme are during the time when the transmitter is setting up a link. Any other transmitter will not be able to disrupt the ongoing communication until it uses the same transmitter code. The overhead in this scheme is the assignment of pseudo-orthogonal codes to every transmitter. In the second method, two codes are assigned to every node.

One of the codes is used for listening to incoming requests and the other code is used for transmitting data. The advantage of this protocol over the first one is that there is a collision only when frames are sent to the same node.

In [17], an improvement was made over the protocol above by using a RTS/CTS mechanism to avoid the loss of data. The basic protocol remains the same except that there is a feedback loop in the setup stage. They named the two protocols the MACA/C-T and the MACA/R-T protocol. A CDMA based CSMA MAC layer protocol was proposed in [18] for wireless LANs. The proposal used the concept of assigning codes dynamically for multiple access based on the communication needs of the nodes. The codes would be chosen from a set of pre-defined codes and a particular node would choose a code which none of its adjacent nodes would be using. The node can gather the information regarding the codes being used in its vicinity by listening to the common channel (where the initial communication setup is done). Using the above protocol they showed tremendous improvement in performance as compared to the CSMA and the RTS/CTS mechanism because there can be multiple sessions going on simultaneously (as adjacent nodes transmitting would ideally not interfere with each other).

In [19], an improvement over the receiver based protocol [16] was proposed which gives the same throughput as the R-T based scheme. Carrier sense is done at the transmitter on the receiver code of the intended receiver before it begins transmission. This reduces the probability of collision. Contention is resolved using CSMA. A similar scheme was proposed in [23]. Other protocols proposed include the receiver based protocol in which a unique code is allocated to each terminal which the node monitors while it is idle. If a node needs to transmit data to another node, it sends the information on the receiving code of the destination node. The receiver gets the message and decodes it. This scheme was analyzed in [20]. A transmitter based protocol was proposed in [21] in which a unique transmitter code is allocated to each terminal. If there are enough codes in the code space then the transmissions from different transmitters should not interfere.

The Transmitter – Receiver based protocol was proposed in [22] in which each node is assigned a unique transmission as well as reception code.

Almost all proposed CDMA based MAC layers rely on static assignment of CDMA codes, which leads to inefficient utilization of the codes. Also as the number of required codes increases, in order to obtain codes with good cross-correlation properties, the code length needs to be increased, which leads to a further reduction in throughput. Also, CDMA schemes suffer from the inherent near-far problem, which leads to an inefficient protocol if all the nodes communicate with one another via the base station.

2.3 MAC Layer Protocols for UWB

Because UWB is a relatively new technology in the communications area, significantly less work has been done on the MAC layer design of such systems. Research for this technology has primarily been in the PHY layer and previously existing MAC layers have been proposed with slight modifications for usage with this technology. As of today, no one has done an extensive analysis of the UWB MAC for an impulse radio based PHY. A comparison of access methods for a multi-hop scenario was made in [24]. Time hopping codes were compared against the CSMA technique for UWB systems. The number of code channels was assumed to be equal to the number of users in the system. A feedback loop in the system was assumed in which a receiver informs the node its current interference levels. Having received this information, each user sends at a rate such that it does not result in such interference that the neighboring nodes cannot receive packets designated for them. A modified CSMA algorithm was also investigated which incorporated a feedback channel to inform the adjacent nodes about the receiver's current interference level. A comparison was done on the basis of average delay versus average throughput and maximum throughput versus the feedback delay.

In [25], the position location properties of UWB were used and a new strategy was proposed for path selection which would lead to the low power path to the destination using multiple hops. An infrastructure for a UWB-based MAC layer was proposed in [26]. They outlined the functionality of the various blocks to be used in a UWB based system. Surprisingly, they did not talk about the position location capability of UWB and did not try to exploit it. UWB suffers from the problem of high acquisition times. The impact of channel acquisition times on the network throughput, utilization and delay was studied in [27]. A novel impulse radio network was proposed in [28]. They highlighted the issue of long acquisition times in UWB networks and proposed a MAC layer scheme called Sustained Link Networks (SLN) to maintain connectivity between the physical layer modules during the whole logical link connection between them. They showed that such a technique did not affect covertness and had a higher system throughput. The authors of [46] proposed a new MAC layer for UWB networks based on dynamic channel coding and interference mitigation. In [47], UWB networks were evaluated in the context of joint optimization, in which power control, scheduling and routing issues were considered.

2.4 Motivation

As mentioned in the previous chapter, UWB (impulse radio) systems are being looked upon as a replacement for Bluetooth for WPAN applications and also for sensor network applications.

Applicability of Channelized Schemes to UWB (FDMA, TDMA)

Since a UWB pulse could occupy a significant part of the spectrum, not many FDMA channels can be supported within the allocated bandwidth. A maximum of 17 channels can be supported (in the current FCC allocated band given the minimum channel bandwidth of 500 MHz), which is very low given the amount of bandwidth allocated to the technology. Since impulse radio uses very low duty cycle pulses for communication, employing a TDMA based channelization

scheme leads would require extremely accurate timing or would result in extremely inefficient spectral usage.

Applicability of Non-Channelized Schemes to UWB (CSMA etc)

Either of the above mentioned non-contention based techniques (Section 2.1.1 and Section 2.1.2) could be used as a MAC for a UWB (impulse radio) based PHY but the low duty cycle communication mechanism leads to a waste of resources.

One question which comes to mind is that why is it not possible to use a high duty cycle communication channel and do a TDMA based MAC? This is certainly possible but since UWB systems operate in an unlicensed band and are limited by the power spectral density specified by FCC (i.e., -41.3 dBm/MHz). This puts a limitation on the maximum achievable range. The following link budget analysis (Table 2.1) aids the discussion.

Table 2.1 Example Link budget for a UWB system

	Uncoded	Coded (K = 8, R = 1/3)
Pulse width (ns)	2	2
Pulse Rate (MHz)	500	500
Pulses per bit	1	3
Bandwidth (MHz)	500	500
Information Data Rate (Rb) (Mbps)	500	167
Average Tx Power (Pt) (dBm)	-14.3	-14.3
Tx Antenna Gain (Gt) (dBi)	1.0	1.0
Center Frequency (fc) (MHz)	3882.0	3882.0
Path loss at 1m (L1)	44.2	44.2
Rx Antenna Gain (Gr) (dBi)	1.0	1.0
Average Noise Power per bit (N) [-174 + 10*log10(Rb)]	-87.0	-91.8
NF (Nf)	7.0	7.0
Average Noise Power per bit (Ntot) [Ntot = N+Nf]	-80.0	-84.8
System Eb/No (S) [10e-5% BER] – Includes 3 dB implementation margin	12.6	8.9
Link Margin (M)	0.0	0.0
Sensitivity	-80.0	-80.0
Rx Power Required [Pr = Ntot + S + M]	-67.4	-75.9
Path loss at d m [L2 = Pt + Gt + Gr - L1 – Pr]	10.9	19.3
Distance at which path loss is achieved (m) [10^(L2/20)]	3.5	9.3

Assumptions:

1) The pulse of 2 ns can be transmitted at -14.3 dBm. Since we are peak power limited and the transmitted pulse would not have a flat spectrum for the entire bandwidth that it occupies, the tx power would be much lower than what is shown here.

2) The path loss has been calculated with center frequency to be the center of the first 500 MHz of allocated UWB spectrum. As we move higher in the spectrum, the center frequency increases, increasing the path loss and reducing range even more.

The above analysis produces the achievable distance of an uncoded system and a coded system in an AWGN channel. As calculated, the achievable distance of a coded system is only 9.3 meters without the presence of multipath and any interference. With the incorporation of multipath and interference (due to

imperfect CCA or narrowband interference) the achievable distance would reduce even further.

UWB is envisioned as a technology to be used with either short distance high speed communications (i.e. Wireless Personal Area Networks) with a range of about 10 meters or for long distance low data rate communication. For long range communications ranges of the order of kilometers would be required which is definitely not achievable by transmitting a single pulse/bit. This leads us to investigate other mechanisms to improve the achievable range of the system and also mechanisms which give highest throughput in a network spread over a particular geographical area. In order to increase the achievable range, one must increase the energy transmitted per bit. This can be done either by simply repeating a pulse multiple times or spreading the signal using some kind of spreading scheme. By spreading we mean that the pulse is repeated multiple times and the amplitude/polarity/phase of the pulse depends on the chip value of the spreading sequence. Note that the energy transmitted per bit is now the original energy transmitted per bit times the spreading factor. This leads to an increased in the transmitted energy per bit. Although this would increase the energy per bit, it reduces the throughput by the number of times the pulse is repeated. Also this technique is not efficient if the network architecture requires multiple communication links to be operating simultaneously. Another technique is to spread using well defined spreading codes. This technique also reduces the throughput by the number of times the pulse is repeated but improves the performance of the network as multiple communication links can be operated simultaneously. This technique of using different spreading codes for different users has been adopted extensively in cellular technology and becomes a viable solution for UWB based wireless LANs due to the inherent nature of short pulses.

This thesis proposes and compares a CDMA based network architecture with a traditional CSMA based network architecture and brings forth the advantages and disadvantages of each of them. It also compares the proposed architecture with a

receiver based code assignment scheme proposed in the literature and compares them on various grounds.

Chapter 3

3 System Model

3.1 Introduction

The objective of this chapter is to describe in detail the system model used for simulation (including both the MAC layer and physical layer) as well as the algorithm proposed for Medium Access control of Ultra-Wideband systems. The assumed model will be used to examine the performance of the MAC algorithms and to compare the proposed scheme with other schemes presented for UWB in the literature. Simulation results obtained using the model described in this chapter are discussed in Chapter 4. The system was developed independently by the author in MATLAB.

3.2 Proposed CDMA-based MAC Algorithm for UWB

3.2.1 Overview

Spread Spectrum based Packet Radio Networks (PRNs) have been widely studied in the literature [16] – [23], [34] – [40] and are discussed in detail in Chapter 2. Some of the advantages of spread spectrum based communication are that it allows multiple users to communicate simultaneously and does not require network wide synchronization. In spread spectrum based PRNs, although no system wide synchronization is required, such networks are limited by the amount of mutual interference seen in the network [36], [37]. Spread spectrum based networks also lead to a more graceful degradation of overall network performance as compared to other schemes. This is similar to the advantage that spread spectrum based systems enjoy in cellular networks. Throughput analysis for spread spectrum networks has been performed by various authors [41].

CDMA or Code Division Multiple Access is a natural access technique for spread spectrum based networks. It is based upon the assignment of different spreading waveforms (*i.e.*, different spreading codes) to different users in the network, which then can communicate simultaneously. In theory, it is possible to have completely orthogonal codes assigned to each user. The orthogonality between the codes is normally only possible if the users are time synchronous. This is very hard to achieve in a practical network as signals reach each user with different code phases (*i.e.,* different shifts in the transmitted code) due to various propagation delays in the channel. In centralized networks where each user communicates through a central receiver, synchronization is feasible on the downlink (from access point to a node) but is difficult to achieve on the uplink (from the node to the access point). Additionally, if communication is peer-to-peer, synchronism is nearly impossible to achieve. Hence it is not usually possible to eliminate all interference in a spread spectrum based network. For a practical network, it is the job of the system designer to assign spreading codes in such a manner as to provide minimum interference to each node. This brings up the interesting problem of code assignment.

Code assignment has also been widely studied and various algorithms have been presented in order to optimally assign the codes to avoid "collisions" in code assignment [16], [42] - [45], [48], [49] (by "collision" in the context of code assignment, we mean two users in close proximity being assigned the same spreading code). As discussed in Chapter 2, in [16] a receiver based code assignment algorithm (RCA) was proposed. In [49] a transmitter based code assignment algorithm (TCA) was proposed. A different scheme based on pair-wise code assignment (PCA) was proposed in [43]. In PCA, a code is assigned to each transmitter-receiver pair and codes are assigned in such a manner that no two pairs use the same code in a particular geographical area. In [45], a distributed code assignment algorithm was proposed which required information about the

transmission codes of nodes 1 and 2 hops away in order to assign codes such that no *primary*[1] interference occurs.

3.2.2 Proposed Code Assignment Scheme for UWB Networks

An ad-hoc network is considered in this work, and the targeted applications are sensor network based applications. These are high density, high redundancy types of systems. Such systems require multiple simultaneous communication links to be established and broken. Either a node is idle, acting as an intermediate router to transfer information from a source to a destination or is the intended source or destination. A higher level protocol (predominantly the network layer) is used to determine the path from a particular source to a particular destination. The problem of routing is outside the scope of the present research. In such systems, due to the high density of nodes, there is a significant amount of interference in a particular area. From a system perspective it would be ideal for all nodes to communicate with their respective receivers simultaneously. A fully centralized system is clearly not the choice of architecture due to the high density of nodes and due to the limitations typical of sensor nodes (*i.e.*, nodes in a sensor network are typically required to be inexpensive and power efficient). A centralized receiver would also entail stringent timing requirements on the nodes and could lead to components such as an on-board GPS device. Clearly, this not consistent with inexpensive and power efficient nodes. This type of a system demands an ad-

[1] In the literature, spread spectrum based interference is typically divided into two categories. Primary interference occurs when two nodes in the vicinity of each other use the same code and hence cause drastic degradation in performance. Secondary interference occurs when two nodes using different codes are in the vicinity of each other. It is always desirable to eliminate primary interference, whereas secondary interference can be tolerated up to a certain limit. The concept of primary and secondary interference has been given various names in the literature. For example, some authors use the terms direct and indirect interference instead of primary and secondary, respectively.

hoc network approach with small areas under centralized control to provide minimum interference to the nodes in that particular area.

Present techniques of multiple access for wireless LAN applications such as CSMA/CA or CSMA/CA with RTS/CTS require the node to listen to the channel before transmitting data. In this scheme, if one node is transmitting, other nodes have to wait till the present communication is over before making an attempt to access the channel. This is inefficient for UWB since the inherent spreading should allow for simultaneous communication. Note that sensing may be very difficult for UWB-based system due to long synchronization times. Additionally, CSMA-based techniques are known to suffer from the hidden node/exposed node problem.

A second set of techniques use a TDMA based approach. This is also inefficient as only a particular user is active at a time when simultaneous communication should be possible. This leads to inherent inefficiencies in the system such as loss of system throughput. UWB is a recent technology which has extremely low power spectral density. For systems using CSMA/CA, access could be very challenging due to the short duty cycle of the pulses. Thus, we propose using a CDMA based MAC for a UWB-based physical layer. A novel technique based on code brokers is proposed in this work. Simulation results comparing our approach to CSMA-based systems are presented in this work.

To motivate the design of the CDMA code assignment scheme, we first need to determine the desirable properties of the scheme. From our point of view the main properties we desire of a spread spectrum based PRN are:

a. The receiver should only be required to listen to a single code rather than multiple codes. This requirement keeps the implementation of the receiver practical. In present spread spectrum based UWB receivers, multiple rake fingers are required in order to capture signal energy for effective communication. Requiring the receiver to simultaneously listen to

multiple codes increases the complexity of the receiver to unacceptable levels.

b. The network should be asynchronous, as opposed to traditional CDMA based cellular networks, which require base stations to be synchronized. This is not a very practical requirement for PRNs since a piconet may be geographically located in a very small area and spatially separated from other piconets. In such networks, the goal of the designer should be to maximize the "local throughput" of the system.
c. There should be minimum or no *primary* interference. *Secondary* interference is a by-product of using spread spectrum based PRNs and is unavoidable.
d. Network performance should degrade gracefully.

Keeping these requirements in mind, a new MAC layer protocol has been developed for UWB based networks. The proposed protocol is based on limited centralized control and is thus not entirely distributed. Central to this scheme is the concept of a "code-broker," which will be explained below.

A piconet is a wireless ad hoc data communications system which allows a number of independent data devices (DEVs) to communicate with each other [33]. Each piconet has a network controller (which we term a "code-broker"). The adjacent piconets are assumed to be uncoordinated. Unlike traditional centralized architectures (e.g. 802.11 (except for the ad-hoc configuration)) in which all the communication goes through the network controller (or access point in 802.11 terminology), such an arrangement is not required in this scheme. This scheme works on peer-peer communication. The network controller is only used as a "code-broker." A code-broker is a node that is responsible for assigning codes to different users in the network. It does not have to participate in any communication (although it may have communication of its own to transmit). The code-broker is always listening to incoming requests for code assignments so that two nodes in a network can communicate with each other using the assigned code.

Such an arrangement allows multiple links to be operational simultaneously and hence increases the local throughput of the system. Figure 3.1 below illustrates two such piconets.

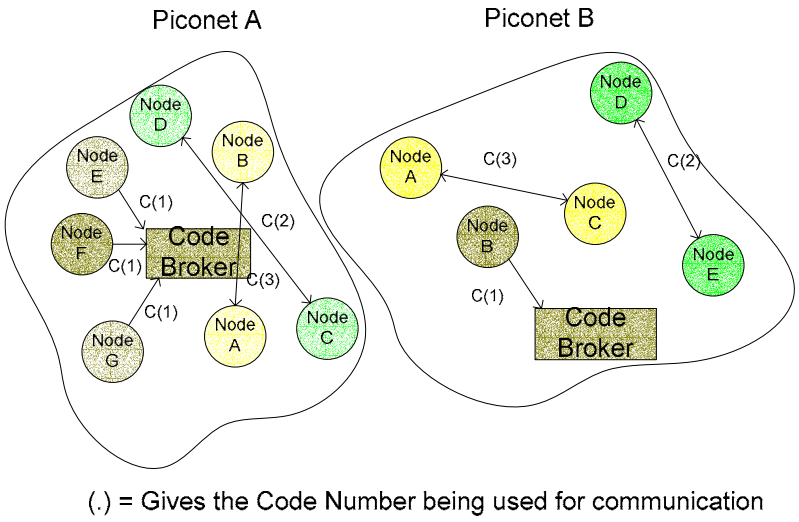

Figure 3.1 Piconet Structure for Spread Spectrum based UWB Networks

Each node in a piconet is depicted in Figure 3.1 as Node A, Node B and so on. As shown in the figure, in piconet A, nodes E, F and G are making requests to the code-broker to join the network. Although all three nodes are in the network association stage (*i.e.*, trying to obtain a code from the code-broker), they are not necessarily transmitting their requests simultaneously. Which node out of the three transmits at a particular time is determined by Algorithm 1 described below. In Piconet A, Nodes A and B as well as Nodes C and D are simultaneously transmitting to each other on their respective codes. Another uncoordinated piconet (Piconet B) is also shown in the figure above, in which Node B is requesting a code from the code-broker. Simultaneously Nodes A and C and Node D and E are communicating with each other.

Each piconet has multiple sets of codes to choose from. Whenever a node wants to start a new piconet, it either

1) Scans the available code space for the best set of codes to choose from. (This would be determined by the interference it observes in each of the code sets) or
2) Communicates with the rest of the piconets in order to make a decision on the code set it could use for its own communication.

The methodology for how the code sets are assigned to different piconets has not been investigated. An example of how a node would start a piconet or associate itself with an existing piconet is illustrated in Figure 3.2 below. Once a node becomes a code-broker, it would need to send periodic beacons (i.e., information elements specifying the properties of the network) on a specified code in order for the new users to listen to the presence of the piconet and eventually join the piconet.

In reality it is hard to find a large number of codes with good cross-correlation properties unless the code length is made large, which reduces throughput. On the upside, the assignment of different codes to adjacent piconets takes care of the interference, which arises when two nodes in adjacent piconets are very close to each other and are using the same code. In this thesis, it is assumed that adjacent piconets use different codes.

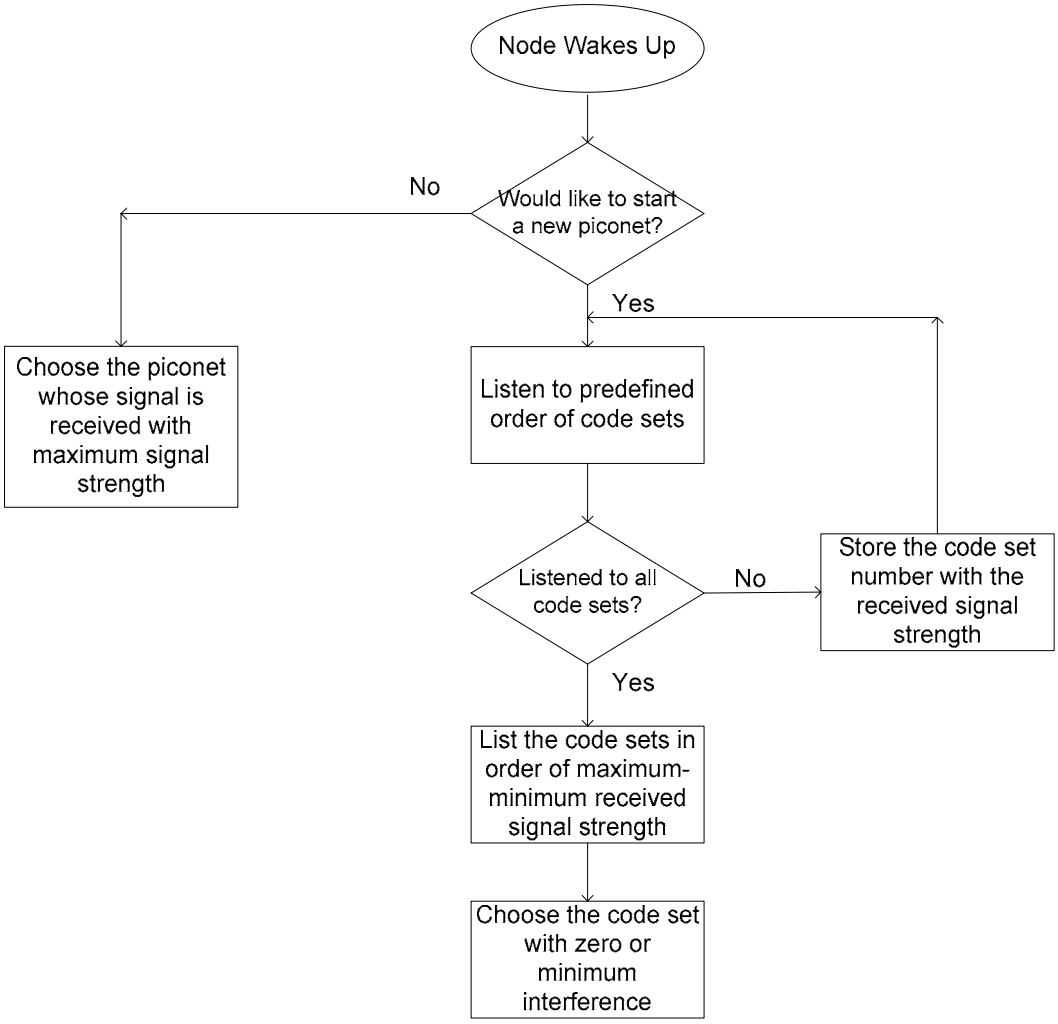

Figure 3.2 Flowchart for piconet formation

Each code-broker maintains a "code assignment table," which is a list of the codes assigned for that particular piconet. The code-broker continuously updates the table. When the network starts, the code assignment table is empty as no nodes are connected to the network. As and when new nodes make requests to join the network to transmit to a particular user, the code-broker examines the table to determine the list of unused codes. Note that code assignment is link based and not user based. If there are any unused codes present in the table, the code-broker assigns one of the unused codes to the requesting node. If there are no left unused codes, the code-broker does not respond to the requesting node. The requesting node upon not receiving any response would time out (as described in Algorithm

1 below) and make another attempt to join the network at a later time. Hopefully at a later point in time, the code-broker would have some unused codes which it could assign to the requesting user. An example of the code-broker's code assignment table is shown in Figure 3.3 below. Note that the code-broker also keeps track of the Node ID to which a particular code is assigned. In addition to the assignment table, the code-broker also needs to maintain a list of the nodes which are a part of the piconet.

Codes	Assigned	Node ID
1	Yes	X
2	No	
N-1	Yes	Z
N	Yes	U

Figure 3.3 Code assignment table maintained by the Code Broker

The ordering of the codes assigned is determined by the code broker. The field "assigned" in the table could be represented by a single bit where a "1" would indicate that the code is being currently used and a "0" would indicate a code currently not being used. The other column is a list of the codes available to the code-broker. The third column associates the code with the nodes ID which has been assigned a particular code. Whenever a node no longer requires a code which it was previously using for communication, it would communicate the message to the code-broker and relinquish control of the code. The code-broker upon receiving such a message would update the corresponding code in the table as unused. It would be beneficial to mandate that an associating node needs to

intermittently communicate with the code-broker in order to indicate its presence in the piconet. This would increase the traffic towards the code-broker as it now would have listen to new incoming requests as well as messages from existing nodes in the piconet who indicate their presence in the network. This would in turn increase the latency to join the network. Another option would be to specify a time-out counter. Whenever a code is assigned the counter is started. Upon expiration of the counter the associating node gives up the obtained code. This mechanism makes sure that no single user can keep an assigned code forever.

Each node upon wakeup associates itself with a particular piconet. A simple mechanism of how a node decides whether it wants to join piconet A or piconet B is described below. Let us consider the scenario where the node is equidistant from the code broker of piconet A and piconet B.

Algorithm 1 (For association of a node to the network – Node's perspective):

1) Every node knows that the request for joining the network has to be transmitted on a particular code (e.g. Code 1). It also knows the reply of the request is always transmitted on a well known code (e.g. Code 2). These codes are chosen from the code set assigned to that particular piconet only. These codes would be different for adjacent piconets as the piconets would use different code sets (*i.e.* Code 1 and Code 2 for piconet A in Figure 3.1 above would be different than Code 1 and Code 2 for piconet B.) Although it is possible that two adjacent piconets might use the same code set, the probability of this scenario happening is very low.
2) Whenever a node wants to join a network it would listen to the medium for any ongoing transmission on Code 1 from any other node to the code-broker.
3) If the node senses an ongoing transmission, it defers its transmission by an amount of time equal to its back-off counter to reduce the interference it would cause to any other ongoing transmission. The back-off counter

could be incremented in a linear or exponential fashion. In other words, CSMA is used for obtaining a code from the network.

4) If upon hearing the channel the node finds the channel empty (*i.e.* no ongoing transmission), it proceeds with the transmission of its "association request" to any of the code-brokers in the range of the node. The request consists of the Node ID and the destination ID (*i.e.* ID of the node the associating node would like to communicate with).
5) The node then waits for a specified time (on Code 2) for an "association request granted" packet.
6) If the node does not receive an "association request granted" packet within the specified time, it times out and repeats the procedure from step 2.

The algorithm is also depicted in Figure 3.4 below.

Algorithm 2 (For association of a new node to the network – Code-Broker's perspective):

1) The code-broker is always listening on a particular code (say Code 1) for incoming requests from prospective members (nodes) of its piconet.
2) Upon receiving a request, the code-broker decodes the packet. If the packet is not decoded successfully the code-broker does not respond to the associating node. A successful/unsuccessful decoding of the packet could be determined by looking at the FCS (Frame Check Sequence) appended to the end of the packet. The received frames' FCS is calculated and checked with the known FCS. If the two sequences match, a successful reception of the frame is declared; else, an error is reported.
3) If packet decoding is successful, the code-broker knows the associating node's ID and the destination node's ID. The code-broker responds to the associating node with an "association request granted" packet on a pre-defined code (say Code 2 for our example) with the new code to be used by the associating node for its communication with the destination node.

The code-broker also informs the destination node to expect a packet on the new code from the associating code.

The code-broker also updates its "code assignment table" with the "new code" in its table marked as USED. Please note that the communication between the code-broker and the associating node for conveying the information about the newly assigned code is assumed to be perfect in this work. The feedback channel is assumed to be perfect in the association stage. In this stage it is assumed that the communication from the code-broker to the associating node and the destination is perfect. In the communication phase, since there is no ACK scheme, there is no feedback channel. Figure 3.5 below shows the algorithm as a flowchart. A timing diagram of the whole association algorithm is shown in Figure 3.6 below.

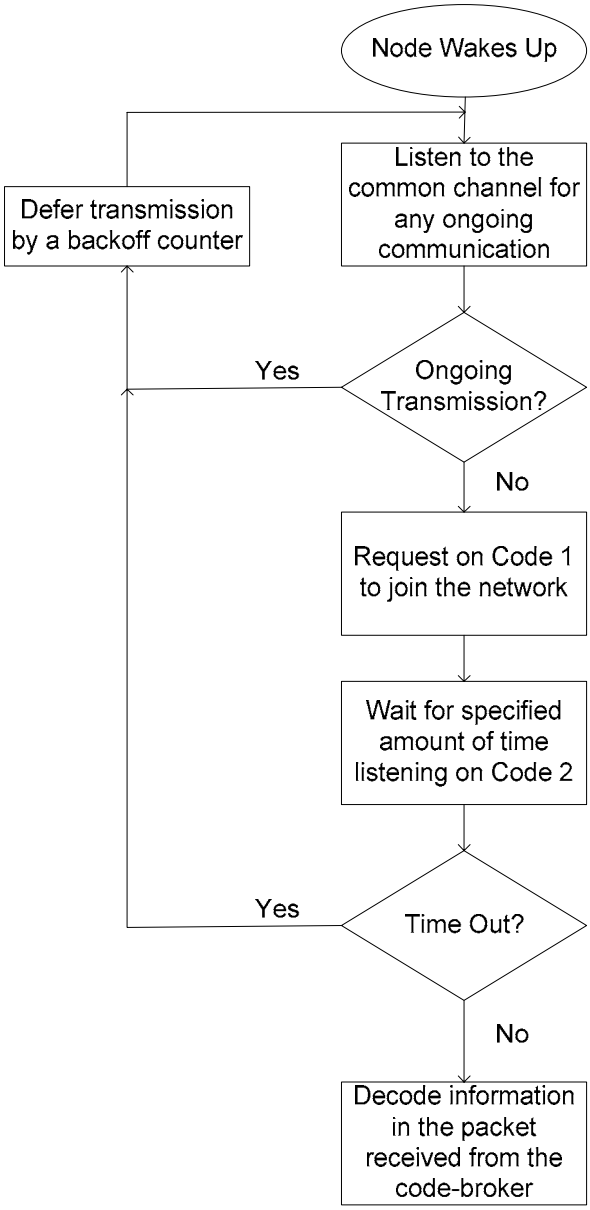

Figure 3.4 Algorithm for association of a node to a network (Node's perspective)

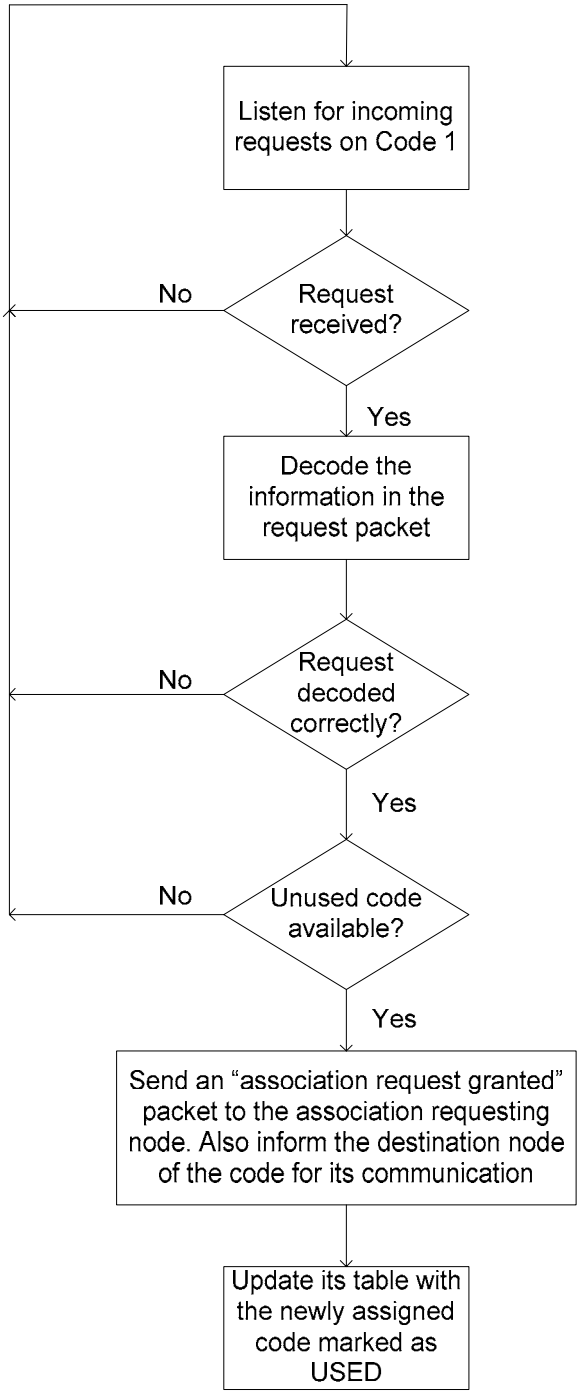

Figure 3.5 Algorithm for association of a node to a network (Code-brokers perspective)

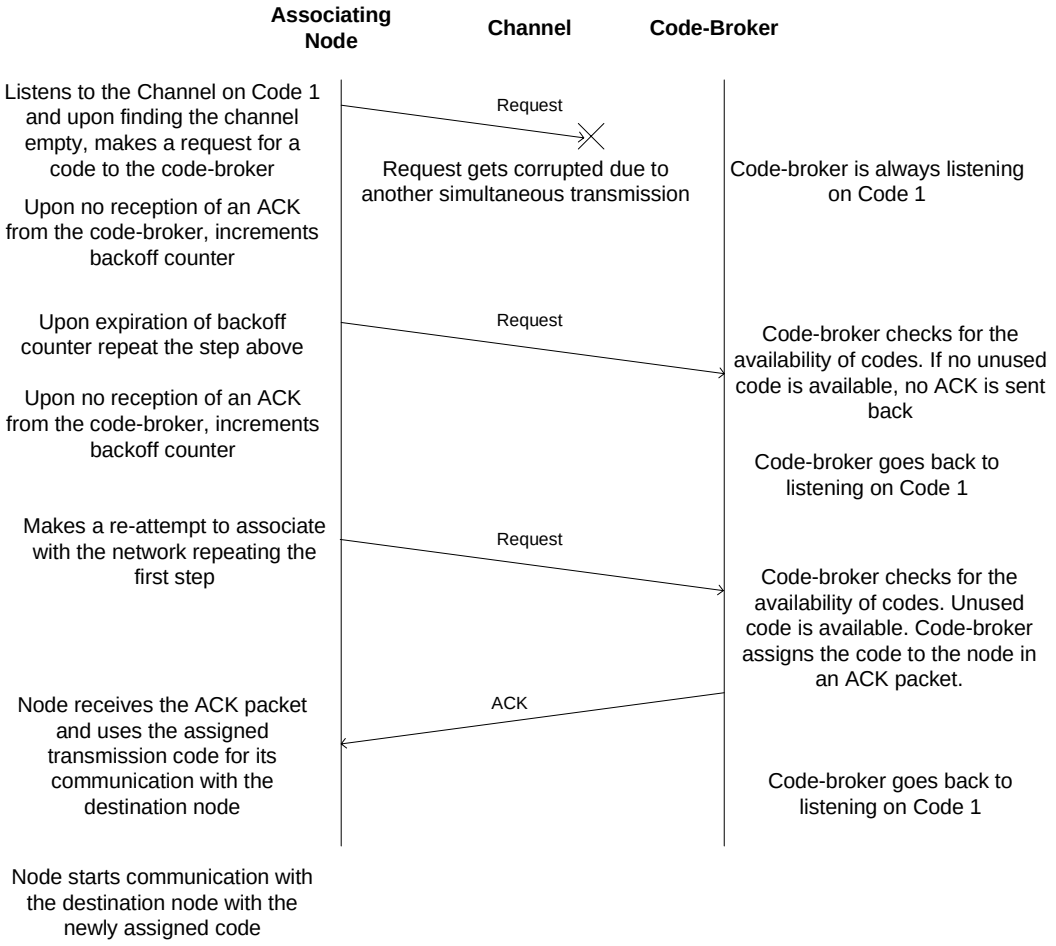

Figure 3.6 Association timing diagram

Algorithm 3 (For the node to get a communication code from the code-broker and disassociation from the network):

1) The node upon receiving an "association request granted" packet from the code-broker decodes the information in the packet to obtain the newly assigned code for its communication with the destination node.
2) It proceeds with communication with the destination node. (Note: The exact algorithm for communication between the two nodes *i.e.* whether it supports immediate acknowledgements (ACKs) for packets transmitted, delayed ACKs or no ACKs etc. is not specified in the algorithm. It would be dependent on the kind of application the MAC is being used for. For example, if the application is time critical (e.g. real-time video) then a no

ACK scheme would be preferable. For file transfer or similar applications a delayed ACK or immediate ACK would be more useful.) The MAC is not responsible for guaranteeing reliable transmission from one node to another. If the application requires reliable transmission, the functionality would be provided by upper layers in the protocol stack such as the network layer or the transport layer.

3) Upon completion of communication, the node informs the code-broker that it is no longer communicating with the destination node using its assigned code and disassociates itself from the network.

   Note: Although the node might be no longer communicating with the destination node, instead of disassociating itself from the network and returning the code back to the code-broker, the node might decide upon keeping the code to itself. It might want to do it if it feels that at a near point in the future it would again have to communicate with the destination node and the setup time in requesting a new code from the code-broker would be too high.

Note: The destination node is assumed to be idle when the source node (or the node requesting the code from the code-broker) is transmitting a packet to it. This is guaranteed by the code-broker before it responds to the associating node with an "association request granted" response. Figure 3.7 below shows the flowchart for communication between the two nodes.

Algorithm 4 (Disassociation of a node from the network – Code-brokers perspective):

1) The code-broker after assigning a new code to the associating node, updates its table with the newly assigned code as USED.
2) Upon reception of a "disassociation request" packet from any previously associated node, the code-broker decodes the Node ID and the transmission code being used by the node. The code-broker updates its table with the previously assigned code to the node marked as UNUSED.

Note: The same control code is used for association/disassociation with the network. Also note that if a time-out mechanism is used, the associating node has to relinquish control of the obtained code after the timeout counter expires.

Figure 3.8 below shows the flowchart for disassociation of a node from the network.

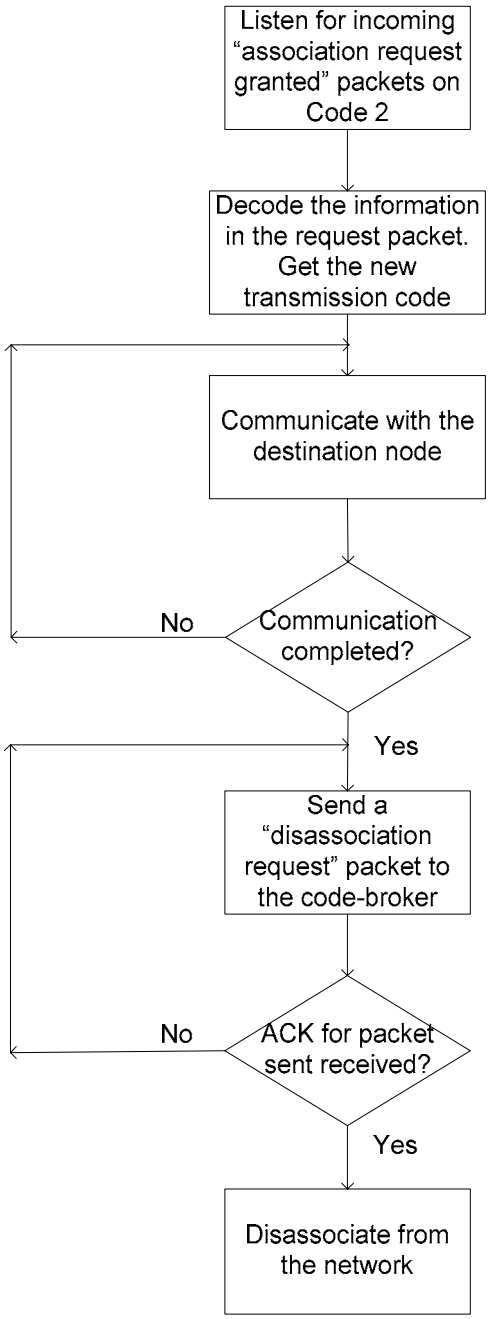

Figure 3.7 Algorithm for communication/disassociation of a node (Node's perspective)

.

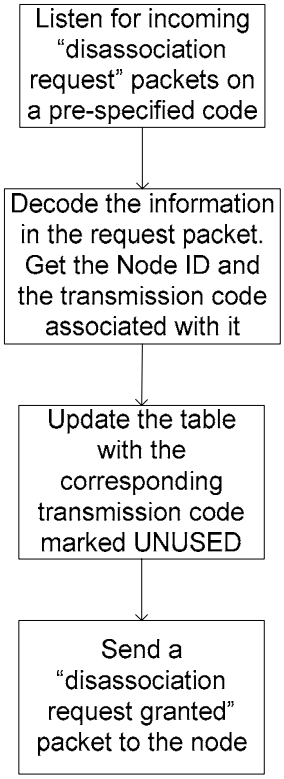

Figure 3.8 Algorithm for disassociation of a node (Code-broker's perspective)

3.3 MAC layer model

The above stated algorithms (with some assumptions) have been simulated for UWB networks and compared to the traditional CSMA based scheme. The proposed code assignment scheme has also been compared to receiver-based code assignment CDMA schemes. The simulation setup for each of the schemes (*i.e.*, CDMA based MAC using a code broker, CSMA based MAC and a CDMA based MAC with receiver code assignment) is described below.

3.3.1 CDMA based MAC with Code Broker (*the proposed scheme*)

The MAC scheme described above has been simulated along with a UWB PHY layer with the assumptions stated below

1) A spread spectrum system can suffer from the imperfect power control and has great amount of multipath. How the actual system deals with these problems greatly affects the performance of the system. In this simulation/analysis, it is assumed that the system takes care of these issues ideally (*i.e.* a perfect rake receiver which collects all of the received energy related to a bit). By doing so, the effects of the protocol can be isolated and studied independent of the system implementation. In practical implementations, a rake receiver is unable to collect all the energy associated with a bit and a factor for degradation could be incorporated in the simulations to include that effect.
2) Communication on the feedback channel (*i.e.* communication from the code-broker to the associating node) is assumed to be ideal.
3) Communication between the code-broker and the destination node is also assumed to be ideal. This communication takes place when the code-broker needs to tell the destination node to switch to a particular code which the associating node will be using for communication.
4) The disassociation algorithm has not been simulated.

Using these assumptions, the following steps are simulated using the MATLAB software package. The simulation can be divided into two phases. “Phase 1” is the association phase (*i.e.*, obtaining a code channel for communication) and “Phase 2” is the communication phase.

Phase 1:

1) At the beginning of the simulation the “code assignment table” of the code-broker is empty.
2) The node listens to the channel to sense any ongoing communication. After sensing for a certain period of time, if the node concludes that the

channel is empty it tries to associate itself with the code-broker. If the channel is sensed to be busy, the node backs off by a certain number of time slots, which increases linearly with time, and then follows the same algorithm again for a certain number of attempts. The mechanism which determines how a code-broker is chosen has not been simulated. In the simulation, a known node is the code-broker.

Note: There are three entities in this phase of the simulation

a) The Code-broker
b) The source node making an attempt to obtain a code
c) The interferers which are present due to imperfect channel sensing.

For each attempt to associate with the code-broker, the same number of interferers is chosen, although the location of the interferers changes. The number of interferers in phase 1 is always less than the number of interferers in phase 2. All the interference in this stage is primary interference since all of the nodes transmitting are using the same transmission code (*i.e.,* the control code). The interfering nodes first listen to the channel to sense if it is empty. If the channel is sensed to be empty, the interferer node goes ahead with the transmission; else, it defers its transmission to some later time. When the later time arrives, the node repeats the algorithm stated. The back-off counter increases linearly with time in the simulation. Sensing is performed by trying to acquire the signal of the transmission. Since the code used for transmission is known and the preamble sequence is known, this operation is similar to that performed by a receiver to acquire the transmitted signal. If a node is able to acquire the signal, it declares the channel busy else it declares it empty.

3) Once the node is successfully able to communicate with the code-broker (i.e. it receives a positive ACK along with the code assignment), it moves on to Phase 2. As mentioned above, the assignment of the code from the code-broker to the node is performed ideally. The code-broker at the same time updates its table with the newly assigned codes marked as USED.

For Phase 1 of the simulation, the hidden nodes in the simulation cause the primary interference observed in the simulations. Since the simulation is based on E_b/N_o, depending on the distance between the interferer and the receiver, the received E_b/N_o differs. If the received E_b/N_o is smaller than a particular value the signal is assumed to be weak and the node is assumed to be hidden. Another way to simulate hidden nodes would be for each interferer to acquire the transmitted signal. If the interferer is unable to acquire the signal, it is assumed to be hidden. This methodology of simulation would lead to huge simulation run times and has been avoided. The prior method has been used to simulate hidden nodes in this work.

Phase 2:

1) In phase 2 of the algorithm, the actual communication between the associated node and the destination node takes place. It is assumed that the destination node has been informed by the code-broker to switch to the code assigned by the code-broker to the associated node. Once the node enters phase 2, it starts communicating with the destination node using the assigned code.
2) Both nodes communicate with each other for a specified number of packets before deactivating the communication link. The packets are transmitted back to back. No traffic model has been assumed in the simulations. During each packet transmission the same numbers of interferers are present for a particular scenario but the location of the interferers is different for each frame.

   In this simulation there are 3 entities

   a) The source node communicating with the destination node
   b) The destination node and
   c) The interferers which are present due to simultaneous communication of other pairs of nodes using different codes. This interference is termed secondary interference as all the nodes are using different codes for communication.

Note: In the proposed scenario, adjacent piconets are assigned different codes and hence there is no primary interference. Please note that there is a possibility (although small) that two adjacent piconets might end up using the same code set. In this case there would be primary interference present in the communication phase.

In the simulation, adjacent piconets having the same code set have not been simulated and the only effects of a single piconet have been considered. Exposed nodes in this scenario do not contribute to any degradation in performance in this scheme[2]. The source node (or the node requesting to associate to the network) and the destination node remain at the same location in a particular scenario.

Both Phase 1 and Phase 2 of the simulation run for a certain number of scenarios to stochastically integrate over the distribution of user positions. The simulation does not take into account retransmissions due to incorrect frames being received. Details on the number of scenarios and the rest of the parameters (*e.g.*, area over which simulations are carried out, etc.) are described in Chapter 4.

3.3.2 CSMA based MAC

In addition to the CDMA based MAC, a CSMA based MAC has also been simulated. The CSMA based MAC is comparatively simpler to implement as compared to the CDMA based MAC. In the CSMA based MAC scheme, each bit of the user is spread by a spreading code whose length is equal to the length of the

[2] The concept of exposed/hidden nodes only comes in consideration when nodes using the same "channel" transmit at the same time and hence cause interference. The term "channel" can be either related to time based channels, frequency based channels or code base channels. In the CDMA simulation all users in Phase 2 are assumed to be communicating using different codes and thus are not on the same "channel." Hence we do not have the hidden/exposed node problem if a single piconet is considered by itself or if neighboring piconets have different code sets.

spreading code used for the CDMA simulations. This has been done to do a fair comparison between the two schemes. As mentioned in Chapter 2, spreading in UWB networks might be unavoidable due to the low power spectral density specified by the FCC. Details of the algorithm simulated are given below.

1) A node listens to the channel to sense if it is busy or not.
2) If the channel is sensed to be busy, the node backs off its transmission counter which increases linearly with time. Once the back-off counter expires, the node again listens to the channel to sense if it is busy or not and the same algorithm repeats.
3) If the channel is sensed to be free, the node goes ahead with its transmission to the destination node.
4) The source node communicates with the destination node for a specified number of packets. The position of the interferers changes with each transmitted frame, whereas the transmitter (source node) and the receiver (destination node) are assumed to be in the same position.

The above algorithm is simulated for a certain number of scenarios. The simulation does not take into account retransmissions due to incorrect frames being received.

Note: All the other nodes in the system also follow the same algorithm of "channel sense and back-off." Due to imperfect channel sensing, the hidden node problem in CSMA networks is still a major problem and cannot be avoided. Any transmission due to imperfect channel sensing leads to the adjacent nodes transmitting using the same code as the node under consideration. This interference is primary interference because all the codes are transmitting using the same code and leads to catastrophic results.

3.3.3 Receiver code assignment based CDMA MAC

For the receiver code assignment based simulations, a transmitter who wants to communicate with a receiver listens on the receiver's code for an ongoing transmission. If it detects an ongoing transmission, it backs-off its counter and again listens to the channel before making an attempt to communicate with the respective receiver.

Once the transmitter detects an empty channel on the receiver's code, it proceeds with its communication with the receiver. In this phase, two or more transmitters could sense the channel as idle at the same time and transmit simultaneously on the same receiver code resulting in primary interference. Moreover, an ongoing communication could be disrupted due to imperfect channel sensing of an adjacent transmitter that wants to communicate with the same receiver, causing drastic interference (primary interference). This phase of the simulation is described below.

Communication Phase:

In this phase of the algorithm, the actual communication between the associated node and the destination node takes place. Both nodes communicate with each other for a specified number of packets before deactivating the communication link. During each packet transmission the same numbers of interferers are present for a particular scenario but the location of the interferers is different for each frame. The interference in this scenario is primary interference and is due to imperfect channel sensing by the adjacent transmitters that want to communicate with the same receiver. Secondary interference is also present in this phase, due to simultaneous communication links in the network.

Note: In this simulation also there are 3 entities

a) The source node (intended transmitter)
b) The destination node (intended receiver) and
c) The interferers (near-by transmitters that want to communicate with same the destination node). This interference is termed

primary interference as all the nodes are using the same receiver code for communication.

Adjacent piconets having the same code set have not been simulated and only the effects of a single piconet have been considered. Exposed nodes in this scenario do not contribute to any degradation in performance. The source node (or the node requesting to associate to the network) and the destination node remain at the same location in a particular scenario.

The whole algorithm has been simulated for a certain number of scenarios to statistically sample the distribution of users. The simulation does not take into account retransmissions due to incorrect frames being received. Details on the number of scenarios and the rest of the parameters (*e.g.* area over which simulations are carried out etc.) are described in Chapter 4.

3.4 Physical (PHY) Layer Model

The block diagram of the UWB based PHY layer model is shown in Figure 3.9 below.

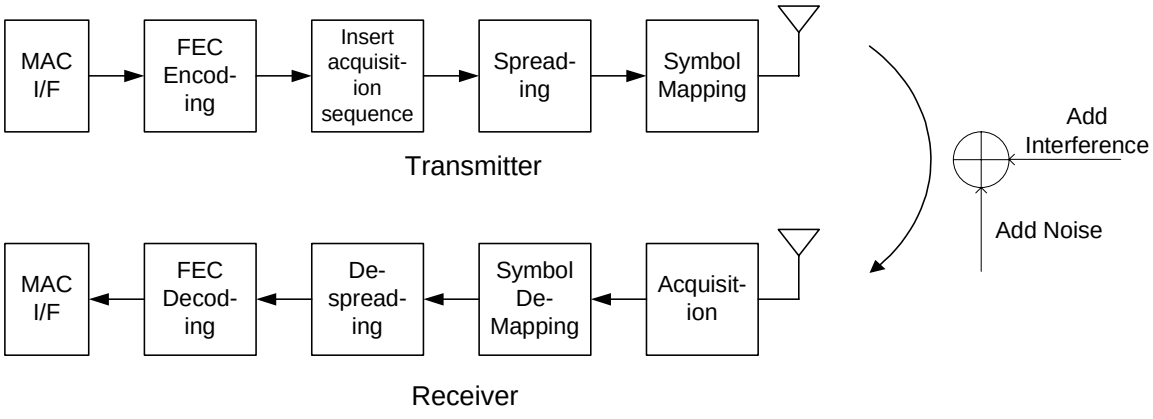

Figure 3.9 Block Diagram of the UWB PHY layer

The frame format used in the simulations is shown in Figure 3.10 below.

Figure 3.10 Frame Structure of packets used in simulations

Each node has a unique ID. The Source ID is the ID of node transmitting the packet. The destination ID is the ID of the destination node with which the source wants to communicate. The payload is the data being sent from the source node to the destination node. Details regarding each of the fields are described in detail in Chapter 4.

The various blocks are described below.

3.4.1 MAC I/F (Interface)

This block requests a clear channel assessment (CCA) from the PHY block and depending on whether the channel is busy or not is sends data to the PHY layer to be transmitted. The MAC layer also keeps track of the code to be used in a particular transmission. The MAC is the owner of the "code assignment table" used in the code-broker node. All the intelligence lies in the MAC block at the transmitter and the receiver. CCA is normally done by making an attempt to acquire a signal in a particular channel for a certain amount of time. If the signal is acquired, the channel is deemed busy.

3.4.2 FEC Encoding/Decoding

All PRNs employ some sort of encoding/decoding mechanism to recover data reliably which has been corrupted by the communications channel. Convolutional codes have emerged as perhaps the most widely used class of codes because of the huge gain in performance they provide with a slight increase in complexity (*e.g.*, 802.11a). Block codes are easier to implement but provide less error

correction capability. Turbo codes can provide large gains (depending on the packet size) but are substantially more complex to implement. Convolutional codes provide the most practical trade-off between performance and complexity and are thus our choice for simulation.

A 1/3 rate, constraint length 7 convolutional encoder was used. The encoder used was specified by 3 generator polynomials $\{133_8, 145_8, 175_8\}$[3]. For every input bit, 3 output bits are produced which are transmitted in the order X, Y, Z as shown in Figure 3.11 below.

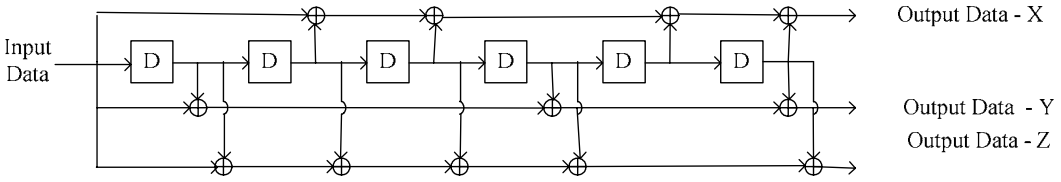

Figure 3.11 Structure for convolutional encoder

Soft decision decoding was implemented using the Viterbi decoder [50]. A trace back depth of 50 was used in the simulations. For a K = 7 convolutional encoder, although the recommended trace back depth is 5K = 35, a slightly larger trace back depth has been used. Some simulations were run using a trace back depth of 35 and negligible difference was observed between the two simulation runs.

3.4.3 Spreader/De-spreader

Various kinds of spreading codes are available in the literature (e.g. Walsh-Hadamard codes, Gold codes, etc.). Codes such as Walsh-Hadamard codes have very good cross-correlation properties when the codes are in-phase (*i.e.* aligned perfectly with respect to each other). When the codes are not aligned, the cross-

[3] The octal number represented when converted to binary consists of 1s and 0s. The 1s in the binary notation represents the bit positions where the shift register needs to be tapped for each output. For example, 133_8 in binary format is $[1011011]_2$. So for output number X (See Figure 3.11 below), the shift register is tapped at 1st, 3rd, 4th, 6th and 7th location starting from the left. Similarly 145_8 corresponds to Output Y and 175_8 corresponds to output Z.

correlation and auto-correlation properties of the codes are not very good. Gold codes on the other hand have good auto-correlation and cross-correlation properties even if the codes are not perfectly aligned. Alignment of codes requires centralized timing between all the nodes, which is generally not feasible in PRNs. Hence Walsh-Hadamard codes are not a very good choice in this system. In the simulation, Gold codes of length 31 have been used. A complete table of the codes used in this work is shown in Appendix A. Please note that in the table a value of "0" is representative of "-1."

In the simulation, Code 0 is always used to communicate with the code-broker. If the communication is successful, the PNC assigns a particular code to the requesting node based of the availability of codes with the code-broker.

In literature, impulse radio based UWB is normally simulated using time hopping codes instead of using direct sequence spreading as used in our simulation. For comparison of a CSMA based MAC with a Spread Spectrum based MAC, the choice of the spreading does not have a strong impact as both would have similar interference characteristics. For a simulation based on time hopping codes the length of the frame over the air would be longer as compared to the length of the frame using a direct sequence spreading mechanism. This increases the simulation time and provides no benefit in terms of system performance. In order to keep the simulation time reasonable, direct sequence spreading was used in the simulations.

3.4.4 Modulation/Demodulation

A bi-phase (*i.e.,* polarity) modulated full duty cycle UWB pulse has been used for simulations. A 0 is represented by an inverted pulse and a 1 is represented by the pulse shown in Figure 3.12. The sampled version of the pulse and its spectrum are also shown in Figure 3.13. Note that the pulse has been over-sampled by a factor of 4.

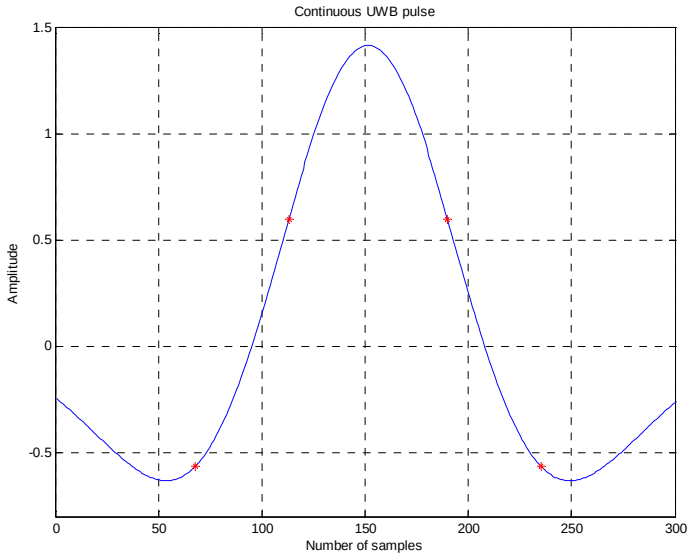

Figure 3.12 Continuous version of the pulse used in the simulations

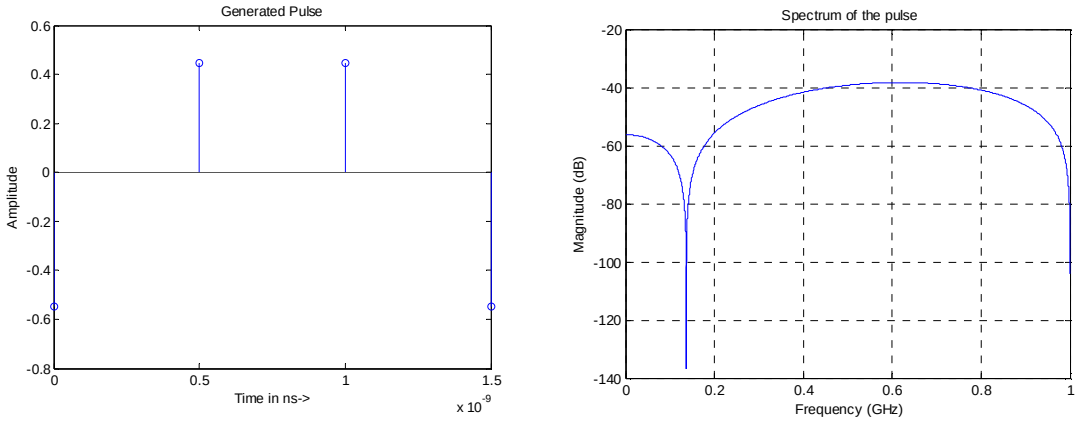

Figure 3.13 UWB Pulse simulated and its spectrum

3.4.5 Gaussian Noise and Energy of the Pulse

In the simulation, the standard deviation of the noise is kept constant and signal energy is scaled in order to achieve a particular E_b/N_o. The noise variance is set to 1 per signal component since the signal is real. The energy of the transmitted signal is calculated as

$$E = \frac{2(E_b/N_o)\,r}{M\sum_{t=1}^{N}|A_t|^2}$$

where r is the coding rate

M is the spreading code length

$\sum_{t=1}^{N} A_t^2$ is the energy of the pulse. (N is the number of samples in a particular pulse.)

The amplitude of each sample is multiplied by $\sqrt{E}$.

Note: The amplitudes of the spreading code need not be scaled by 1/sqrt(M) as the amplitude is taken into account in the energy of the signal.

3.4.6 Path loss

In order to account for path loss in the simulation, the E_b/N_o value at which each bit is transmitted is scaled by the distance between the transmitter and the receiver. The distance between the transmitter and the receiver is known and the E_b/N_o (received) is set to be proportional to 1/distance^2 for a path loss exponent of 2 and to 1/distance for a path loss exponent of 1 (*i.e.,* if the transmitter is close to the receiver, the E_b/N_o would be higher). This is done for each of the interferers also and their E_b would be set accordingly. The minimum distance between the transmitter and the receiver would be 1 m, which would correspond to the maximum possible E_b/N_o. A maximum distance is also defined, which corresponds to the minimum E_b/N_o. The energy at which the bit is transmitted is determined by formula shown in equation(s) below.

For a path loss exponent of 2

$$\text{EbNo\_dB} = \text{EbNo\_max\_dB} - 20*\log10(\text{dist})$$

Equation 3.1 Equation to calculate the energy of the transmitted bit (Path loss exponent = 2)

For a path loss exponent of 1

$$EbNo\_dB = EbNo\_max\_dB - 10*\log10(dist)$$

Equation 3.2 Equation to calculate the energy of the transmitted bit (Path loss exponent = 1)

where EbNo_*dB* is the transmitted energy per bit (in dB scale),

*EbNo_max_dB i*s the maximum possible *energy* in a network (obtained at minimum distance) and

dist is the distance between the transmitter and the receiver

The specific values used in the simulation are discussed in Chapter 4. Also the simulation results are presented and discussed in Chapter 4.

Chapter 4

4 MAC Simulations and Results

4.1 Introduction

In the previous chapter an overview description of the various Multiple Access Control schemes simulated was provided. This chapter of the thesis gives a detailed explanation of the various parameters used in the MAC layer simulations for the different scenarios examined (*i.e.*, CDMA based MAC using a code broker, CSMA based MAC and a CDMA based MAC with Receiver code assignment) and discusses the simulation results in detail. The advantages and disadvantages of the schemes have been compared on the basis of

1) Throughput vs. Latency
2) Throughput vs. Network Load
3) Latency vs. Network Load
4) Packet Error Rate vs. Network Load.

4.2 Simulation Parameters

The piconet simulated is assumed to be distributed over a geographical area of 10m x 10m. The code-broker (represented by a black star in Figure 4.1 below) is assumed to be in the center of the piconet. Figure 4.1 shows multiple example simulation scenarios in which the transmitter (Tx, Red star) and receiver (Rx, Green star) have different positions in each scenario. The blue stars in the figure represent the positions of the various interferers in the network.

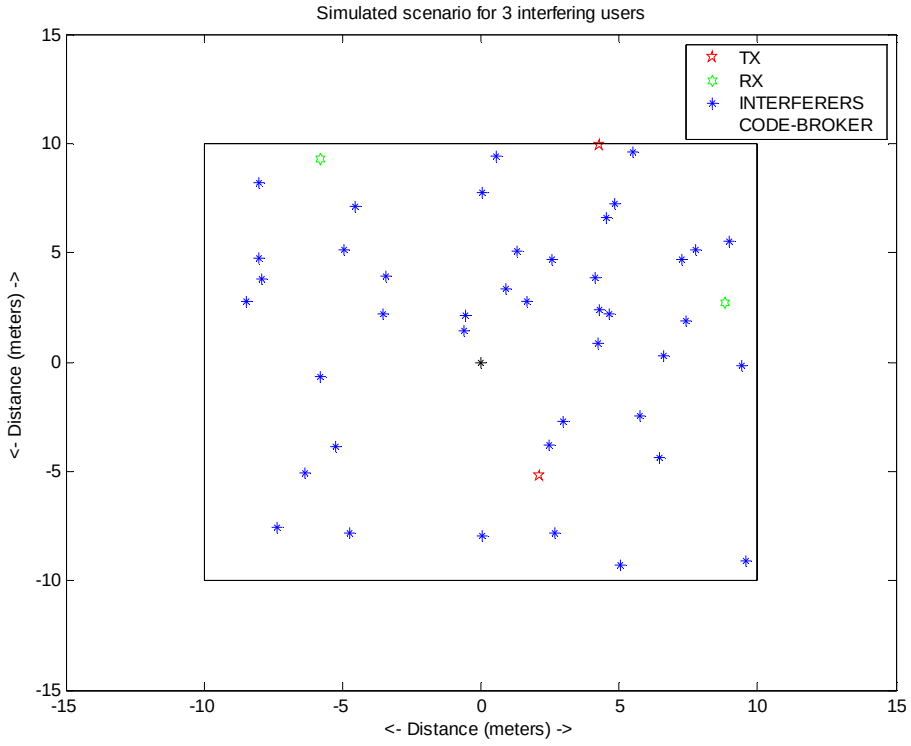

Figure 4.1 Example simulation scenario

The acquisition sequence used for the simulation is {1 -1 1 -1 1 -1 1 -1 1 -1}. Each bit is spread by a length 31 Gold code [50]. The Gold code used is the same as the code assigned to the node for communication. This code is used for the CDMA based code broker scheme, CSMA-based scheme and the Receiver based code assignment scheme. For the CSMA-based scheme, the acquisition sequence is used for doing CCA (Clear Channel Assessment). For the CDMA based code broker scheme, the acquisition sequence is used for determining if the node has been able to successfully establish a connection with the code-broker. It is also used for sensing the channel for an ongoing communication between the code-broker and any other node before making an attempt to communicate with the code-broker. For the Receiver based code assignment scheme the acquisition sequence is used to sense the channel for any ongoing communication at the intended receiver's code. This sequence is also used for determining successful reception of the packet at the destination node for all the above stated schemes.

For a particular scenario (explained below), the transmitters and the receivers are assumed to be stationary. A scenario consists of a number of points (*i.e.*, positions) simulated for every attempt of transmitter/receiver communication. In a particular scenario, a transmitter initially communicates with the code-broker using a fixed gold code (*e.g.*, Code 0). The transmitter makes a certain number of attempts to communicate with the code-broker. If it is unable to communicate with the code-broker, the simulation moves to the next scenario in which the transmitter and the receiver have a different location on the grid. The process continues for a fixed number of scenarios. If in the specified number of attempts, the transmitter is able to communicate with the code-broker, the code-broker gives a different code to the transmitter, as explained in the previous chapter, simultaneously informs the receiver of the code it should use to receive data. The communication between the code-broker and transmitter and code-broker and receiver is assumed to be perfect. In the simulation this is accomplished by enabling appropriate flags. This marks the end of Phase 1 of the simulation as explained in the previous chapter. Once the transmitter/receiver pair knows the code to be used, they communicate for a number of frames (Phase 2 of the algorithm). Each frame is a 512 byte frame (before encoding). The interferers are always transmitting data on a specified code which could be either the same code as the intended transmitters/receiver or could be different depending upon the scenario being simulated. For the CSMA-based scenario all the interferers are transmitting using the same code. It should be noted that in this scenario all the interfering nodes are not always transmitting. They only transmit if they are hidden from the ongoing communication in the piconet. The methodology for determining whether a node is hidden is as explained in the previous sections. Also, all the interference in this case is primary interference as the code for transmission is always the same. In the CDMA-based code-broker approach during Phase 1 of the communication, the interference is primary as all the nodes are using the same code to communicate with the code-broker. During Phase 2, all the interference in this scheme is secondary interference as the interferers are

essentially transmitters using different codes. In this scheme, all the interferers are always transmitting data on different codes. In the Receiver based code assignment scheme, both primary and secondary interference is present in the system. Primary interference occurs if a node is hidden and tries to communicate with a receiver which is already communicating with another transmitter. Secondary interference is also present in the piconet as there are multiple active communication links in the system which are using different codes for communication. Note that in Figure 4.1 .the interferers presented are actually only three interferers but represent multiple positions.

A simulation run is defined as an environment with a particular number of users trying to communicate over a fixed geographical location. The position of the interferers and the intended transmitter/receiver changes in each scenario simulated in a particular simulation run. Multiple scenarios are simulated in each simulation run. In each simulation run, for the CDMA-based code-broker approach, 100 scenarios have been simulated and in each scenario an associating transmitter makes 5 attempts to communicate with the code-broker in Phase 1. If it is unable to establish contact (due to imperfect sensing), it moves on to the next scenario where the same steps are repeated. Once the associating node obtains a code from the code-broker, it communicates with the destination node for 50 frames. Each frame consists of 512 bytes of payload. As explained in Chapter 3, each node transmits with a specified E_b/N_o in the simulation. The maximum possible E_b/N_o has been set to 15 dB (for path loss exponent of 1) and 25 dB (for path loss exponent of 2). This would happen when the transmitter and the receiver are very close to each other (defined as a minimum of 1m in the simulations). The minimum possible E_b/N_o has been set to 5 dB. This happens when the transmitter and receiver are at opposite corners on the square area considered. The actual E_b/N_o used for transmission is calculated using the equation presented in Equation 3.1 in Chapter 3. For the distance between each interferer and the intended receiver, the received E_b/N_o at the receiver due to the respective interferer is calculated using that equation which determines the amount of interference

caused by other users in the system Interfering users could either cause primary interference or secondary interference. Primary interference occurs primarily due to hidden nodes in the system whereas secondary interference occurs due to the presence of other users communicating on a different code. For the CSMA based approach also each node makes 5 attempts to listen to the channel. If it finds an empty channel, it communicates with the intended receiver else the simulation moves to another scenario. One hundred scenarios are considered in each simulation run. The rest of the parameters for the CSMA-based scheme are similar to the CDMA-based code-broker scheme. A similar approach is used for the Receiver-based code assignment scheme simulations.

The basic unit for communication in the simulation is a mini-slot as it is a common granularity in the existing literature. In the simulation, a mini-slot is defined to be equal to a frame length. Acquisition of the frame, as well as decoding, is performed in the same mini-slot. All users are assumed to have an infinite amount of data to send (*i.e.*, all users always have data to send to their intended receiver.) No traffic flow model has been considered in the simulations.

Note: In the simulation, Code 0 is always used to communicate with the code-broker. If the communication is successful, the code-broker assigns a particular code to that particular node. This scheme is very effective if all the nodes want to have peer-peer communication. The work of the code-broker is just to allocate codes to different users and it should never be involved in continuous communication with a node in the network. In sensor network applications since there is a great redundancy in the nodes, making one of the nodes the code-broker would incur minimal overhead. Note that in this scheme nodes could also take turns to be a code-broker.

Hidden nodes are also simulated in the CSMA based scheme as well as the Receiver code assignment based scheme. The methodology for classification of hidden nodes is explained in Appendix B.

4.3 Calculation of basic system parameters

4.3.1 Single User Throughput Calculation

Frame length = 512 bytes

*Total number of pulses (after encoding and spreading) = Bits/Byte * PAYLOAD LENGTH * 1/R * S + ACQ LENGTH*S*

where

Bits/Byte = 8,

PAYLOAD LENGTH = Total Number of Bytes in the payload,

R = Encoding Rate (*i.e.*, 1/3),

S = Length of Spreading Code and

ACQ LENGTH = Acquisition sequence length

Thus,

Total number of pulses (after encoding and spreading) = 8*512*3*31 + 10*31.

Note: The second term is due to the acquisition sequence which is of length 10 and is spread by a 31 length spreading code.

Pulse time = 2 nsec.

Total frame length = 0.7625 msec.

If all bits are received correctly then the maximum possible throughput is 8*512/Total frame length = 5.372 Mbps.

Note: The throughput has been calculated based on the total number of correct frames received*number of bits/frame.

4.3.2 Maximum Throughput Calculation

*Maximum throughput = Max. Throughput per user * number of users*.

As calculated above, the maximum throughput per user is 5.372 Mbps. For various numbers of users the throughput could be calculated using the formula above.

4.3.3 Network Load Calculation

Packets/sec. = 1/Total frame length (Shown in Section 4.3.1 above).

Network load = Numbers of users * Packets/sec.

4.3.4 Latency Calculation

Whenever an associating node is not able to successfully communicate with the code-broker it increments its latency counter. Each time the latency increases it indicates that the latency to join the network has increased by the total frame length (a mini-slot) times the number of mini-slots the node has backed off. When the back-off counter expires, the associating node again tries to establish connection with the code-broker.

For the CSMA-based scheme, the latency in the simulation is due to the fact that each node listens to the channel for an ongoing communication before transmitting its own data. Note that the factors amounting to the latency for this system are different as compared to the CDMA-based code-broker scheme. In the later scheme, the latency is due to obtaining a code from the code-broker whereas for the CSMA-based scheme, it is due to the fact that a node needs to listen for any on-going communication in the entire piconet before attempting its own transmission. Also the node backs-off its transmission upon hearing any other ongoing communication. For the Receiver-based code assignment scheme, the latency is again due to the fact that a node needs to listen for any on-going communication on the intended receivers' code prior to attempting its own transmission. Also, the node backs-off if it hears any transmission on the intended receivers' code.

In the simulations, the latency is stored for each particular scenario (i.e. each transmitter - receiver separation) and the final latency is calculated by averaging the latency calculated for each scenario over all the scenarios. One hundred scenarios have been considered, which is representative of all the transmitter

receiver distances and hence would give a good measure of the latency required in joining the network for a particular number of users in the system.

4.4 Simulation Results

4.4.1 Comparison - Perfect CSMA based scheme vs. proposed CDMA based code-broker approach

In the sections below we initially discuss the results of each of the schemes before making a comparison between the schemes.

4.4.1.1 CDMA-based Code Broker MAC

The results of the CDMA based code-broker approach are discussed below. Figure 4.2 plots the resulting throughput vs. latency to join the network for a path loss exponent of 1 and 2. Two different path loss exponents were simulated in the system for all the cases as some of the indoor measurement results in the literature report path loss exponent values lower than 2 for UWB signals [58]. As the number of interferers increases the throughput of a particular user is reduced. This is expected as the interference increases with an increase in the number of nodes in a piconet. Also as the latency in the system increases due to an increase in the network load, the throughput of the user deteriorates. The increase in the latency is due to the fact that a large number of users are making an attempt to get a code from the code-broker. Since the node needs to listen to the channel before making its own request to the code-broker, with a larger number of users, the probability of the channel being busy increases which in turn increases the latency. Also as more users are present in the system, the throughput of the user decreases, since it can access the code broker less frequently. For a path loss exponent (n) of 2 it is observed that the latency to join the network is lower as compared to a system with a path loss exponent of 1. This is attributed to the fact that when n = 2, the interference seen by the code-broker is lower as compared to when n = 1. Also it

is noticed that for the same throughput the latency to join the network is greater when n = 1.

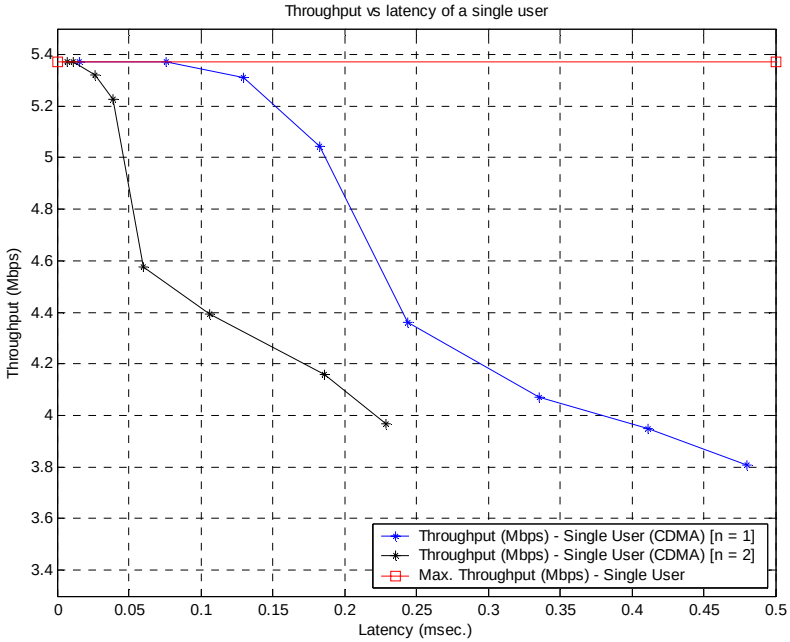

Figure 4.2 Throughput vs. Latency of a single user

Figure 4.3 shows the throughput vs. latency for the entire piconet under consideration. The curves for both n = 1 and n = 2 have been plotted below. It should be noted that the number of users in a system directly affects the network throughput as well as the latency to join the piconet. As the number of interferers increases, the throughput of the whole system saturates, *i.e.*, the system starts to behave like an interference limited system. Although the throughput of a particular user is decreasing, the total system throughput remains nearly constant as the number of users communicating increases. Also as the number of interferers increase, the latency to join the network increases as explained in the paragraph above. The total system throughput is higher for a system in which n = 2 again attributed to lower interference in the system. Also the latency to join the network in such a scenario is lower. The latency is also lower due to the fact that there are less number of hidden nodes in the system when n = 2. This is due to the fact that the total E_b/N_o range of the network varies from 5 – 25 dB and any signal

whose received E_b/N_o is below 8 dB is deemed hidden. For the n = 1 case, the E_b/N_o range of the network is from 5 – 15 dB. It should be noted that the latency axis in both Figure 4.2 and Figure 4.3 is the same i.e., the same number of interferers simulated for both the cases is the same. Thus, we see that with an increase in the latency to join the network, the total system throughput increases but after a certain amount of latency, the system throughput starts to saturate and the net gain of adding more users to a particular piconet reduces. This could be used to calculate the optimal number of users which should be present in a particular piconet in order to get maximum benefits in terms of maximum throughput capacity of the system and minimum latency in joining the network.

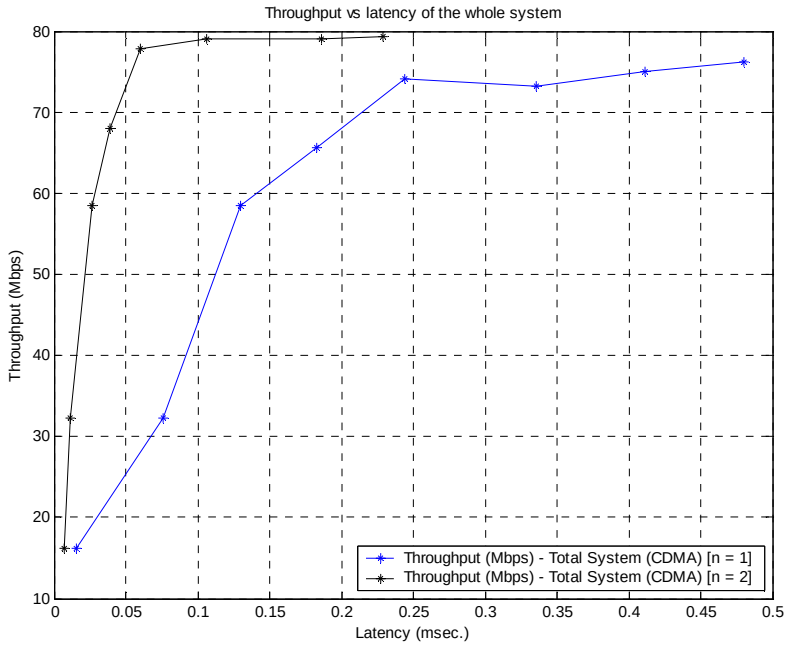

Figure 4.3 Throughput vs. Latency of the whole system

The simulated total throughput has been plotted versus network load in packets per second along with the maximum possible throughput in the system in Figure 4.4. The network load calculation in shown in Section 4.3.3 above. It is seen that for higher network load the system throughput saturates. This is due to the fact that as the network's load increases, the amount of interference in the system increases leading to more packet errors in each communication link. But since

there are more users in the system, there are more active communication links at a higher network load as compared to a lower network load which offsets the increase in packet error per user. If the whole piconet is considered, even though the throughput of each link reduces, the total system throughput continuous to increase until it reaches a saturation point. This is true for both n = 1 and 2. For n = 2, the total system throughput is higher as compared to a system in which n = 1.

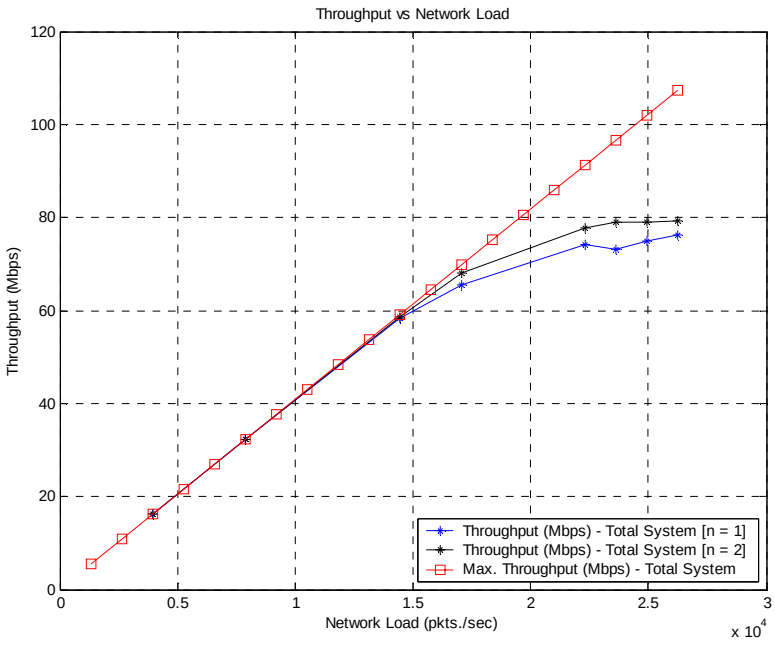

Figure 4.4 Throughput vs. Network Load of the whole system

The relationship between the network load and latency is not exactly one-one but it is close for low values of network load as seen in Figure 4.5. As the network load increases, the number of codes which are used also increases and the interference seen by a transmitter-receiver pair in general increases. Although the exact interference depends on the correlation properties of the codes for a given number of users, in general it will increase with the number of users. It is noticed that the latency increases non-linearly for high network loads. This is attributed to the fact that with a high number of users in the system, there are more users attempting to obtain a code from the code-broker. Since a node needs to listen to the channel before making an attempt to request a code from the code-broker, the

channel is busy for a large amount of time and the intended transmitter needs to back-off for a longer time which increases the latency to join the network. For n = 2, the latency to join the network is lower for the same network load. This is due to the presence of fewer hidden nodes in the system and greater attenuation of secondary interferers due to greater path loss and hence lower secondary interference is observed at the intended receiver.

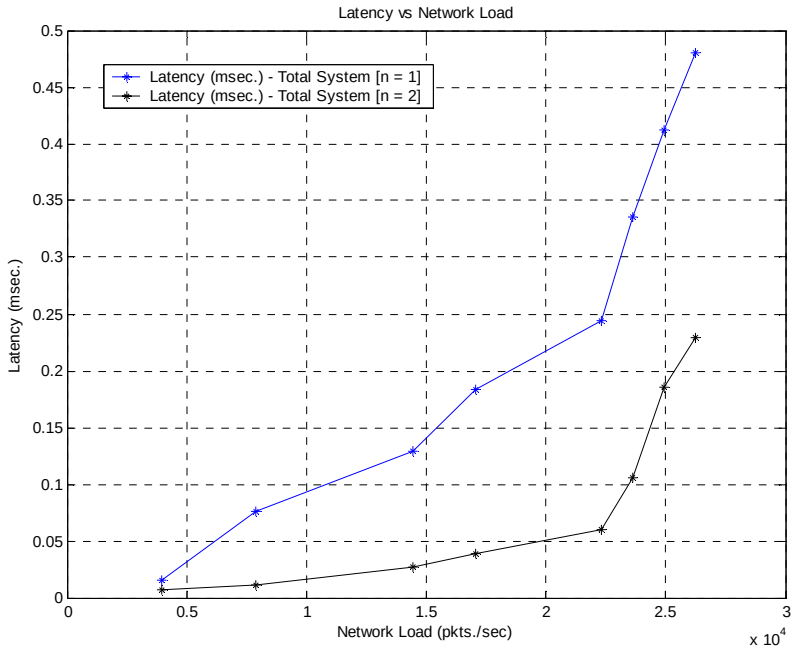

Figure 4.5 Latency vs. Network Load of the whole system

The packet error rate vs. the network load in the system is plotted in Figure 4.6 below. As the network load in the system increases, the number of simultaneous transmissions in a piconet increases. This leads to higher secondary interference and hence leads to an increase in the packet error rate in a transmission. The packet error rate initially increases drastically due to an increase in the number of communication links. The initial drastic increase is also due to the near-far problem in the system. It is possible that an interfering communication links' transmitter is closer to the intended receiver as compared to the intended transmitter leading to a high packet error rate. It is noticed that the packet error

rate starts to saturate for higher network loads. This is due to the fact that even at higher network loads, the cross-correlation properties between the different Gold codes are robust which limits the interference seen by a particular user. For n = 2, due to less amount of secondary interference the packet error rate of the system is lower as compared to n = 1.

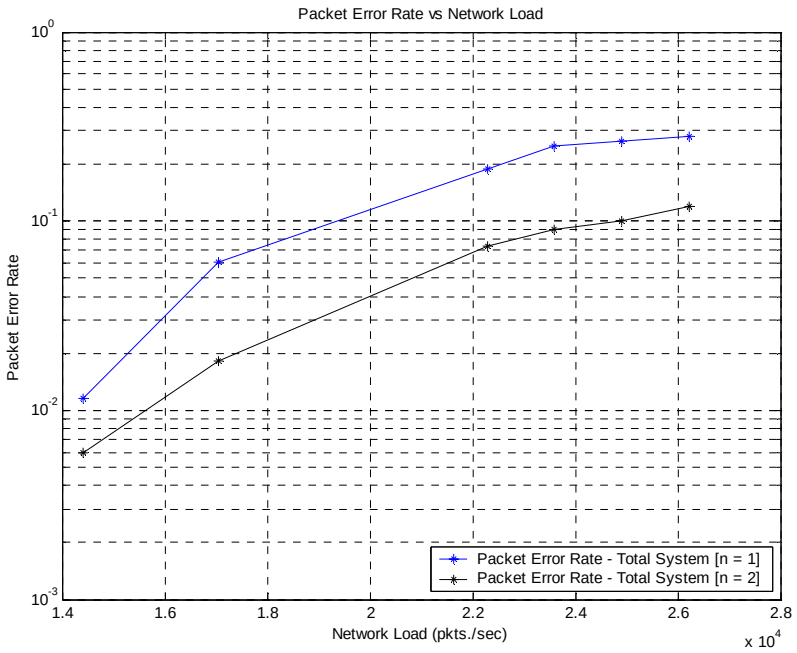

Figure 4.6 Packet Error Rate vs. Network Load of the whole system

4.4.1.2 CSMA-based MAC

In the CSMA-based MAC scheme, in this set of simulations, no hidden nodes have been simulated in the system. This means that once the channel is determined to be empty, the user starts its transmission and no other user in the channel communicates. The only element incorporated in the simulation is channel sensing in which each node wishing to communicate listens to the channel for any ongoing communication before transmitting to a particular user. Also note that no back-off mechanism has been simulated. This means that if the channel is not sensed to be empty, the node senses the channel at the next slot to again determine if the channel is busy or free. If the back-off mechanism is

incorporated in the system, this would lead to higher latency in starting a communication link. This scenario has also been simulated and the results are presented in the succeeding sections. The simulated results using this CSMA based scheme are discussed below.

Figure 4.7 plots throughput vs. latency for a single user using a CSMA-based MAC scheme for both n = 1 and n = 2. In this simulation, since hidden/exposed nodes have not been simulated in the communication phase, an increase in the number of interferers does not have any effect on the throughput. However, note that the latency increases tremendously. This is attributed to the fact that every time a user wants to communicate it needs to listen to the channel first to determine if it is empty. If the channel is busy, it must wait. Since there are many users trying to communicate at any point in time (at high loads), the probability of the node transmitting is very low and hence the latency is very high.

In the simulation, it is assumed that in the particular area under study, every node can hear every other node. So in a CSMA scheme because there is only one possible ongoing communication, the total system throughput would be the same as the single user throughput. Thus, Figure 4.7 below also represents the system throughput of the entire piconet. This is true for both when the system has a path loss exponent (n) of 1 and 2. A greater path loss decreases the latency in the system as explained above but has not impact on throughput as no primary interference is simulated in the system (due to hidden nodes).

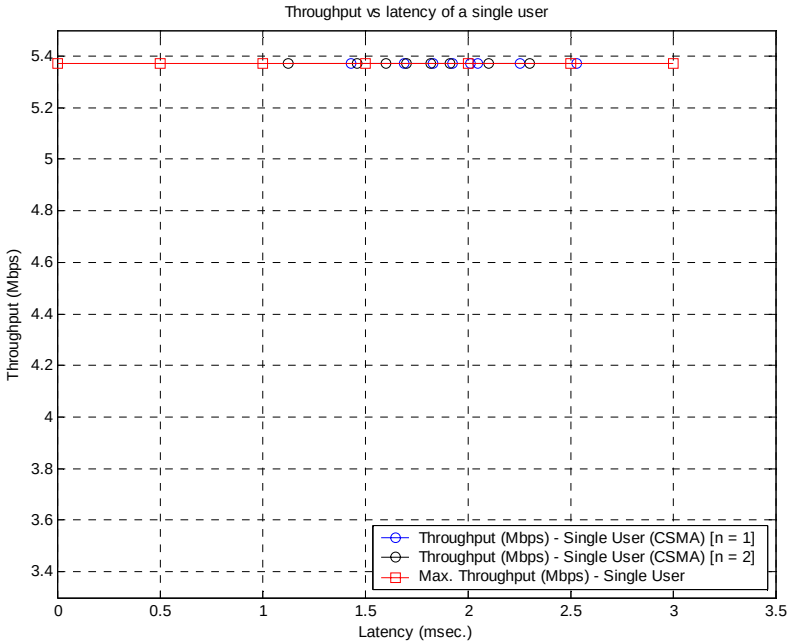

Figure 4.7 Throughput vs. Latency of a single user/whole system

The total throughput obtained from the actual simulation has been plotted along with the maximum possible throughput possible in Figure 4.8 (for both n = 1 and n = 2). All the users are assumed to be able to communicate when they want to. As the hidden/exposed nodes have not been simulated in this set of simulations, there is no primary interference in the system and hence the total system throughput is equal to the maximum throughput of a single user. This is due to the fact that only one user can transmit in the whole piconet at a particular time. A significant difference is noted between the actual system throughput and the maximum possible system throughput. It is also noted that the throughput remains constant with network load as no hidden/exposed nodes have been simulated in this part of the simulation.

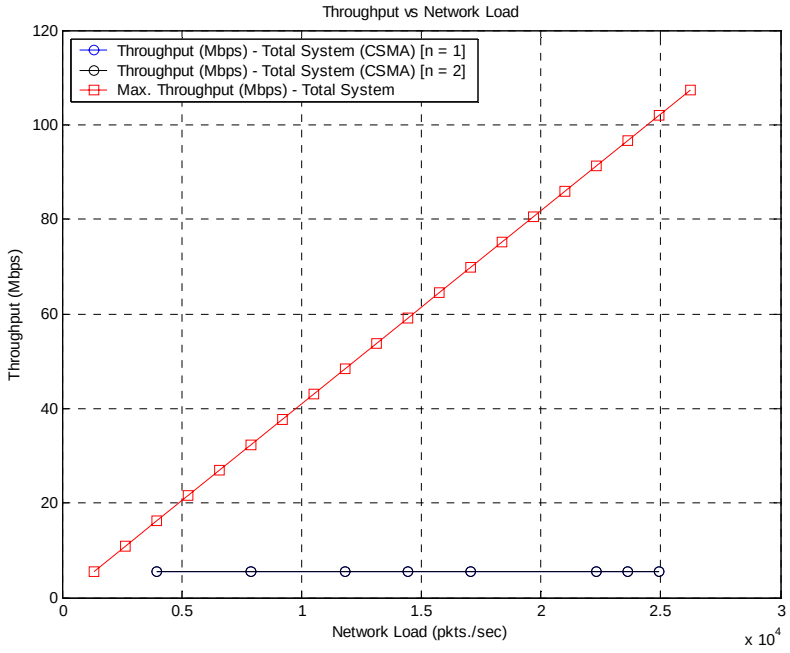

Figure 4.8 Throughput vs. Network Load of the whole system

The effect of the latency in the network with an increase in the network load has also been analyzed for a CSMA based system as has been done for the code-broker based approach. Figure 4.9 plots the resulting curve. For lower network loads the latency increases linearly. It is also noticed that as the network load becomes very high, the latency to join the network increases rapidly. This is due to the fact that a node is unable to find a clear channel for a long period of time when the load is high. For n = 2, again due to the presence of less number of hidden nodes, the latency to join the network is lower as compared to when n =1.

The packet error rate of the system vs. the network load has not been plotted. Since there are no hidden nodes in the system, there is no other node communicating while the intended transmitter/receiver pair is communicating with each other and hence there are no packet errors. The packer error rate in this system is 0%. Note that due to the incorporation of the hidden nodes, there would be primary interference which would leads to some packet error rate. This simulation has been considered in the next section.

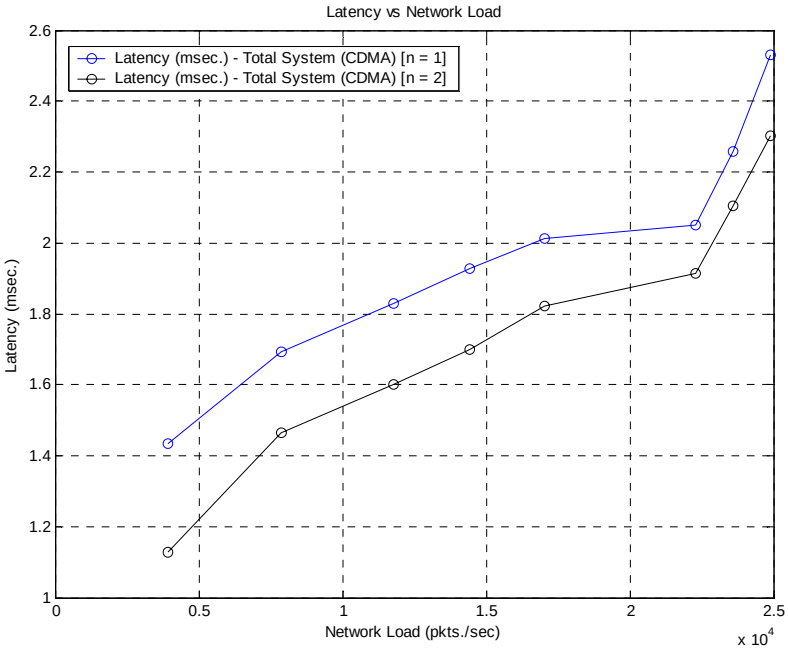

Figure 4.9 Latency vs. Network Load of the whole system

4.4.1.3 Comparison – Code-broker approach vs. Perfect CSMA approach

The results presented above are now compared with each other. Figure 4.10 presents the throughput vs. latency curve for both the CDMA-based code-broker scheme and the CSMA-based scheme. As can be seen, the throughput of a single user goes down quickly in the CDMA-based code-broker scheme due to secondary interference in the piconet. This is true for both n = 1 and n = 2. For the CSMA based scheme, the throughput remains the same as hidden nodes have not been simulated.

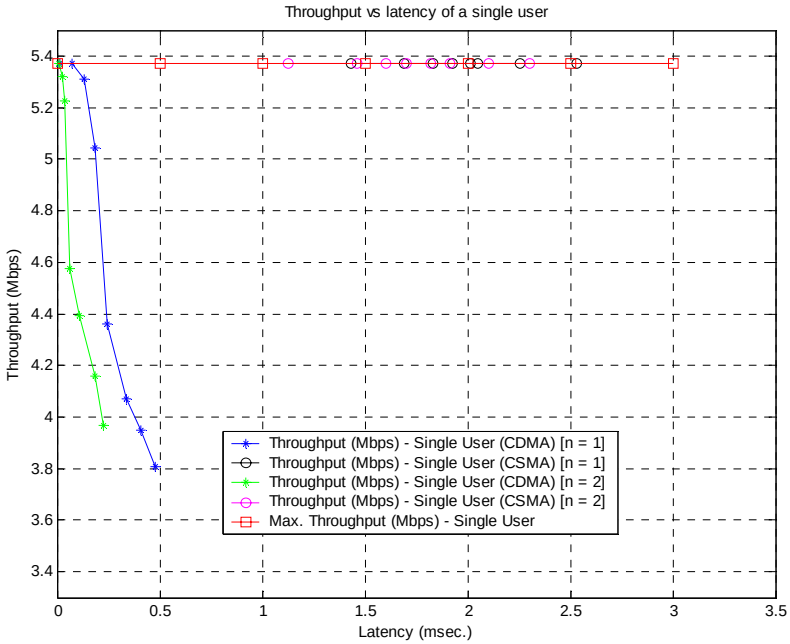

Figure 4.10 Throughput vs. Latency of a single user

However, we notice that the total system throughput increases with an increase in the network load for the CDMA-based code-broker approach but not for the CSMA based MAC (Figure 4.11 below). This is due to the fact that in the CSMA-based system only one user can communicate at a particular time instant whereas in a CDMA-based code-broker approach multiple active communications links are possible which increases the total system throughput. Thus, even though the throughput of a single user in a CDMA-based code-broker decreases (due to secondary interference), the total system throughput is still very high. This makes the CDMA based code-broker MAC better than the CSMA based MAC in terms of throughput. It should also be noted that the latency of the CSMA based network is much greater as compared to the CDMA based network. This is due to the fact that over time there are less number of users in the CDMA based code-broker MAC which are requesting a channel to communicate with their respective receiver as compared to the CSMA based MAC scheme. Also in the CSMA based scheme, the user needs to listen to the channel every time it wants to communicate with its intended receiver whereas in the proposed MAC, once the

user has obtained a code, it can communicate until the whole communication is over. Furthermore, the CDMA based MAC scheme has even higher throughput as compared to the CSMA based scheme when n = 2.

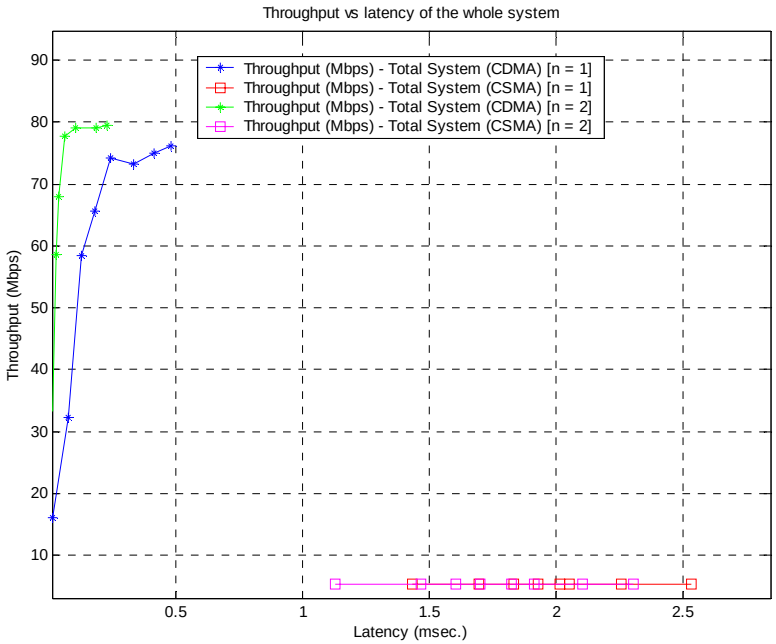

Figure 4.11 Throughput vs. Latency of the whole system

Figure 4.12 below shows the throughput vs. the network load. Here again it is noticed that for low-mediocre network loads, the CDMA-based code-broker scheme approaches the maximum possible system capacity whereas the CSMA-based scheme has very low system throughput (even in the absence of hidden nodes (*i.e.*, primary interference)). The situation would become worse for the CSMA-based scheme in the presence of such interference. For higher network loads, due to high level of secondary interference, the packet error rate increases slightly which is offset by the increase in the number of active communication links in the network and hence the system throughput starts to saturate. For n = 2, the system saturates at a higher level as compared to when n = 1.

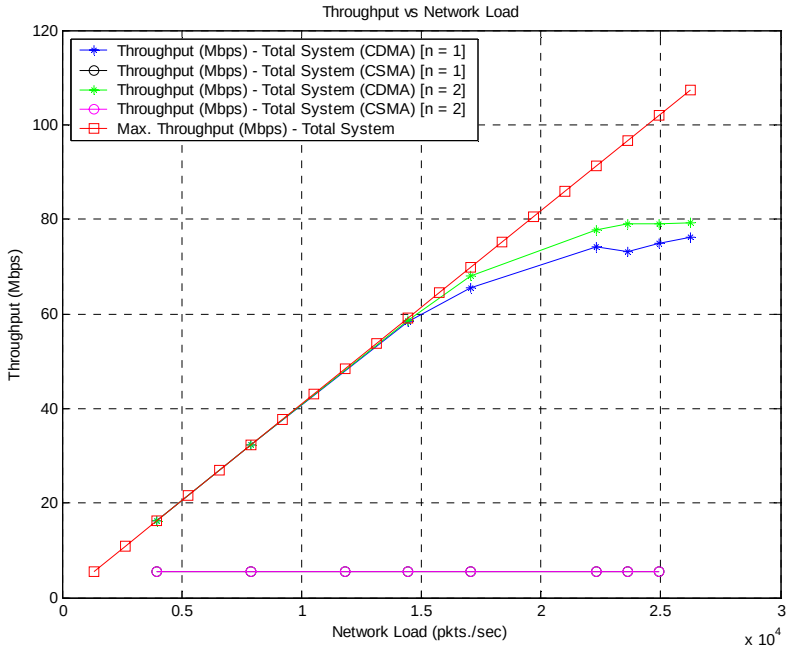

Figure 4.12 Throughput vs. Network Load of the whole system

The main reason for this advantage is that CSMA cannot take advantage of the fact that the information rate in UWB is much lower than the bandwidth. In a traditional system (i.e., with no spreading) CSMA could transmit at a higher rate than a CDMA-based scheme. However, since UWB will typically involve a minimum spreading factor (unless extremely high data rates are desired), a CDMA-based approach more efficiently uses the system bandwidth in terms of system throughput.

The latency to join the network and get a communication link started vs. the network load is plotted in Figure 4.13 below. The CSMA scheme incurs more latency to join the network as compared to the CDMA-based scheme due to the fact that in the CSMA based scheme all the users who want to communicate are listening to the channel and making an attempt to transmit data. In the CDMA based scheme the latency is due only to obtaining a code from the code-broker. There is no additional latency incurred from first listening to any on-going transmission in the whole network prior to starting communication with the

intended receiver. Also in the CSMA based scheme, the user needs to listen to the channel every time it wants to communicate with its intended receiver whereas in the proposed MAC, once the user has obtained a code, it can communicate until the whole communication is over. This is a source of latency for the CSMA-based scheme as well as the receiver code assignment based scheme. For both the proposed CDMA based scheme and the CSMA based scheme for n = 2, the latency to join the network is lower for the same network load. As explained above, for the CDMA based scheme as well as CSMA based scheme this is due to the fact that the number of hidden nodes in the system is smaller as compared to when n = 1.

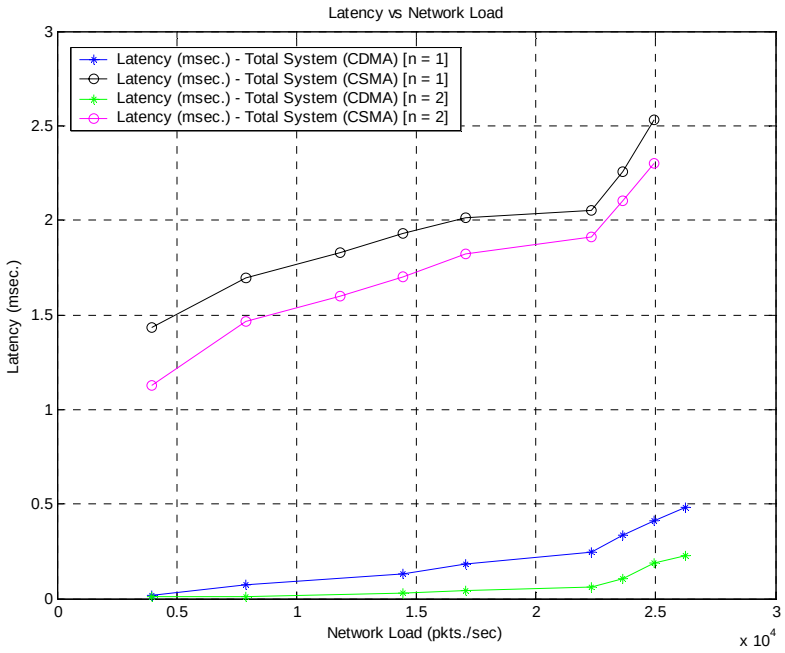

Figure 4.13 Latency vs. Network Load of the whole system

For the same network load, in the CSMA based scheme, all users listen to the channel and make an attempt to obtain it for their respective transmission whereas for the CDMA based scheme not all users are simultaneously making an attempt to request a code from the code-broker. This leads to reduced latency as compared to the CSMA based scheme.

The packet error rate (PER) vs. the network load for the CDMA-based code-broker scheme has not been plotted. For the CSMA-based scheme (as stated in previous discussion), for this set of simulations as no hidden nodes have been simulated, the packet error rate in the system is zero. Thus if a perfect CSMA-based scheme is compared with the CDMA-based scheme, the former scheme has better PER vs. network load characteristics. A comparison of the PER vs. the network load for a CSMA-based scheme incorporating hidden nodes has been performed in the next section.

4.4.2 Conclusions – Code-broker approach vs. perfect CSMA approach

As seen in the figures above, the CDMA-based code-broker approach outperforms the CSMA-based approach in terms of throughput as well as latency to join the network. In terms of throughput this is due to the fact that in the CSMA-based scheme, the code is spread by the Gold Code sequence. As explained in various sections above, due to the lower power spectral density of UWB devices, each bit must be transmitted multiple times in order to achieve the desired energy per bit. This leads to an effective reduction in data rate of each user by a factor equal to the spreading factor (approximately). In our case, this is an effective reduction of data rate by 31 times which leads to a much reduced throughput for the CSMA-based case firstly because the throughput of a each user is reduced by approximately 31 times and secondly because only one transmission is allowed in the entire piconet which limits the net system throughput. The CSMA-based scheme and the CDMA-based code-broker approach can be compared on two different grounds.

1) If a comparison is made between both the systems using a UWB spread spectrum system i.e. each pulse being spread by a length 31 Gold code, then as seen in the plots above, the proposed CDMA scheme outperforms the CSMA scheme completely.

2) Another way to do a comparison is to assume that ONLY the proposed system uses spread spectrum system and is spread by a length 31 code and the CSMA based scheme is not spread. In this case, for CSMA the net throughput of the user/system increases by approximately 31 times (~31*5.372 ~= 166 Mbps) and outperforms CDMA even if the number of simultaneous users in the system is more than 31 as the network throughput saturates at about 80 Mbps.

Thus, as we would expect, CSMA will outperform CDMA in a single cell scenario when spreading is not mandatory. But as discussed above, due to the FCC limit of the low spectral density of UWB devices, spreading is inevitable for even moderate distances making the proposed approach very attractive for UWB networks. Additionally, when multiple cell scenarios are considered, spreading is absolutely necessary to allow multiple piconet operation unless an FDMA approach is used for piconets. However, as cellular systems have shown, CDMA-based approaches are generally superior to FDMA or TDMA based approaches that require frequency reuse patterns.

4.4.3 Comparison - CSMA-based scheme (with Hidden nodes and Back-off) vs. proposed CDMA-based code-broker approach

The explanation of how hidden nodes are modeled in a system in given in Section 4.2 above.

4.4.3.1 Simulation Results

In this section the CSMA-based scheme is again compared with the CDMA-based code-broker approach. Now, however, in the CSMA-based scheme, hidden nodes have been also simulated. A linear increase-linear decrease back-off mechanism has also been incorporated in the simulations. The results are presented below.

Figure 4.14 presents a comparison between the two schemes. As expected, due to incorporation of hidden nodes in the system, the throughput of the CSMA based scheme decreases. Also due to the incorporation of a back-off mechanism the latency to start a communication link increases by a large amount. For the CDMA based code-broker approach, the reduction in throughput is due to the presence of secondary interferers in the system. For n = 2, the latency of the system in lower as explained in previous sections. This is true for both the CDMA based scheme and the CSMA based scheme. The maximum possible throughput of a single user has also been plotted.

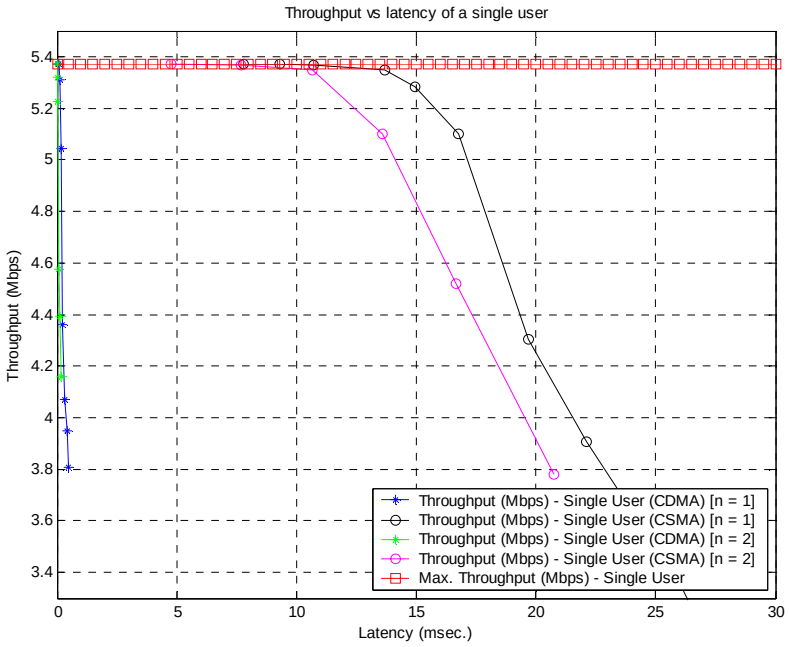

Figure 4.14 Throughput vs. Latency of a single user

The latency vs. throughput for the CDMA based scheme has been zoomed and shown in Figure 4.15 below. Again, it is observed that the latency for a system with n = 2 is lower than a system with n = 1.

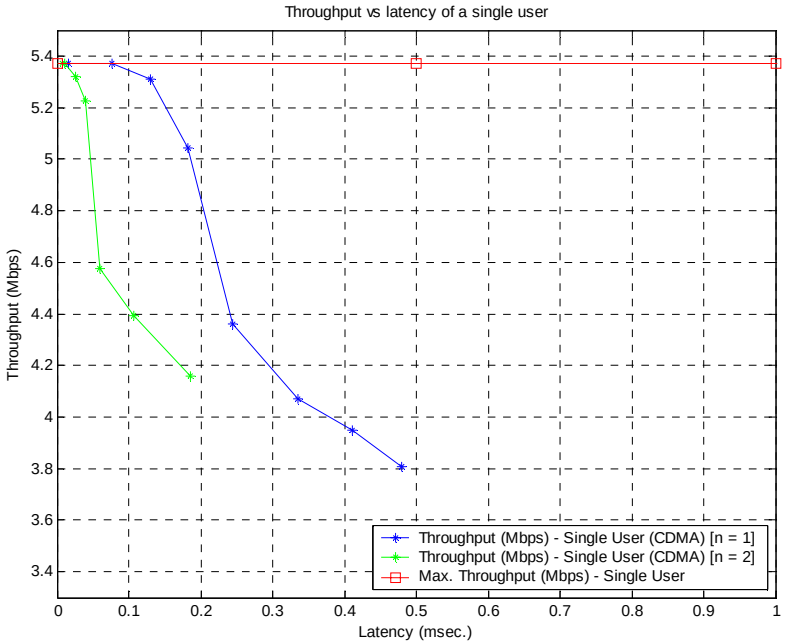

Figure 4.15 Throughput vs. Latency of a single user (CDMA based scheme – Zoomed)

Figure 4.16 plots the total system throughput versus the latency to join the network. For the CDMA based code-broker approach, we notice that the latency to join the network is very low whereas the maximum network load approaches ~75 Mbps (for n = 1) and ~ 79 Mbps (for n = 2). On the other hand for the CSMA based approach, due to back-off, the latency to start a communication link is very high. Also in the CSMA based scheme, the user needs to listen to the channel every time it wants to communicate with its intended receiver whereas in the proposed MAC, once the user has obtained a code, it can communicate till the whole communication is over. The total throughput of the system on the other hand is very low as only one link is possible in the entire piconet.

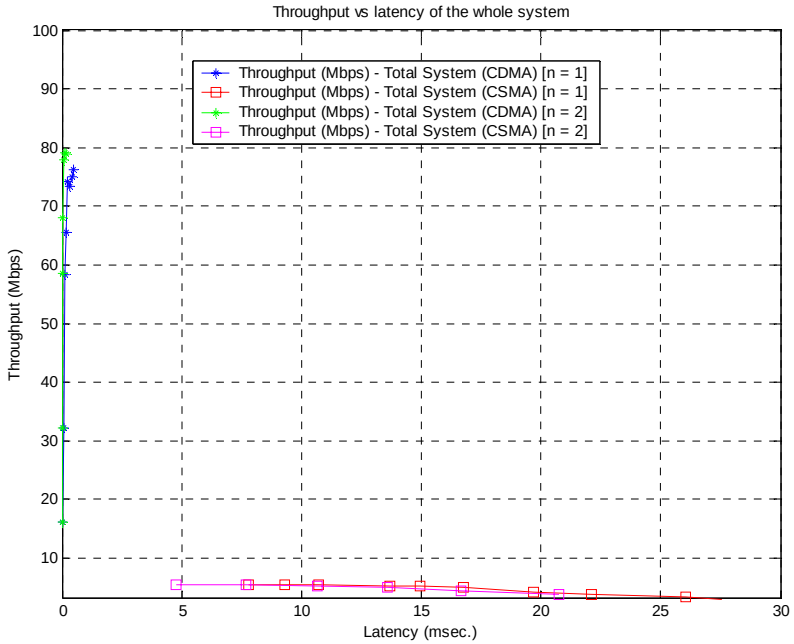

Figure 4.16 Throughput vs. Latency of the whole system

A zoomed latency vs. throughput curve of the CDMA based scheme is plotted in Figure 4.17 below. The network saturates at a higher throughput for n = 2 as compared to n = 1. This is due to the presence of less secondary interference in the system due to greater path loss. Also a zoomed latency vs. throughput curve of the CDMA based scheme is plotted in Figure 4.18 below. For the same throughput the system latency for n = 2 is lower as compared to n = 1. An increase in path loss exponent reduces the latency but also increases the system throughput but due to a greater reduction in latency the curve for n = 2 is towards the left of the curve for n = 1.

The total system throughput is compared with the network load in Figure 4.19 below. Here also we observe similar effects. Due to the presence of just a single link, the total system throughput is very low. The CDMA based code-broker approach scheme on the other hand approaches the system capacity for lower network load. For high network load the system behaves like an interference-limited piconet and the total throughput starts to saturate. For n = 2, the

throughput for the CDMA based scheme is higher than for n = 1. The total system throughput of the CSMA based scheme is very low as compared to the CDMA based scheme.

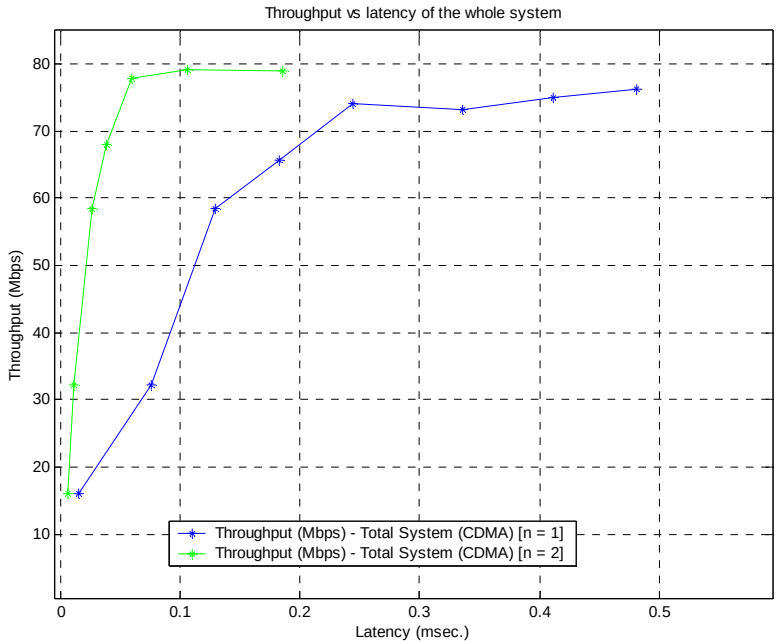

Figure 4.17 Throughput vs. Latency of the whole system (CDMA based scheme – Zoomed)

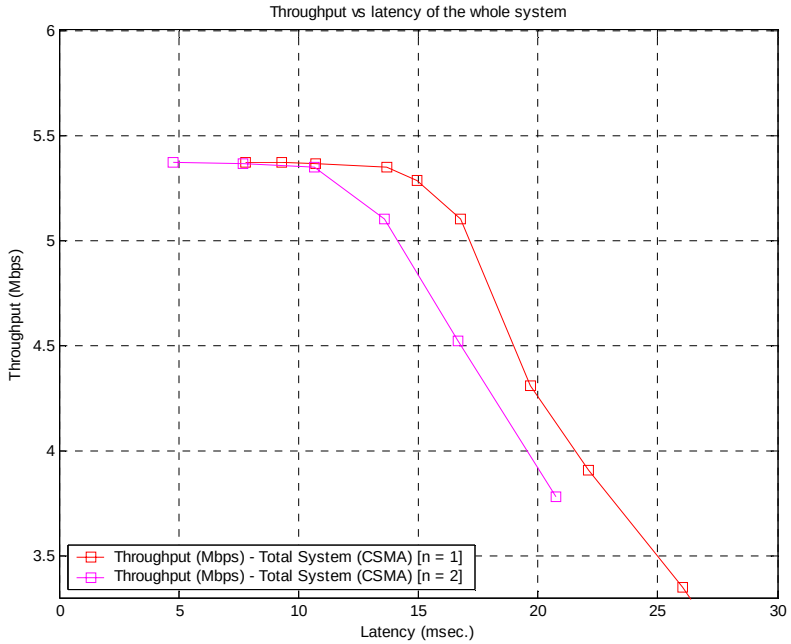

Figure 4.18 Throughput vs. Latency of the whole system (CSMA based scheme – Zoomed)

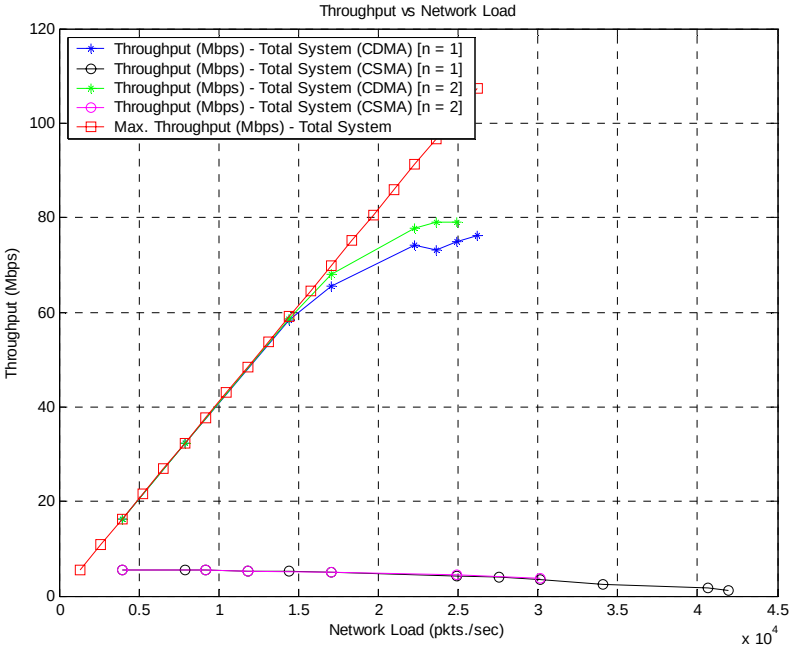

Figure 4.19 Throughput vs. Network load of the whole system

As seen in Figure 4.20 below, as the network load increases the latency to join the network for the both the CSMA and CDMA based schemes increases in a similar manner. The total latency for the CSMA based scheme is very high as compared to the CDMA based scheme. For n = 2, the latency for both the CSMA and CDMA based scheme is lower for the same network load. This is more evident for the CDMA based scheme in Figure 4.21 plotted below.

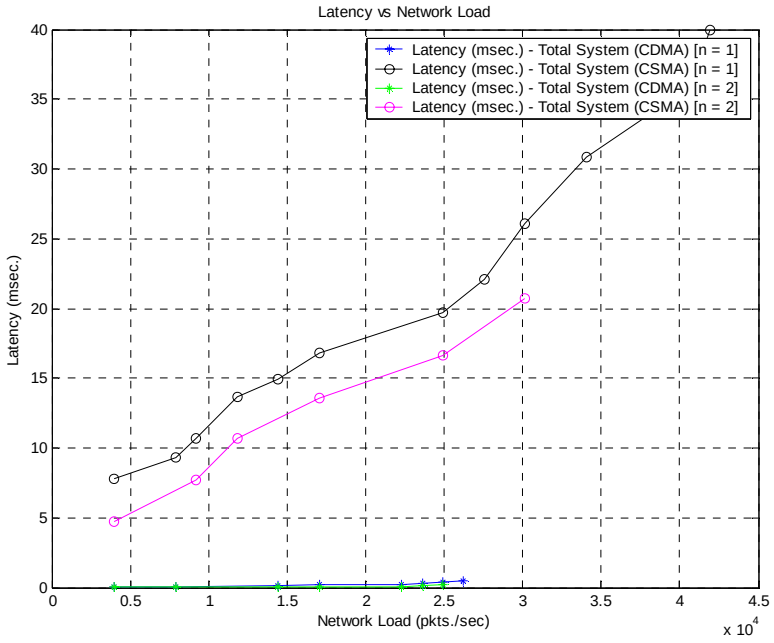

Figure 4.20 Latency vs. Network load of the whole system

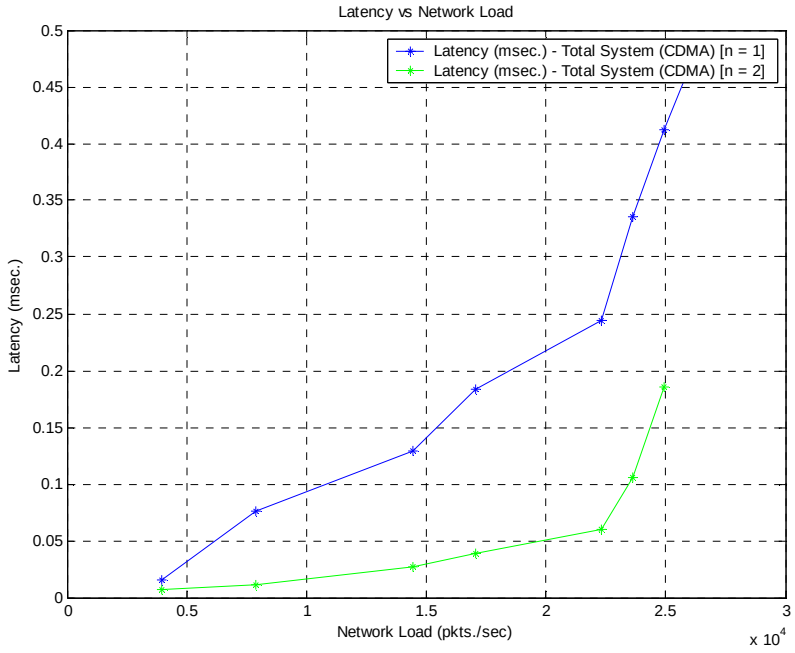

Figure 4.21 Latency vs. Network load of the whole system (CDMA based scheme – Zoomed)

The network load vs. the packet error rate of the entire system is plotted in Figure 4.22. With an increase in the network load, the packet error rate for both the schemes increases. To achieve a particular PER, we notice that the CDMA-based scheme outperforms the CSMA-based scheme. For example, to achieve an 8% PER, the CDMA based scheme needs a network load of 1.82 x 10^4 pkts./sec (for n = 1) which from Figure 4.19 above results in a throughput of ~67.4 Mbps while the CSMA based scheme needs a network load of 1.97 x 10^4 pkts./sec (a throughput of ~4.82 Mbps, again for n = 1). This is an improvement of 62.58 Mbps throughput for the entire network. If a similar analysis is done for a system with n = 2, the net system gain is 79.42 Mbps.

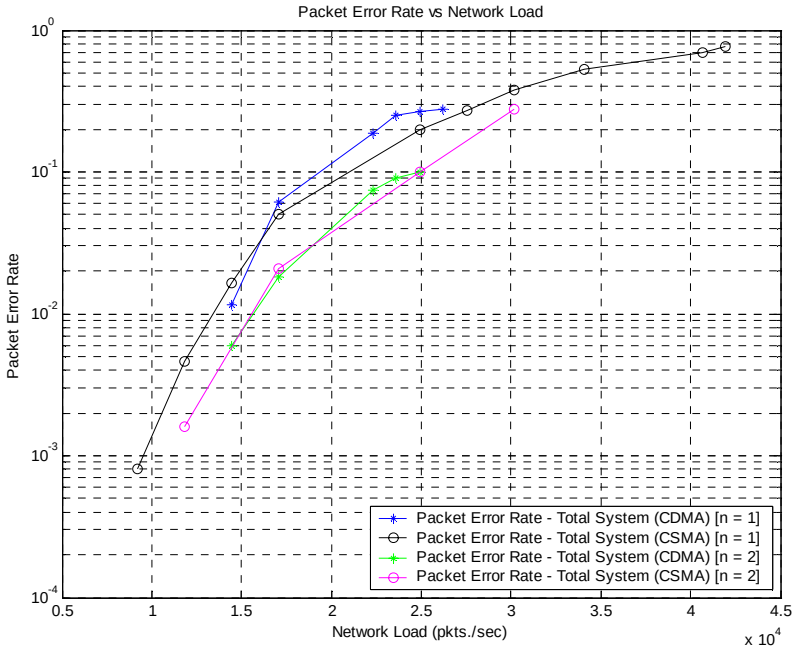

Figure 4.22 Packet Error Rate vs. Network load of the whole system

4.4.4 Conclusions

As seen in the figures above, the CDMA based code-broker approach outperforms the CSMA based approach in terms of throughput as well as latency to join the network.

Based on the results obtained from both the sections above we conclude that if the CSMA-based scheme is also spread by the same length spreading code as the CDMA-based code-broker approach, the latter approach dramatically outperforms the CSMA-based scheme. In other words, the CDMA based code-broker scheme has better throughput-delay characteristics that a simple single-channel CSMA system. On the other hand, if that is not the case (i.e., if we have a single piconet and no spreading) then the CSMA scheme would outperform the proposed scheme in terms of latency as well as throughput. The reason why the CDMA based scheme performs better than the CSMA based scheme is simply due to the fact that in the CDMA based scheme many pair of nodes can communicate at the

same time even though they are in close proximity to each other. Also a system with a higher path loss performs slightly better as compared to a system with a lower path loss. This is true for both the schemes analyzed in the system. The latency for both the systems (CDMA based and CSMA based scheme) reduces for a higher path loss exponent system due to the presence of less number of hidden nodes in the system.

4.4.5 Comparison – Code-broker approach vs. Receiver based code assignment scheme

4.4.5.1 Simulation Results

A comparison of the proposed code-broker scheme has been made with the receiver-based code assignment scheme [16] and the results are shown below. In the receiver-based code assignment scheme, each receiver is assigned a unique code. The advantage of this scheme is that each user only has to monitor its own code but due to multiple users transmitting at the same time to the same user (hidden nodes*) primary* interference can be caused at a receiver. For this scheme, the node first listens at the intended receivers' code for an on-going transmission. If there is any communication happening on that code, the node backs-off and listens to the channel again once the back-off counter expires. If there is no on-going transmission, the node goes ahead with its communication with the intended receiver. During communication with the receiver, *primary* as well as *secondary* interference is present at each receiver. Primary interference occurs due to the presence of hidden nodes in the system. The hidden nodes are simulated using the same technique as described in Section 4.2 above. Secondary interference occurs due to the presence of simultaneous on-going transmissions on different codes in the entire piconet.

Figure 4.23 shows a comparison of the throughput of a single user in the system vs. the latency in the network. In terms of throughput, the receiver code assignment based scheme performs slightly worse than the proposed scheme. In the simulations it was observed that some of the errors in the receiver code assignment based scheme were due to acquisition errors whereas some of the errors are attributed to the secondary interference present in the system. Collisions occur due to the fact that multiple users can simultaneously transmit using the same code (hidden node problem). It should also be noted that for the receiver based code assignment scheme the same throughput as compared to the proposed code-broker approach is achieved at a much lower latency. It is also observed that for n = 2, the throughput for both the proposed CDMA based MAC and the receiver based code assignment scheme increases. This is due to less number of hidden nodes in the system for the later scheme and less amount of secondary interference for the former scheme. For the later scheme too, the presence of less amount of secondary interference increases the throughput of the system.

The throughput of the system vs. the latency incurred in joining the network is plotted in Figure 4.24 below. Here also it is observed that the total system throughput reduces due to *primary* conflicts in the channel. It is seen that the proposed system has a net throughput advantage of ~10 Mbps (for n = 1 and 2). A drawback of the proposed scheme is that it has a longer latency in starting a communication link. This is true for both the path loss cases. Although the absolute values in the system changes, the relative values in the system remains approximately the same. This is due to the fact that in the proposed code-broker scheme all the users are contending for the channel to communicate for the code-broker whereas in the receiver based code assignment scheme only some users are contending to communicate with the intended receiver. In the simulation as all the nodes have an infinite queue of data to send, it is assumed that $1/3^{rd}$ of the nodes in the system are attempting to communicate with the intended receiver. This assumption would have some implications on the results obtained in the

simulation. If a traffic model (*e.g.*, Poisson) were assumed in the simulation, this condition could be removed and improved results could be obtained.

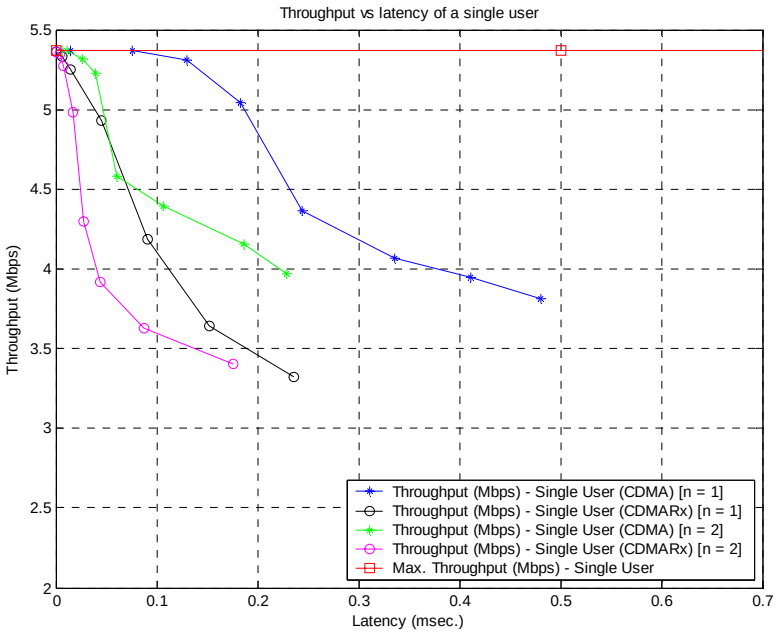

Figure 4.23 Latency vs. throughput of a single user

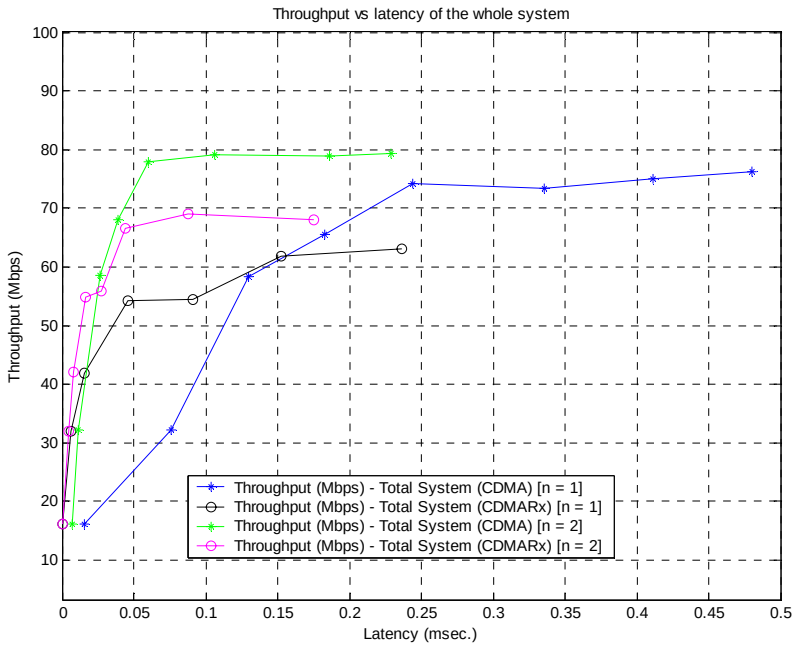

Figure 4.24 Latency vs. throughput of the whole system

The total system throughput achieved by both the systems versus network load is compared to the maximum possible throughput in the network (Figure 4.25 below). It is seen that both the systems saturate (*i.e.*, start behaving as interference limited systems) at high levels of network load. The net throughput of the proposed system is higher as compared to the receiver based code assignment scheme for the same network load in the system (for both n = 1 and 2). This is due to the presence of primary as well as secondary interference in the receiver code assignment scheme as opposed to the presence of only secondary interference in the proposed code-broker scheme. For the case when n = 2, due to less number of hidden nodes in the system, the throughput of the receiver based code assignment scheme is higher. For the proposed scheme due to higher path loss, the amount of interference reduces which leads to a greater throughput in the system.

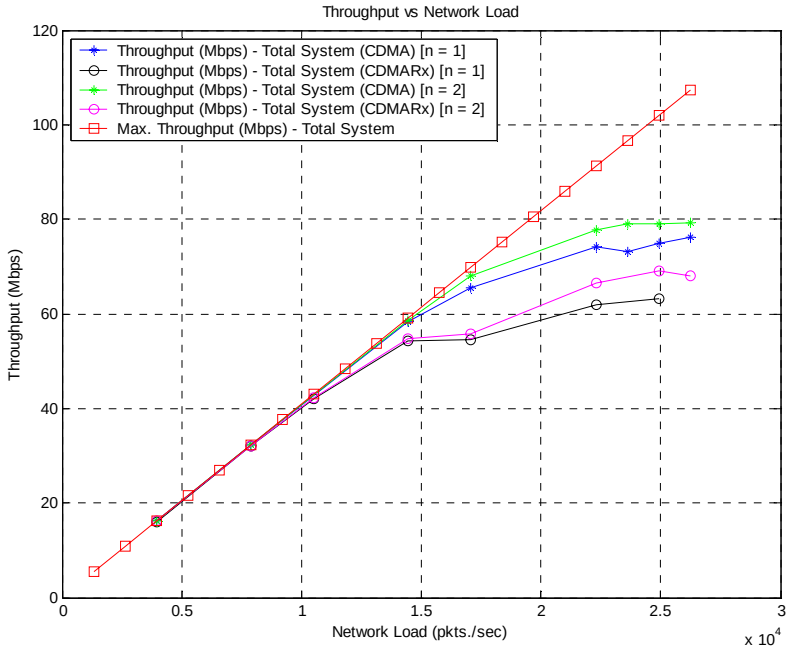

Figure 4.25 Network load vs. throughput of the whole system

The network load has been plotted against the latency of the two systems in Figure 4.26 below. The receiver based code assignment scheme incurs slightly less latency as compared to the proposed code-broker scheme for the same network load. The same effect is observed for both n = 1 and 2. The latency in the network for the proposed scheme is a function of the time taken by a node to obtain a code from the code-broker. For the receiver based code assignment scheme it is a function of the amount of users contending to communicate with a particular receiver. Further more for a higher path loss exponent, the number of primary interferers (hidden nodes) in the system is less as compared to a lower path loss exponent system which reduces the latency of the system further.

Figure 4.27 plots the network load vs. the packet error rate in the system. It is noticed that the packet error rate for the receiver based code assignment scheme is higher as compared to the proposed scheme. This increase in the packet error rate is attributed to the presence of *primary* as well as *secondary* interference in the piconet. For the proposed scheme, only secondary interference is present in the

system. Again for n = 2, the packet error rate reduces for both the systems as the amount of *primary* and *secondary* interference in the system reduces with higher path loss.

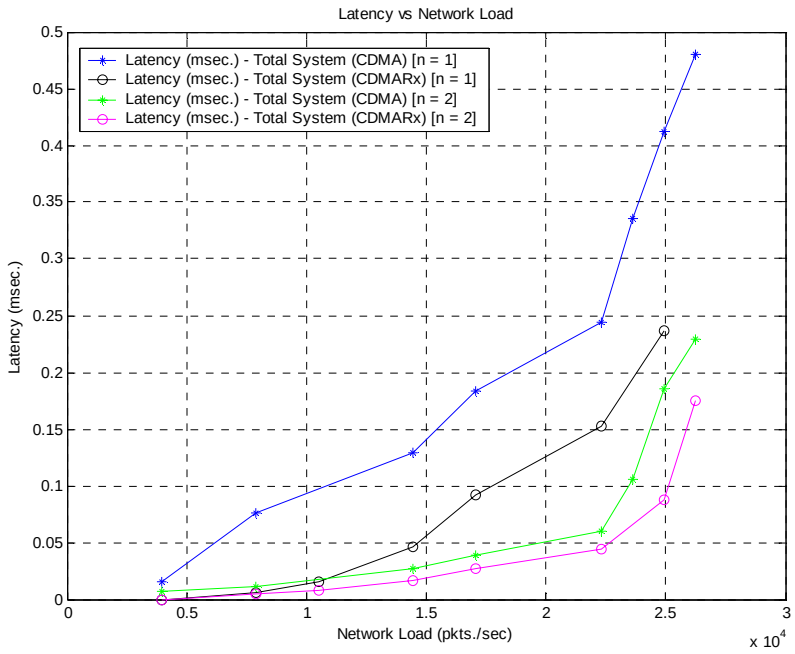

Figure 4.26 Network load vs. latency of the whole system

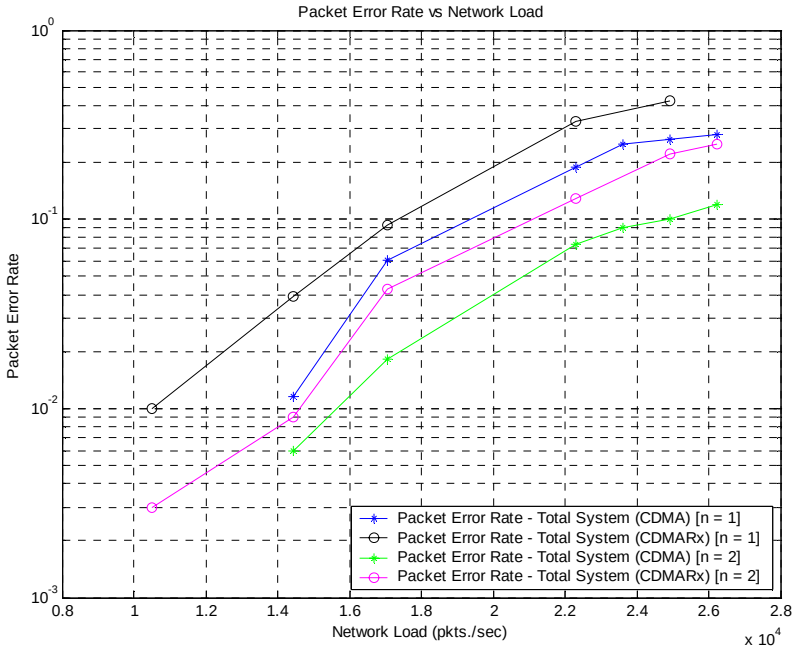

Figure 4.27 Network load vs. packet error rate of the whole system

4.4.6 Conclusions

As seen in the figures above, the CDMA based code-broker approach performs slightly better than the receiver-based code assignment scheme in terms of throughput. This is primarily due to the fact that in the receiver based code assignment scheme *primary* as well as *secondary* interference disrupts the communication. A downside of the proposed code-broker approach is that the latency to start a link is higher as compared to the receiver based code assignment scheme. This is due to the fact that in the proposed scheme all the nodes are contending to obtain a code from the code-broker whereas in the later scheme, only some of the nodes are contending to communicate with the intended receiver. The absolute performance of both the schemes changes with a change in the path loss exponent but the relative performance of both the schemes remains the same for different path loss exponents.

Chapter 5

5 Multiband-OFDM based UWB

Although Impulse Radio is generally what researchers imply when they use the term "Ultra-Wideband", recently alternative flavors of UWB have emerged. In the following two chapters we will examine one such version of UWB which is similar to Orthogonal Frequency Division Multiplexing (OFDM) [53]. Specifically, the following two chapters of this thesis concentrate on the IEEE 802.15.3 standard MAC layer protocol proposed for the 802.15.3a protocol which is being termed as the "Alternate PHY". This chapter gives an overview of the 802.15.3 MAC layer protocol and the Multiband-OFDM based Physical layer proposed for UWB applications. In the next chapter one of the issues examined is the issue of interference due to simultaneously operating piconets is examined. Since the 802.15.3a physical layer proposal uses the 802.15.3 MAC layer the problem of simultaneously operating piconets has been tackled from the physical layer point of view. It is not possible to make changes to the already existing MAC layer whereas the physical layer proposal is still under development. For the Impulse Radio based network topology (discussed in the previous chapters) as there is no standard MAC layer defined, the problem of simultaneously operating users is tackled from the MAC layers' perspective.

5.1 Overview of 802.15.3 MAC layer protocol

The IEEE standard 802.15.3 MAC layer [51] is based on a centralized, connection-oriented topology which divides a large network into several smaller ones termed "piconets". Note that this term has also been used previously for our Impulse Radio based MAC layer proposal Each piconet consists of a Piconet Network Controller (PNC) and DEVs (DEVices) and spans over an area of about 10 meters^2. Such a piconet is envisioned for Wireless Personal Area Network (WPAN) applications in which multiple devices in close proximity of an end user

communicate with each other. The piconet concept comes from the development of ad-hoc networks, where piconets are formed "on-the-fly" without any prior infrastructure.

IEEE 802.15.3 MAC is designed based on the following goals [51]

1) Fast connection time
2) Ad hoc networks
3) Data transport with quality of service (QoS)
4) Security
5) Dynamic membership
6) Efficient data transfer

The standard also allows for the formation of child piconets and neighbor piconets. The original piconet is called the parent piconet and the child/neighbor piconets are called the dependent piconets. These piconets differ in the way they associate themselves to the parent piconet. The general structure of a piconet is shown in Figure 5.1 below.

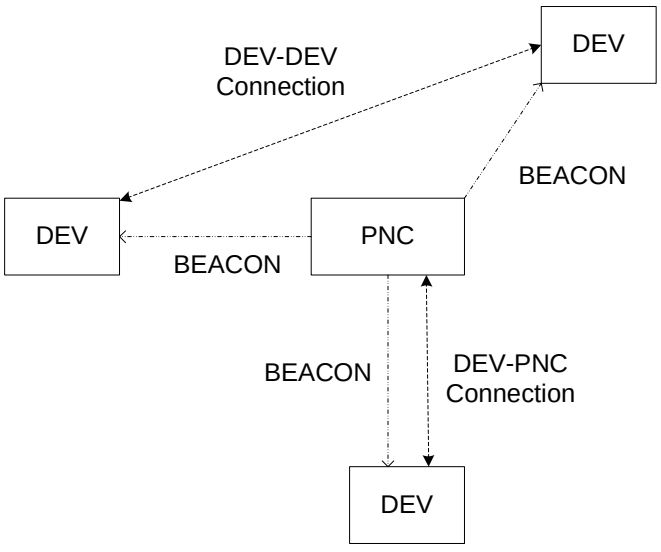

Figure 5.1 Piconet structure

The Piconet Network Controller (PNC) controls network timing, admission to the piconet and authenticates new DEVs (DEVices). The PNC can also seamlessly handover its duties to any DEV in its network. This happens without interruption of any existing ongoing communication. Guaranteed time slots (GTS) are used to allocate fixed bandwidth to the devices (QoS). The 802.15.3 standard supports multiple power saving modes and multiple ACK policies (NO ACK, Imm-ACK, Del-ACK, Implied ACK). For more information about different acknowledgment schemes please refer to [51]. It is very robust and supports coexistence with the other WLAN technologies such as 802.11. In the 802.15.3 MAC protocol, although communications are connection–based under the control of the PNC, connections and data transfer can be made with peer to peer connections.

The 802.15.3 protocol defines a super-frame for transmissions. The maximum length of a super-frame is 65.536 msec. The super-frame structure is shown below.

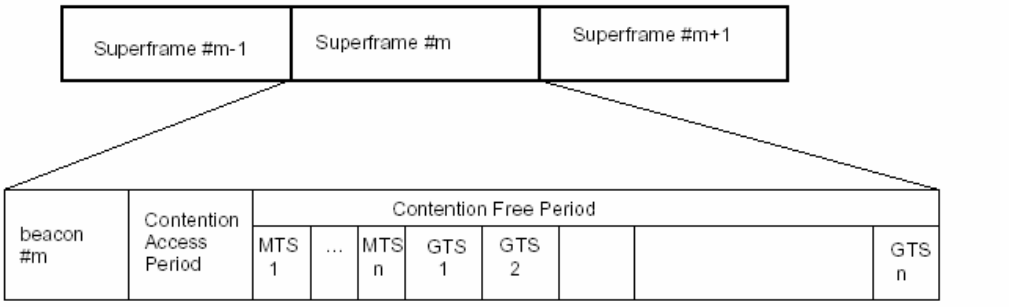

Figure 5.2 Super-frame structure for the 802.15.3 MAC layer

As shown above, the 802.15.3 MAC frame consists of 3 parts

1) Beacon

This is used to transmit control information, the allocated GTS (Guaranteed Time Slot) per stream index for the current super-frame and to provide network wide timing information. All the nodes in a piconet synchronize to the PNC clock at the beginning of the BEACON preamble.

2) Contention Access Period (CAP) – Uses CSMA/CA with back-off procedure

Communication during this part of the frame uses the CSMA/CA protocol with back-off procedure. This period is used for stream-less data, channel time requests, authentication, association request/response, asynchronous data and other commands in the system. The PNC governs what can be sent in the Contention Access Period.

3) Contention Free Period (CFP)

This part of the frame is composed of GTS (Guaranteed Time Slot) and MTS (Management Time Slot). Each device makes a channel time request during the CAP. The PNC responds by allocating GTS/MTS units to the each DEV depending on the QoS requirements of the DEV. The information concerning the assignment of GTS/MTS to a DEV is transmitted during the BEACON portion of the frame. This is a TDMA-based scheme to guarantee the DEVs their negotiated QoS. This is very important to support real time video/audio applications as they have very stringent requirements on timing jitter, end-to-end delay etc.

A GTS is specified by a start time, a source ID, a destination ID and duration. This feature is very crucial for power saving mode as the devices can go to sleep when not scheduled to send or receive data. GTS can be either asynchronous or isochronous. The isochronous mode is used for DEVs which require a guaranteed time slot every super-frame (for example, streaming video kind of applications). These DEVs are assigned a fixed time slot in every super-frame. Asynchronous connections are given to DEVs which have little QoS requirements. This leads to dynamic allocation of time slots.

The MTS is used for PNC-DEV communications. The MTS is normally used to substitute for CAP. Some slots in the frame are defined as MTS which are like the CAP period. Although the CAP can be used for various purposes, MTS are used for specific purposes. MTS can be of three different types: Normal MTS, Open

MTS and association MTS. Normal MTS time slots use TDMA for communication. An Open MTS slot is used by any associated device to send a command frame to the PNC. An Association MTS slot is used for devices to associate to the piconet. A slotted ALOHA access is used for open and associated MTS communication.

5.2 Overview of MB-OFDM "Alternative PHY"

The Multiband-OFDM [30] proposal was originally proposed by Texas Instruments (TI) and has been recently backed by most of the leading Consumer Electronics companies and other leading Ultra-Wideband companies. The proposed UWB system works on OFDM (Orthogonal frequency division multiplexing) over a bandwidth of 528 MHz. OFDM was first proposed in 1966 [52] and has been a highly favored technology for various wireless LAN applications e.g., 802.11a/g. The proposed 802.15.3a standard supports data rates of 55, 80, 110, 160, 200, 320 and 480 Mbps in which the support for 55, 110 and 200 Mbps is mandatory.

The proposed system divides the spectrum into 14 bands each 538 MHz wide in the allotted UWB spectrum from 3.1 – 10.7 GHz. The system defines a total of 5 logical channels, of which 4 logical channels are comprised of 3 bands and one logical channel is comprised of 2 bands. The frequency allocation for the different bands is shown in the Table 5.1 below.

Table 5.1 OFDM PHY band allocation

Channels	Band No.	Lower Frequency	Center Frequency	Upper Frequency
Logical Channel #1	1	3168 MHz	3432 MHz	3696 MHz
	2	3696 MHz	3960 MHz	4224 MHz
	3	4224 MHz	4488 MHz	4752 MHz
Logical Channel #2	4	4752 MHz	5016 MHz	5280 MHz
	5	5280 MHz	5544 MHz	5808 MHz
	6	5808 MHz	6072 MHz	6336 MHz
Logical Channel #3	7	6336 MHz	6600 MHz	6864 MHz
	8	6864 MHz	7128 MHz	7392 MHz
	9	7392 MHz	7656 MHz	7920 MHz
Logical Channel #4	10	7920 MHz	8184 MHz	8448 MHz
	11	8448 MHz	8712 MHz	8976 MHz
	12	8976 MHz	9240 MHz	9504 MHz
Logical Channel #5	13	9504 MHz	9768 MHz	10032 MHz
	14	10032 MHz	10296 MHz	10560 MHz

Each logical channel supports four piconets which are distinguished by a time-frequency code (TF code). A general structure of 3 geographically located piconets is shown in Figure 5.3 below.

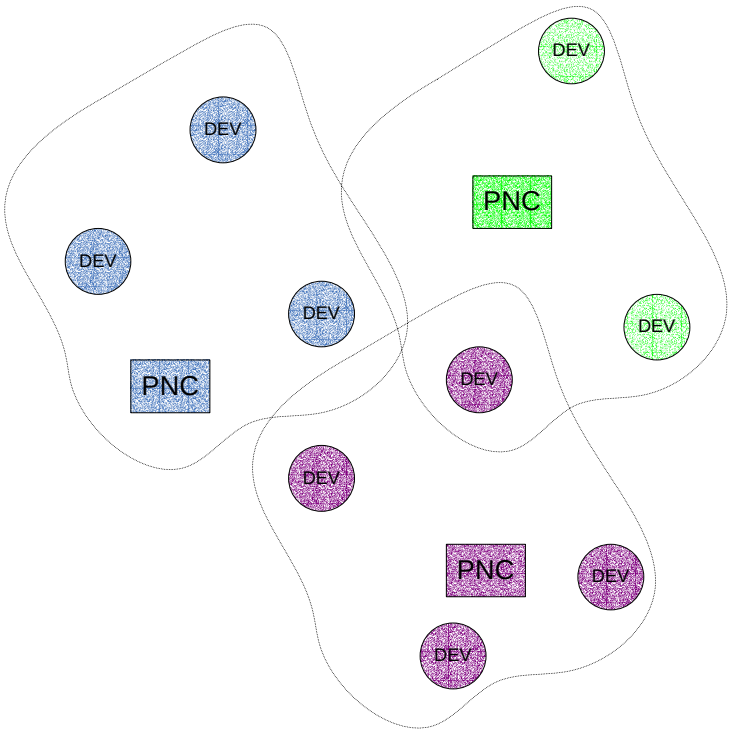

Figure 5.3 Example structure of 3 geographically located piconets

Each TF code interleaves the coded data over all the three frequency bands in each logical channel. Presently, support for the lowest 3 bands is mandatory. The rest of the channels could be added to a device over time. The time-frequency codes and their transmission sequence between the frequencies in a particular logical channel are shown below. The TF code for logical channel 5 has not been defined yet.

Table 5.2 Time Frequency code definitions

Piconet Number	*Length 6 Time Frequency Code*					
1	*f1*	*f2*	*f3*	*f1*	*f2*	*f3*
2	*f1*	*f3*	*f2*	*f1*	*f3*	*f2*
3	*f1*	*f1*	*f2*	*f2*	*f3*	*f3*
4	*f1*	*f1*	*f3*	*f3*	*f2*	*f2*

Each OFDM symbol consists of a cyclic prefix of 32 samples, a guard interval of 5 samples and data worth of 128 samples making it a total of 165 samples. Some of the timing related parameters are shown in Table 5.3 below [30].

Table 5.3 Timing-related parameters an OFDM symbol

Parameter	Value
N_{SD}: Number of data subcarriers	100
N_{SDP}: Number of defined pilot carriers	12
N_{SG}: Number of guard carriers	10
N_{ST}: Number of total subcarriers used	122 (= N_{SD} + N_{SDP} + N_{SG})
Δ_F: Subcarrier frequency spacing	4.125 MHz (= 528 MHz/128)
T_{FFT}: IFFT/FFT period	242.42 ns ($1/\Delta_F$)
T_{CP}: Cyclic prefix duration	60.61 ns (= 32/528 MHz)
T_{GI}: Guard interval duration	9.47 ns (= 5/528 MHz)
T_{SYM}: Symbol interval	312.5 ns (T_{CP} + T_{FFT} + T_{GI})

A frame consists of 5 major sections which are shown Figure 5.4. An assigned slot consists of multiple such frames. The number of frames transmitted depends on the amount of time allocated to a DEV in a particular time slot.

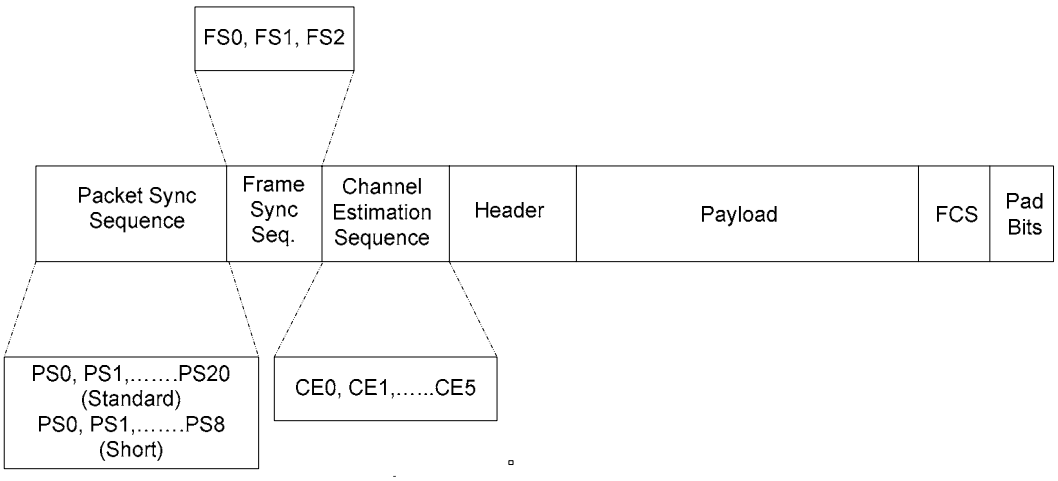

Figure 5.4 Frame Structure for a Multiband-OFDM frame

The packet synchronization sequence, frame synchronization sequence and channel estimation sequence form the preamble. The preamble can be of two types

a) SHORT preamble consisting of 9 repetitions of the packet synchronization sequence, 3 repetitions of the frame synchronization sequence and 6 repetitions of the channel estimation sequence. This preamble is used in BURST MODE to increase the throughput of the system. The total time duration of the long preamble is 5.625 μs. This results in an overhead per frame. The amount of overhead depends on the number of bytes transmitted and the data rate at which the transmission takes place. To send the same number of bytes, a larger frame is required if transmitting at 55 Mbps as compared to 110 Mbps. For example, to send a 1024 byte packet at 110 Mbps, the overhead is 3.6 %.

b) LONG preamble consisting of 21 repetitions of the packet synchronization sequence, 3 repetitions of the frame synchronization sequence and 6 repetitions of the channel estimation sequence. The LONG preamble is also known as the standard preamble. The total time duration of the long preamble is 9.375 μs. For example, to send a 1024 byte packet at 110 Mbps, the overhead is 5.88 %.

The packet synchronization sequence is a time domain sequence which is distinct for each of the piconets. The frame synchronization sequence is an inverted version of the packet synchronization sequence. Each packet synchronization sequences is defined over 128 samples. As stated previously, each OFDM symbol is pre-appended with a 32-sample cyclic prefix and appended with 5 guard samples resulting in a total of 165 samples. The preamble is used for synchronization, carrier-offset recovery and channel estimation at the receiver.

Each OFDM symbol is comprised of 128 sub-carriers 100 of which are data sub-carries, 22 are pilot sub-carriers (which are further divided into regular pilot sub-carriers and 10 user-defined sub-carriers). Each of the sub-carriers is QPSK modulated. A convolutional encoder of rate 1/3 is used which is punctured to achieve the proposed data rates. The different puncturing rates used are 11/32, ½, 5/8 and ¾. Generator polynomials $\{133_8, 145_8, 175_8\}$ are used for the encoder.

The header is always transmitted at 55 Mbps whereas the payload could be transmitted using any of the data rates shown above. This allows the header to be decoded more reliably as compared to the payload. The information regarding the RATE, LENGTH etc. is transmitted in the PHY Header which is a part of the total HEADER field shown in Figure 1.4 above. For data rates of 55 and 80 Mbps, the input to the IFFT is complex conjugate symmetric in order to obtain a real valued output. This saves some power due to the requirement of using only 1 DAC. For the rest of the data rates, the input to the IFFT is not complex conjugate symmetric. The different data rates and their relationship to the puncturing patterns, modulation scheme etc. are shown in Table 1.5 below.

Table 5.4 RATE dependent parameters [30]

Data Rate (Mb/s)	Modulation	Coding rate (R)	Conjugate Symmetric Input to IFFT	Time Spreading Factor	Overall Spreading Gain	Coded bits per OFDM symbol (N_{CBPS})
55	QPSK	11/32	Yes	2	4	100
80	QPSK	½	Yes	2	4	100
110	QPSK	11/32	No	2	2	200
160	QPSK	½	No	2	2	200
200	QPSK	5/8	No	2	2	200
320	QPSK	½	No	1	1	200
480	QPSK	¾	No	1	1	200

The proposed standard document [30] also explains in more detail the various blocks (some of which have been described in the next chapter) and formally defines the values of pilot sub-carriers, guard sub-carriers, concept of time domain spreading, calculation of HCS etc. These have not been included in the above description of the standard for the sake of simplicity.

Chapter 6

6 Multiband-OFDM - System Model and Simulation Results

In this chapter the current Multiband-OFDM system [30] is simulated and studied in detail. A novel technique has been presented which improves performance of the system by taking advantage of the inherent frequency diversity in the system. This scheme has been termed "bit-order reversal." The effect of time interleaving on the system has been studied. In the end, various schemes proposed to mitigate the effect of simultaneously operating piconets have been simulated and their performance has been compared. As stated previously since the 802.15.3a physical layer proposal uses the 802.15.3 MAC layer, in this thesis this problem has been tackled from the physical layer point of view. It is not possible to make changes to the already existing MAC layer whereas the physical layer proposal is still under development. For the Impulse Radio based network topology (discussed in the previous chapters) as there is no standard MAC layer defined, the problem of simultaneously operating users was tackled from the MAC layers' perspective.

6.1 System Model

In order to determine the impact that different physical layer techniques have on the operation of simultaneously operating piconets, the complete physical layer proposal of the MB-OFDM system was simulated. The following sections present the system model assumed for the simulation. A block diagram of the system is presented in Figure 6.1 below. A brief description of the various blocks is presented in the following sub-sections.

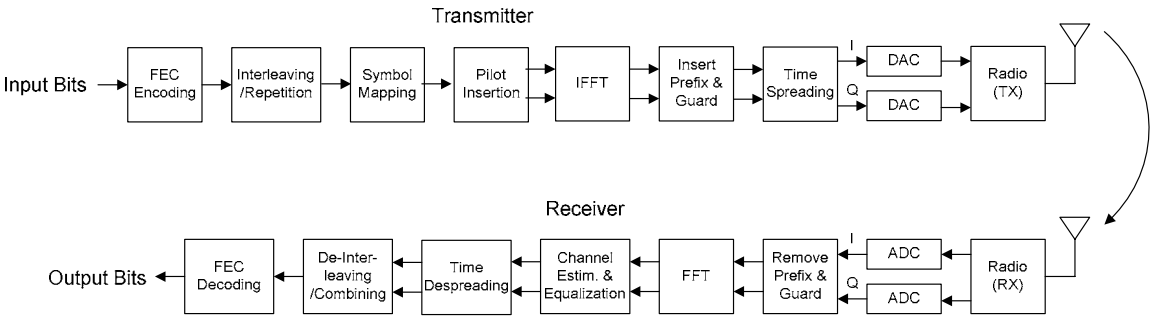

Figure 6.1 Block Diagram of the Tx-Rx implementation

6.1.1 FEC Encoding/Decoding and Puncturing/De-puncturing

A 1/3 rate, constraint length 7 convolutional encoder was used. The encoder used was specified by 3 generator polynomials $\{133_8, 145_8, 175_8\}$ [50]. For each input bit 3 output bits are produced which are transmitted in the order X, Y, Z as shown in Figure 6.2 below.

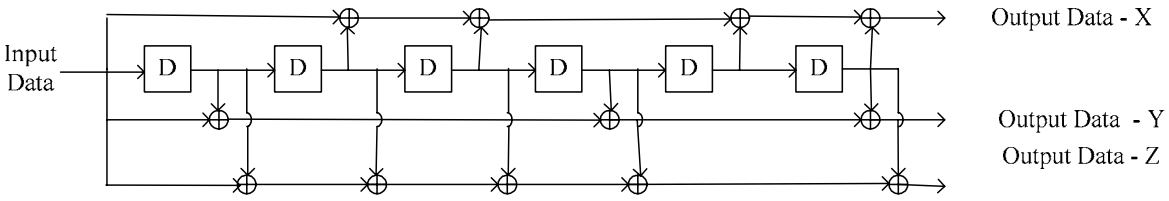

Figure 6.2 Encoder Structure

Soft decision decoding was implemented using the Viterbi decoder [50]. A trace back depth of 80 was used in the simulations.

As stated in Chapter 5, different data rates are derived from the rate 1/3 convolutional encoder using various puncturing schemes. Only a data rate of 110 Mbps in the payload was simulated in this work. The header is always transmitted at 55 Mbps. Both of these rates use a punctured code rate of 11/32. Furthermore, the 55 Mbps header performs a complex conjugate frequency domain spreading operation before sending data into the IFFT. For every 11 bits into the encoder, 33

bits are generated at the output of the encoder. For every 33 bits, the last bit is "stolen" i.e. not transmitted which gives a 11/32 rate code. At the receiver, a dummy bit is inserted at that particular location. If hard decision decoding is used, the dummy bit inserted should be randomly chosen from 0 or 1. If soft decision decoding is used, the dummy bit inserted should always be zero.

6.1.2 Interleaving/De-interleaving

The MB-OFDM specification performs two types of interleaving: symbol interleaving and tone interleaving. The two types of interleaving are performed to achieve different levels of frequency diversity. In the first type of interleaving, bits are interleaved over 3 OFDM symbols to achieve frequency diversity since the 3 OFDM symbols are transmitted in different frequency bands. The tone interleaver is used for interleaving bits in each OFDM symbol to exploit potential frequency diversity in that particular OFDM symbol. Both of the interleavers were simulated in the system. The interleaving operations are described below.

The symbol interleaver works on $3N_{CBPS}$ bits where N_{CBPS} is the number of coded bits per OFDM symbol. If *A(i)* and *B(j)* represent the input and output bits of the symbol interleaver respectively at position *j*, the relationship between the two is given by

$$B(j) = A\left\{ \text{floor}\left(\frac{i}{N_{CBPS}} \right) + 3\text{mod}\left(i, N_{CBPS}\right) \right\}$$

Equation 6.1 Input/Output bit relationship of the symbol interleaver

where

N_{CBPS} = number of coded bits per OFDM symbol

i, j = 0, 1, 2, ….. N_{CBPS}

floor gives the integer value smaller and closest to the value in the bracket

mod gives the remainder after division by N_{CBPS}

The above interleaver uses a block of size 3 x N_{CBPS}.

The output *B(j)* is passed through the tone interleaver block. The tone interleaver block works on N_{CBPS} bits. If C*(i)* and D*(j)* represent the input and output bits of the tone interleaver respectively, the relationship between the two is given by

$$D(j) = C\left\{\text{floor}\left(\frac{i}{N}\right) + 10\text{mod}(i, N)\right\}$$

Equation 6.2 Input/Output bit relationship of the tone interleaver

where

N_{CBPS} = number of coded bits per OFDM symbol

i, j = 0, 1, 2, ….. N_{CBPS}

floor gives the integer value smaller and closest to the value in the bracket

mod gives the remainder after division by N_{CBPS}

The above interleaver uses a block of size N x 10 where N = N_{CBPS}/10. One method of implementing the above equation would be by writing the bits into a block interleaver row-wise and reading them out of the block interleaver column-wise. At the de-interleaver (receiver), tone de-interleaving was performed before the symbol de-interleaving to reverse the operations performed at the transmitter.

6.1.3 Symbol Mapping

QPSK modulation was used in the simulations. The bits were gray coded. The mapping from bits to I and Q samples is shown in Table 6.1 below.

Table 6.1 Constellation Mapping for QPSK Modulation

Input bit	*I*	*Q*
00	*-1*	*-1*
01	*-1*	*1*
10	*1*	*-1*
11	1	1

At the receiver, I and Q samples are directly mapped to the soft decision bits going into the Viterbi decoder.

6.1.4 OFDM Modulation

As mentioned previously, the header is always transmitted at 55 Mbps. Only a data rate of 110 Mbps was simulated for the payload. For the 55 Mbps mode, 50 complex numbers are generated for every OFDM symbol which are complex conjugated and spread to form 100 OFDM symbols. The mapping of the complex numbers to the sub-carriers is shown below. Let c_n denotes the complex number at sub-carrier number n and d_n denotes the input complex number. The relationship between the two is given by

$$c_n = d_n \qquad n = 0, 1, \ldots, 49$$
$$c_{(n+50)} = d^*_{(49-n)} \qquad n = 0, 1, \ldots, 49$$

For 110 Mbps, the relationship is given by

$$c_n = d_n \qquad n = 0, 1, \ldots, 99$$

6.1.5 Pilot Insertion

An OFDM symbol consists of 128 sub-carriers, of which 100 are data sub-carriers, 12 are pilot sub-carriers, 10 are guard sub-carriers and the remaining 6 sub-carriers are zero. No information is transmitted at the sub-carrier at DC so that DC offset does not affect the information in that particular sub-carrier. The sub-carriers are defined from -61 to +61. The pilot sub-carriers are placed at

locations -55, -45, -35, -25, -15, -5, 5, 15, 25, 35, 45, 55. The guard sub-carriers are placed at locations (-61) through (-57) and 57 through 61. The rest of the locations contain the data sub-carriers. The pilots are QPSK symbols which are defined for each sub-carrier and are modulated by a length 127 pseudo-random sequence which changes for each OFDM symbol.

The pilot sub-carriers are defined as

$$P_n = \begin{cases} \frac{1+j}{\sqrt{2}} & n = 15,45 \\ \frac{-1-j}{\sqrt{2}} & n = 5,25,35,55 \\ 0 & n = \pm 1...,\pm 4,,\pm 6,...,\pm 14,\pm 16,...,\pm 24,\pm 26,...,\pm 34,\pm 36,...,\pm 44,\pm 46,...,\pm 54,\pm 56 \end{cases}$$

For modes with data rates less than 110 Mbps:

$$P_{n,k} = P^*_{-n,k}, \qquad n = -5,-15,-25,-35,-45,-55$$

while for 110 Mbps and all higher rate modes:

$$P_{n,k} = P_{-n,k}, \qquad n = -5,-15,-25,-35,-45,-55$$

The regular pilots were used in the simulation for phase error estimation at the receiver.

6.1.6 IFFT Operation

A 128-point IFFT was used in the simulation. If the IFFT input is numbered from 0 – 127, 0 is sent as an input at location 0. Sub-carriers 1 through 61 are sent at locations 1 – 61. Five (5) zeros are sent at locations 62 through 66. Sub-carriers (-61) through (-1) are sent at locations 67 – 128.

An IFFT/FFT operation is performed at the transmitter/receiver respectively. At the receiver after performing the FFT the sub-carriers with zeros and guard tones

are discarded. Only the data and pilot sub-carriers are used for rest of the receiver processing.

6.1.7 Time Spreading/De-spreading

In the time spreading block, each OFDM symbol is transmitted twice. At the receiver the OFDM symbols are combined before being sent to the de-interleaver block.

After the time spreading block, the guard samples and prefix samples are inserted which are then fed to the DAC and subsequently fed to the radio. At the receiver, the signal is down converted, acquired and fed through the rest of the data path for demodulation.

6.1.8 RF Radio

In the simulation all the RF components namely the DAC, ADC, Mixer, Frequency Synthesizer, LNA, Tx/Rx filter, VGA etc. have been simulated. All the components are assumed to be ideal and no non-linearities (e.g. phase noise, IP2 etc.) have been taken into account.

6.1.9 Channel Models

Four channel models are defined for the IEEE 802.15.3a simulations. The channel models vary in their statistical properties (*i.e.*, delay spread, amount of clustering of multipath rays etc.) Six key parameters differentiate between the four channels [54].

Λ = cluster arrival rate;

λ = ray arrival rate, i.e., the arrival rate of path within each cluster;

Γ = cluster decay factor;

γ = ray decay factor;

σ_1 = standard deviation of cluster lognormal fading term (dB).

σ_2 = standard deviation of ray lognormal fading term (dB).

σ_x = standard deviation of lognormal shadowing term for total multipath realization (dB).

The main characteristics of the channel which the model parameters try to meet is [54]

1) Mean excess delay
2) RMS delay spread
3) Number of multipath components (defined as the number of multipath arrivals that are within 10 dB of the peak multipath arrival)
4) Power decay profile

The channel models are named CM1, CM2, CM3 and CM4. The statistical properties of the different channel models are shown in Table 6.2 below [54].

Table 6.2 Channel Model Summary

Target Channel Characteristics[5]	**CM 1**[1]	**CM 2**[2]	**CM 3**[3]	**CM 4**[4]
Mean excess delay (nsec) (τ_m)	5.05	10.38	14.18	
RMS delay (nsec) (τ_{rms})	5.28	8.03	14.28	25
NP_{10dB}			35	
NP (85%)	24	36.1	61.54	
Model Parameters				
Λ (1/nsec)	0.0233	0.4	0.0667	0.0667
λ (1/nsec)	2.5	0.5	2.1	2.1
Γ	7.1	5.5	14.00	24.00
γ	4.3	6.7	7.9	12
σ_1 (dB)	3.3941	3.3941	3.3941	3.3941
σ_2 (dB)	3.3941	3.3941	3.3941	3.3941
σ_x (dB)	3	3	3	3
Model Characteristics[5]				
Mean excess delay (nsec) (τ_m)	5.0	9.9	15.9	30.1
RMS delay (nsec) (τ_{rms})	5	8	15	25
NP_{10dB}	12.5	15.3	24.9	41.2
NP (85%)	20.8	33.9	64.7	123.3
Channel energy mean (dB)	-0.4	-0.5	0.0	0.3
Channel energy std (dB)	2.9	3.1	3.1	2.7

[1] This model is based on LOS (0-4m) channel measurements reported in [55].

[2] This model is based on NLOS (0-4m) channel measurements reported in [55].

[3] This model is based on NLOS (4-10m) channel measurements reported in [55], and NLOS measurements reported in [56].

[4] This model was generated to fit a 25 nsec RMS delay spread to represent an extreme NLOS multipath channel.

[5] These characteristics are based upon a 167 psec sampling time.

Only Channel model CM3 was used for the simulations below. A path loss exponent of 2 was assumed for large scale fading in the simulations.

6.2 Techniques for Improving MB-OFDM

In section 6.2.1, the importance of time interleaving over 3 OFDM symbols is studied. While studying the MB-OFDM proposal, a method to improve the frequency diversity of the system was proposed and simulations were run in order to show that the performance of the current system could be improved by employing the technique. This will be discussed in section 6.2.2. A disclosure has also been filed with regards to the proposed technique. Both of these techniques are physical layer techniques for improving physical layer performance.

Simulations were also run in order to evaluate techniques to improve the performance of Simultaneously Operating Piconets (SOP). This topic is discussed in Section 6.2.3. Here we examine physical layer techniques to improve MAC performance.

6.2.1 Effect of time interleaving

Simulations were run in order to determine the effect of interleaving on the performance of the system. Figure 6.3 below shows the performance of the current MB-OFDM system in the absence/presence of symbol and tone interleaving in Channel model CM3.

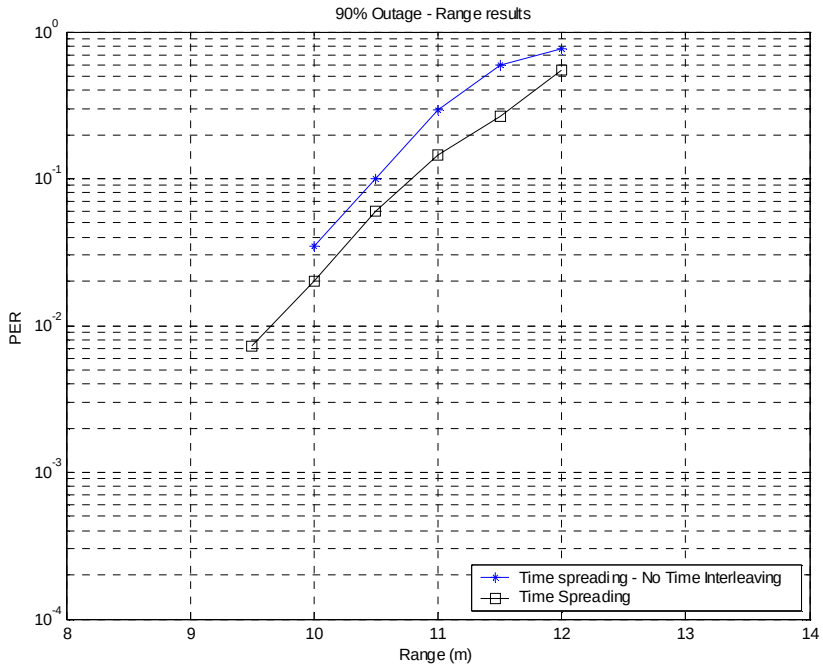

Figure 6.3 Effect of time and tone interleaving in a MB-OFDM system

It is noticed that without the presence of symbol and tone interleaving, the performance of the system deteriorates slightly. The reason for the reduction in range is the reduced frequency diversity of the system. If the bits are not interleaved, all the adjacent bits are transmitted in the same frequency band. If the coherence bandwidth of the channel is very large, then all the adjacent sub-carriers in that bandwidth experience similar fading conditions which lead to adjacent bits being corrupted. The coherence bandwidth of the channel is of the order to 3 - 4 MHz. This is not a desirable effect as the Viterbi decoder is not very efficient in correcting burst errors. On the other hand if the bits are interleaved, adjacent bits no longer appear in the same frequency band and hence the system has more frequency diversity.

Figure 6.4, Figure 6.5 and Figure 6.6 show the performance of the system in the presence of interfering piconets.

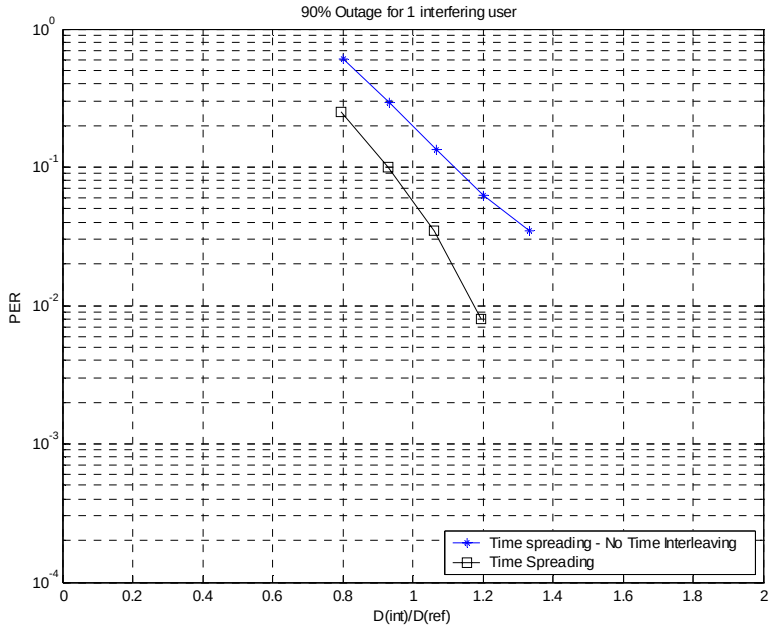

Figure 6.4 SOP Performance Comparison – 1 interfering piconet (Effect of Time Interleaving)

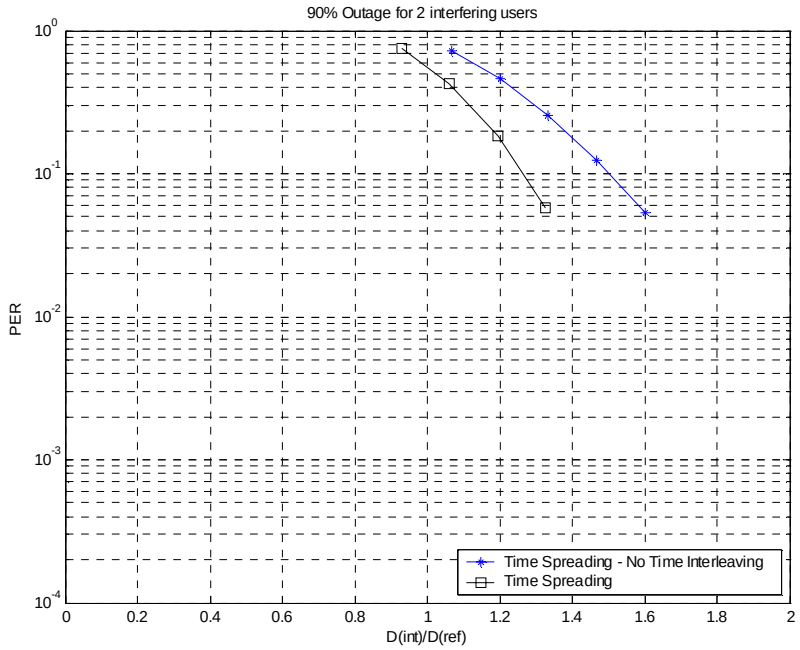

Figure 6.5 SOP Performance Comparison – 2 interfering piconets (Effect of Time Interleaving)

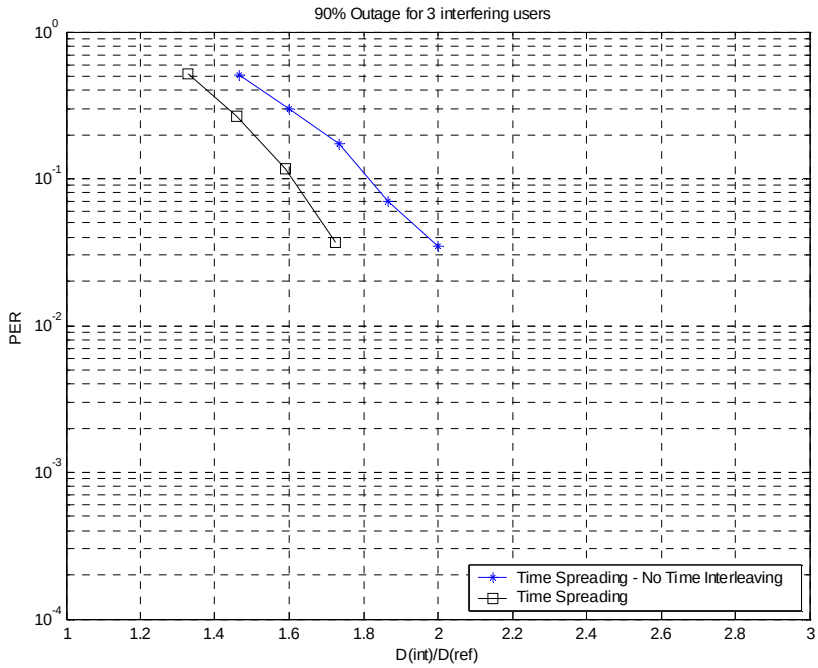

Figure 6.6 SOP Performance Comparison – 3 interfering piconets (Effect of Time Interleaving)

As noticed in the figures above, the performance of the MB-OFDM system deteriorates without symbol and tone interleaving. The primary reason for this is that if a particular hop band is hit due to the presence of another piconet and if the bits are not interleaved, all the adjacent bits get corrupted. This leads to burst errors which the Viterbi decoder is unable to correct effectively. On the other hand, if the bits are interleaved and a particular band is hit by interference, the bits corrupted are far apart (after de-interleaving) and hence such a system is more resilient to interfering piconets.

A summary of the results presented in this section are tabulated in Table 6.3 and Table 6.4 below.

Table 6.3 Simulation Results – Range Performance comparison (No time spreading vs. Time Spreading)

Schemes	Time Spreading (Current MBOA proposal)	Time Spreading (without symbol/tone interleaving)
Range (8% PER, @110 Mbps)	10.7 meters	10.35 meters

Table 6.4 Simulation Results – SOP Performance (@110 Mbps)

@ 110 Mbps	1 interfering piconet (dint/dref)	2 interfering piconets (dint/dref)	3 interfering piconets (dint/dref)
Time Spreading (Current MBOA proposal)	0.95	1.3	1.62
Time Spreading (without symbol/tone interleaving)	1.15	1.55	1.82

6.2.2 Bit-order reversal for MB-OFDM

The current MB-OFDM solution does not take complete advantage of the frequency diversity provided by the system due to different frequency bands used in the system. The following discussion explains the concept in more detail.

As explained in Section 6.1.2, the MB-OFDM system interleaves bits out of the convolutional encoder between three OFDM symbols and again within an OFDM symbol. For data rates greater than 110 Mbps we know that each OFDM symbol consists of 200 bits. For complete interleaving over three OFDM symbols 600 bits would be required. Let us number the bits coming out of the convolutional encoder/puncturer block 1 to 600. The mapping of the bits to different frequency bands and OFDM symbols is shown in figure below.

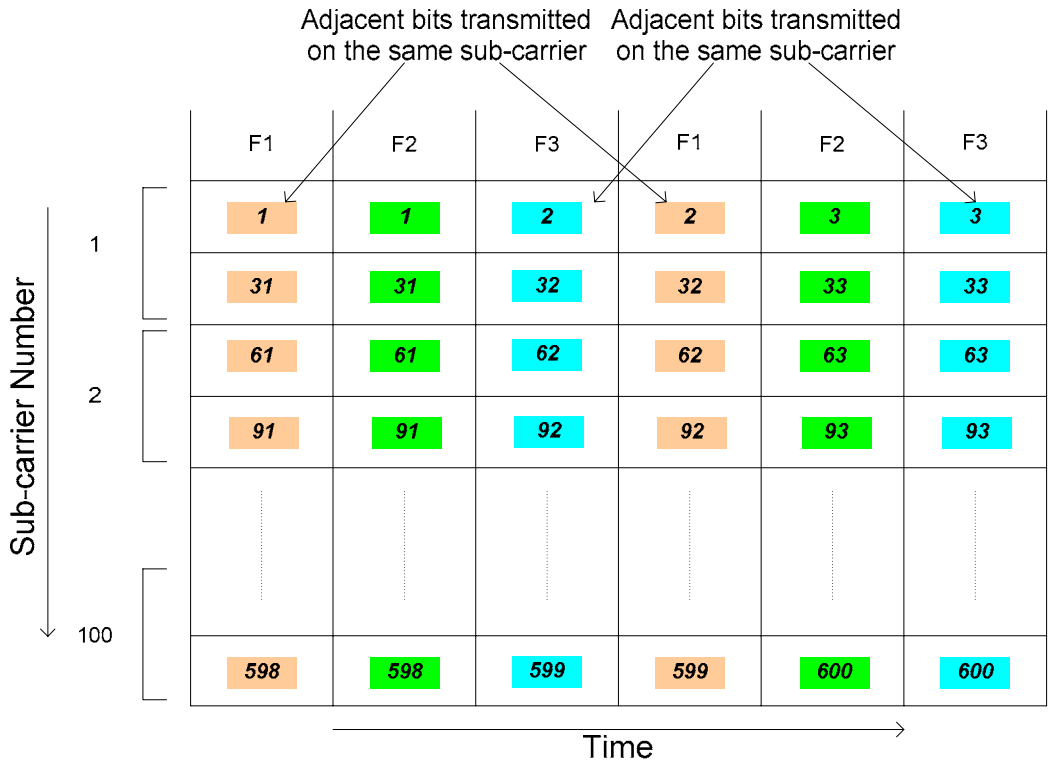

Figure 6.7 Time Spreading for current MB-OFDM system

As we see in Figure 6.7 above, adjacent bits from the puncturer block appear on the same sub-carrier in the same frequency band. This means that if a particular sub-carrier is in a deep fade, then the adjacent bits would be affected. This is not very desirable because the Viterbi decoder does not work very well in the presence of burst errors. This interleaving scheme does not take complete advantage of the frequency diversity offered by the system.

In order to take care of this problem it should be made sure that adjacent bits are not transmitted on the same sub-carrier. This would reduce the number of burst errors which in turn would lead to better performance by the Viterbi decoder. A technique called bit-order reversal was proposed which takes care of the problem with no increase in the complexity of the system and very minimal increase in power consumption. Several other techniques were investigated but this was

finally proposed to the MB-OFDM technical sub-committee due to the ease of implementation of the technique.

In the bit-order reversal scheme, the bits transmitted in the time repeated version of the original symbol are sent after reversing the order of the bits of the original symbol. The bits transmitted for the new scheme is shown in Figure 6.8 below.

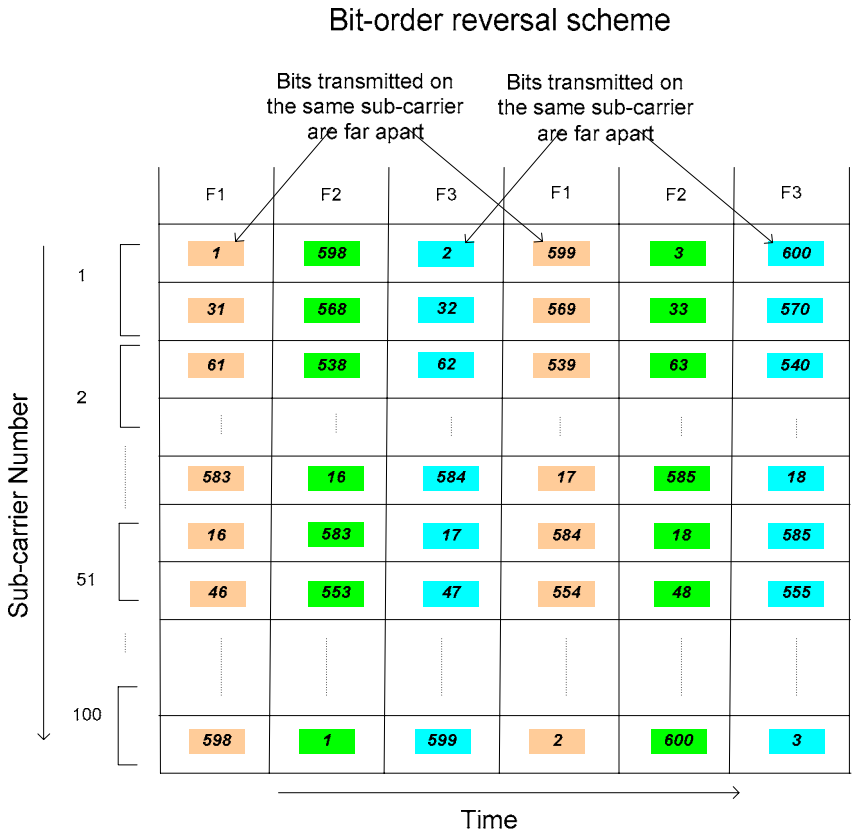

Figure 6.8 Bit-order reversal scheme for MB-OFDM systems

As we see in Figure 6.8, adjacent bits out of the puncturer are no longer transmitted on adjacent sub-carriers which leads to fewer burst errors and hence should improve the performance of the system.

For 55 and 80 Mbps modes, since the bits are complex conjugate repeated in each OFDM symbol, a bit order reversed OFDM symbol appears to be similar to the

original time spread OFDM symbol and hence would not give any improvement in performance. To take care of the problem for lower data rates the following scheme was proposed. For data rates 55 and 80 Mbps, we know that 300 bits are required for interleaving (as each OFDM consists of 100 bits and an interleaver block is 3 OFDM symbols deep). For these cases, only the 100 bits in an OFDM symbol are bit-order reversed and then the bits are complex conjugated. Figure 6.9 below illustrates the methodology both for the lower and higher data rates.

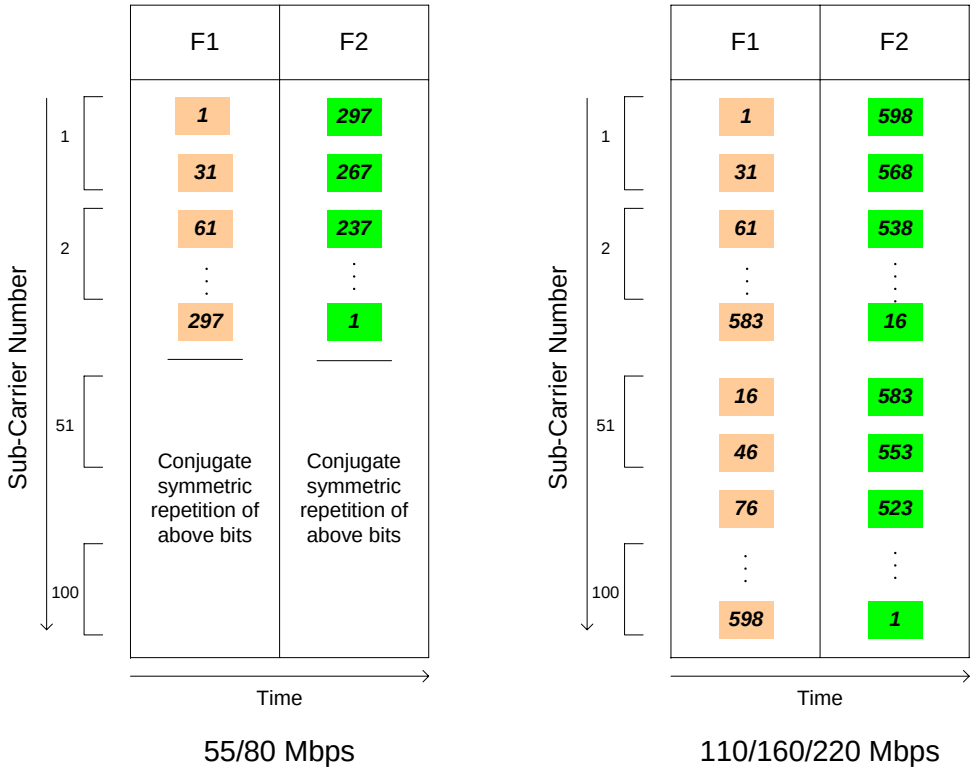

Figure 6.9 Bit-order reversal for 55/80 Mbps and 110/160/200 Mbps

Range and performance of the system under simultaneously operating piconets was simulated and the results are shown below. The range of the proposed scheme was compared against the present MB-OFDM scheme.

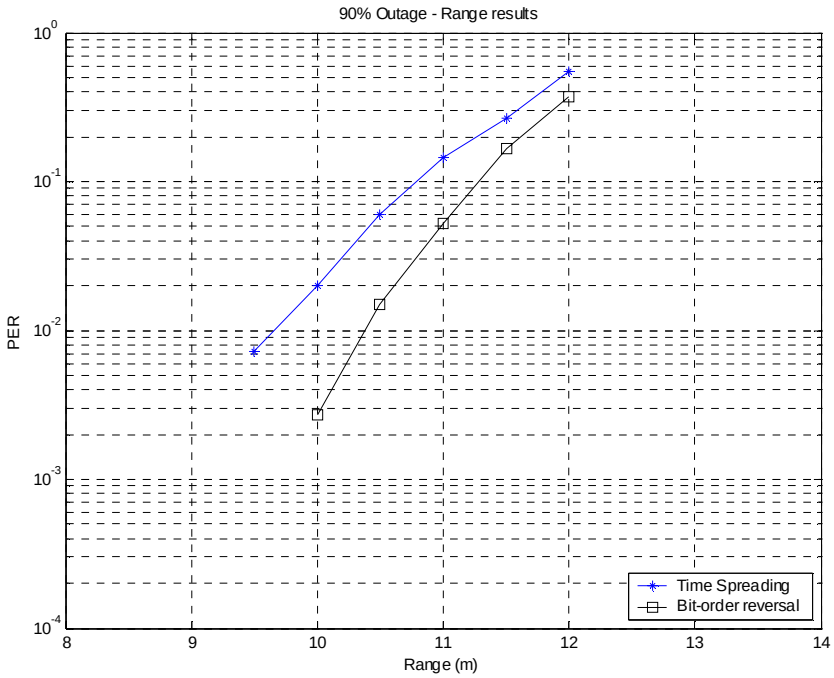

Figure 6.10 Range comparison – Bit order reversal vs. Current MB-OFDM (110 Mbps)

In Figure 6.10, the 90% outage probability for a packet error rate has been plotted versus range. The methodology for calculating the 90% outage probability is described below. For each channel model (CM1 – CM4), 100 channel realizations were simulated. The channels were ordered best to worst on the basis of the error probability of the channel. Out of the 100 channel realizations, the worst 10 channels are discarded and out of the remaining 90 best channels, the error probability of the 90th channel is chosen to give the 90% outage error probability.

It is seen that the proposed system increases the performance of the existing time spreading system by ~0.5 meters (~0.3 dB) at a data rate of 110 Mbps. It should also be noted that systems with higher data rates (for example 200 Mbps) would have less frequency diversity in the system and this scheme should give even greater improvement in range.

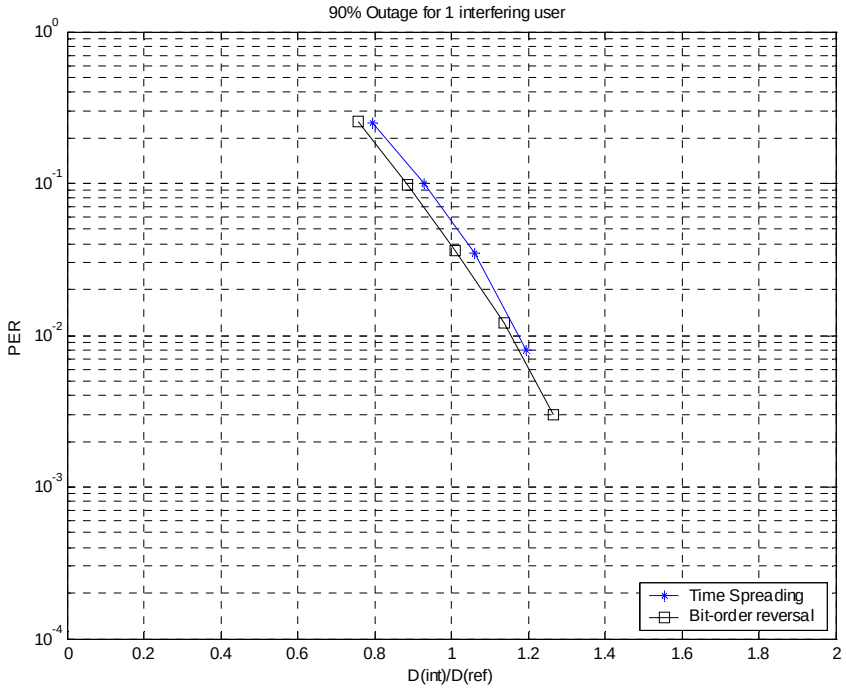

Figure 6.11 SOP Performance comparison – 1 interfering piconet

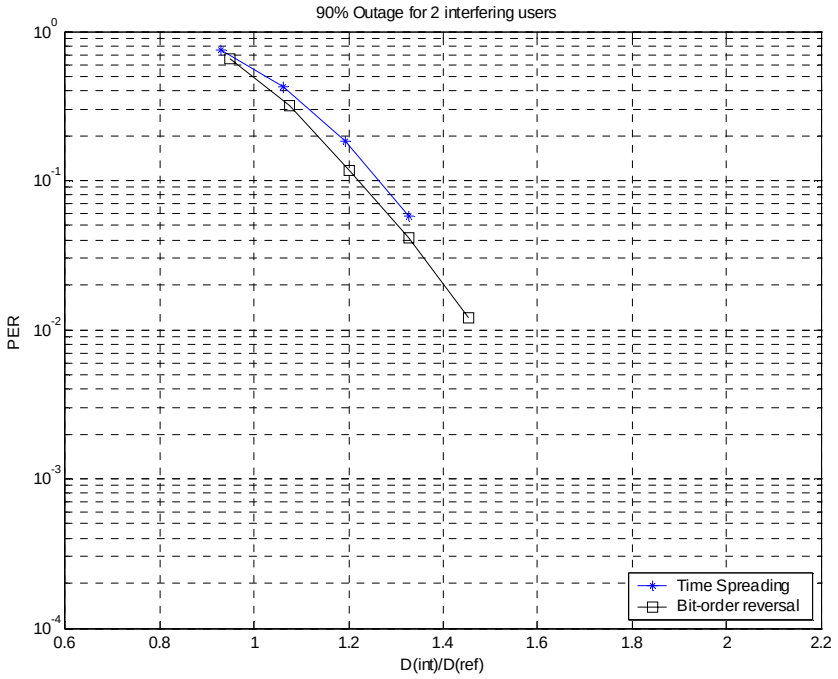

Figure 6.12 SOP Performance Comparison – 2 interfering piconets

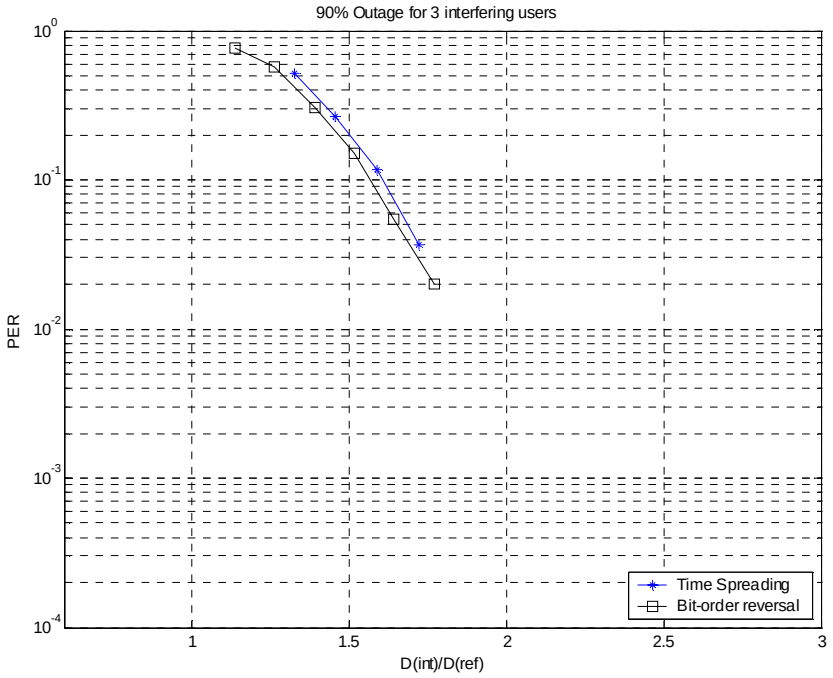

Figure 6.13 SOP Performance Comparison – 3 interfering piconets

In Figure 6.11, Figure 6.12 and Figure 6.13 the performance of the proposed scheme has been simulated in the presence of un-coordinated piconets and compared to the present MB-OFDM scheme. "Un-coordinated piconets" refers to the fact that the hop timing of each of the piconets is independent with respect to each other. The reference piconet uses time frequency code 1 whereas the interfering piconets use the rest of the time frequency codes. Each interfering piconet used a different time frequency code. For the SOP simulations the reference piconet was assumed to be operating at 3dB higher power than required for an 8% outage packet error rate in the absence of other piconets. Shadowing was turned off for the SOP simulations. On the x-axis, the ratio of the distance of the interfering piconet (d_{int}) from the receiver to the distance of the reference piconet from the receiver (d_{ref}) is plotted. On the y-axis, the 90% outage packet error rate is plotted. In practice a d_{int}/d_{ref} of 0 is always desired for any amount of interfering piconets. For the plots above, the reference piconet is kept at a fixed distance from the receiver and the distance of the interfering piconet is varied to

get different d_{int}/d_{ref} quantities. In the case of multiple piconets, all the piconets are assumed to be at equal distance from the receiver.

As seen in the figures above, the proposed scheme does not improve the performance of the current MB-OFDM system in the presence of interference. This is expected because the proposed bit-order reversal scheme should only help increase the frequency diversity of the system and hence should increase the range of the system. How well a system performs in the presence of interference is dependent on how many OFDM collide with those of the interfering piconet(s). The small discrepancies in the curves for SOP performance are expected due to simulation noise.

A similar comparison for range was done for the 55 and 200 Mbps modes. The results are shown in Figure 6.14 and Figure 6.15.

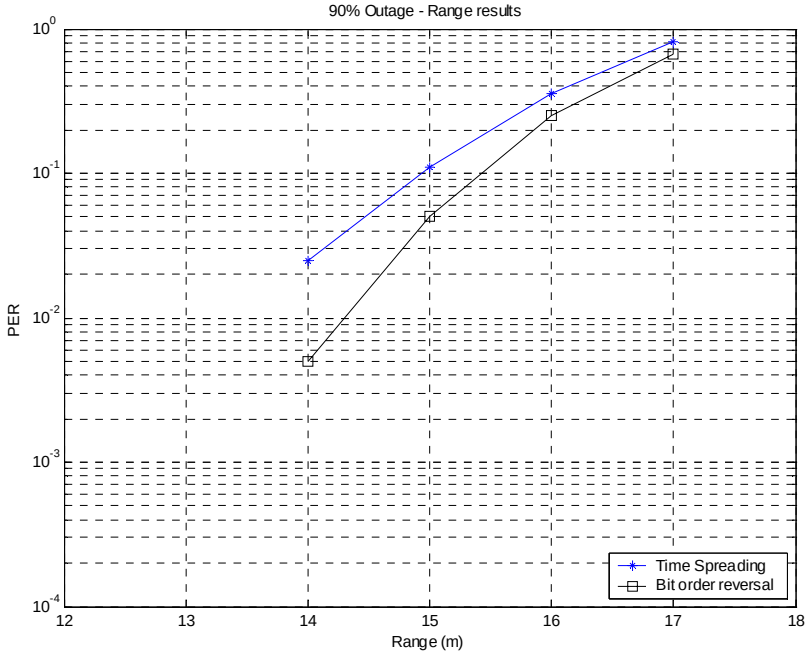

Figure 6.14 Range comparison - Bit order reversal vs. Current MB-OFDM (55 Mbps)

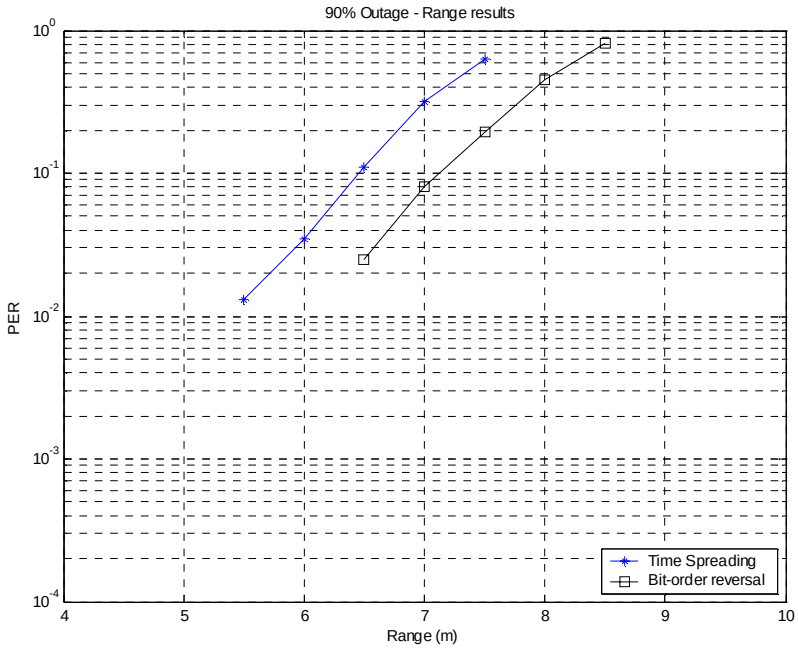

Figure 6.15 – Range comparison - Bit order reversal vs. Current MB-OFDM (200Mbps)

As shown in Figure 6.14 and Figure 6.15 above, the proposed scheme outperforms the present proposal for the 55 Mbps and 200 Mbps modes. A similar pattern is expected to be seen for the rest of the data rates, although they were not simulated. The amount of improvement in performance is dependent upon the amount of frequency diversity already present in the system. If the frequency diversity in the system is less, the gains would be more as in the case of 110 Mbps or higher data rates. If there is already significant frequency diversity, the gains would be less as for the 55 Mbps mode.

A summary of the results is given in Table 6.5 and Table 6.6 below.

Table 6.5 Simulation Results – Range Performance

Schemes	Range (55 Mbps)	Range (110 Mbps)	Range (200 Mbps)
Current MBOA proposal	14.9 meters	10.7 meters	6.4 meters
Bit-order reversal	15.3 meters	11.2 meters	7 meters
Improvement	0.4 meters	0.5 meters	0.6 meters
Improvement (dB)	~0.3 dB	~0.5 dB	~0.7 dB

Table 6.6 Simulation Results – SOP Performance (@110 Mbps)

@ 110 Mbps	1 interfering piconet (d_{int}/d_{ref})	2 interfering piconets (d_{int}/d_{ref})	3 interfering piconets (d_{int}/d_{ref})
Current MBOA proposal	0.96	1.29	1.64
Bit-order reversal	0.91	1.24	1.6

As seen below the proposed technique increases the performance of the system substantially in terms of range. For SOP the performance of the system remained unchanged. It is currently being actively considered as an option to replace the existing time spreading proposal. The proposed scheme requires a very minimal change in logic in order to swap the bits coming out of the puncturer. For data rates 110, 160 and 200 Mbps, the same effect could also be achieved by swapping In-phase (I) and Quadrature (Q) components of the complex signal coming out of the IFFT for every OFDM symbol and re-transmitting that OFDM symbol. For example, if the first OFDM symbol transmitted from the IFFT is F1, the bit-order reversed version of the same symbol could be obtained by swapping I and Q components of the signal F1 and transmitting it again. The same procedure would be followed for the rest of the OFDM symbols. For 55 and 80 Mbps modes, the bit-order reversal needs to be done before the IFFT which leads to sending the same OFDM twice through the IFFT and increases the power consumption slightly.

6.2.3 Half Pulse Repetition Frequency (PRF) vs. Time Spreading

Various schemes have been proposed to improve the SOP performance of the MB-OFDM system. In this section, a half pulse repetition frequency (PRF) scheme is compared against the time spreading scheme in terms of range and SOP. Identical simulation scenarios were created for both the cases as was done for all the simulations presented above. In the original proposal, the 55, 80, 110, 160 and 200 Mbps modes have complex conjugate symmetry around the center frequency. In the time spreading scheme 200 bits are being transmitted in each OFDM symbol. Each OFDM symbol is now transmitted two times which reduces the data rate by a factor of two. In the end there the data rate of the system remains the same.

Half PRF was a technique initially proposed by Wisair to improve the SOP performance of the system. The idea was to increase the number of coded bits per OFDM symbol by getting rid of the complex conjugate symmetry. The same data rate is then maintained by transmitting bits for half of the time in a particular dwell in each band. This concept is similar to that of time spreading since complex conjugate symmetry is removed in the time spreading scheme also. The only difference is that in time spreading the OFDM symbol is transmitted all the time during its dwell in a particular frequency band. The data rate is kept the same by transmitting the same OFDM symbol twice.

Figure 6.16 below illustrates how Half PRF is expected to improve the SOP performance of the system over the time spreading scheme.

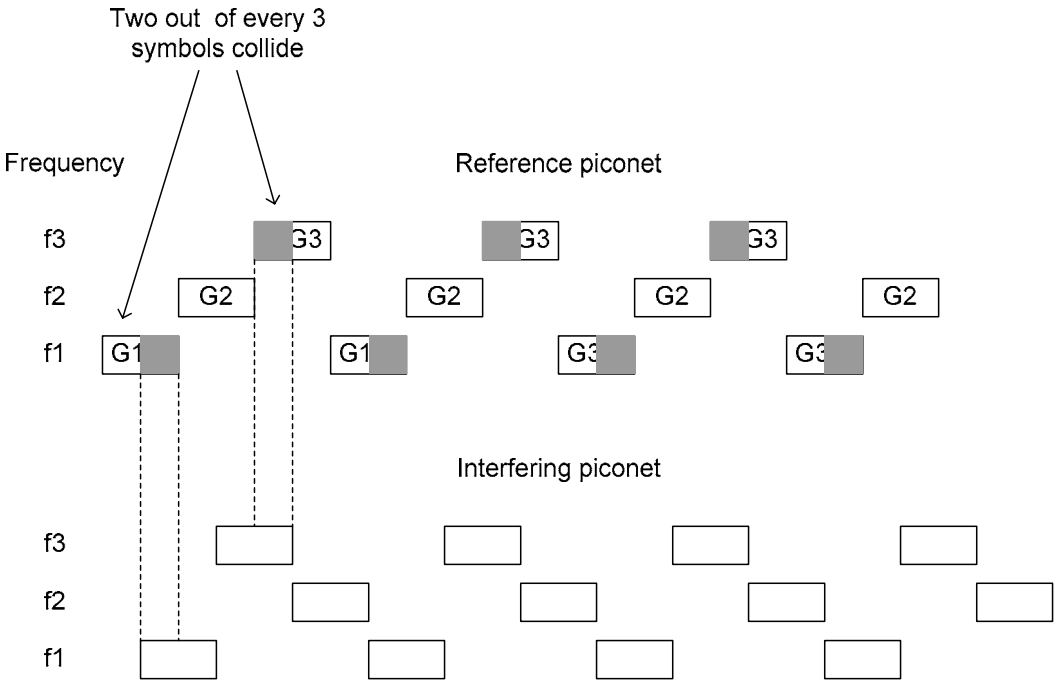

Figure 6.16 SOP Scenario - Original MB-OFDM proposal

In the above figure let G1, G2 and G3 represent the outputs of the 3 generator polynomials from the convolutional encoder (The same nomenclature will be used for the figures shown below). In order to have minimum error in the decoding process, it is desirable that all the bits in the three OFDM symbols corresponding to the three generator polynomials are received without any interference. In the original MB-OFDM proposal, an example SOP scenario is shown in Figure 6.16 above. It is seen that in the presence of 1 interfering piconet, on an average 2 out of three of the bits of the generator polynomial are destroyed which increases the error in the decoding process. An example SOP scenario using half PRF scheme is shown in Figure 6.17 below. It is noticed that in the half PRF scheme the user is only transmitting for half the amount of time in each dwell. As a result, only one out of three OFDM symbols collide which is expected to increase the performance of the system. It should be noted that in the half PRF scheme, the bits should be transmitted with 3 dB more power to achieve the same energy per symbol since they are transmitted only for half the amount of time.

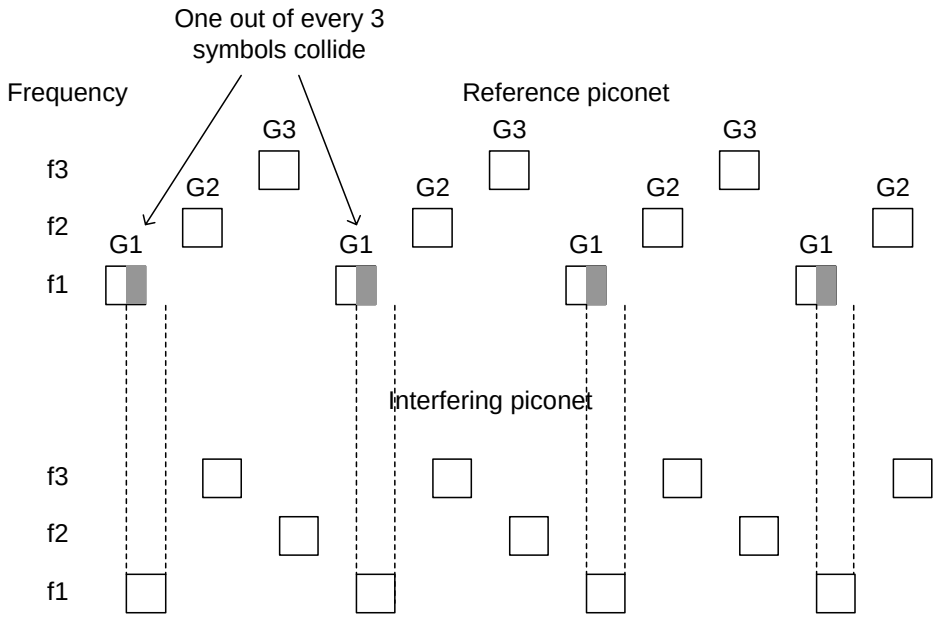

Figure 6.17 SOP Scenario – Half PRF proposal

A similar illustration with the time spreading scheme and the effect of 1 interfering piconet is shown in Figure 6.18 below. It is again noticed that since the bits are transmitted all the time more OFDM collide. However, it should be noted that since the same OFDM symbol is transmitted twice, the system is more resilient to collisions. Even though the bits in one particular band might be corrupted due to collision, the same bits would be transmitted in the adjacent frequency band which may not be corrupted by collisions. Combining the two OFDM symbols would negate the effect of more of the collisions in the time spreading scheme as compared to the Half PRF scheme. It should also be noted that the transmitted power in this scheme is not 3dB more than the original scheme.

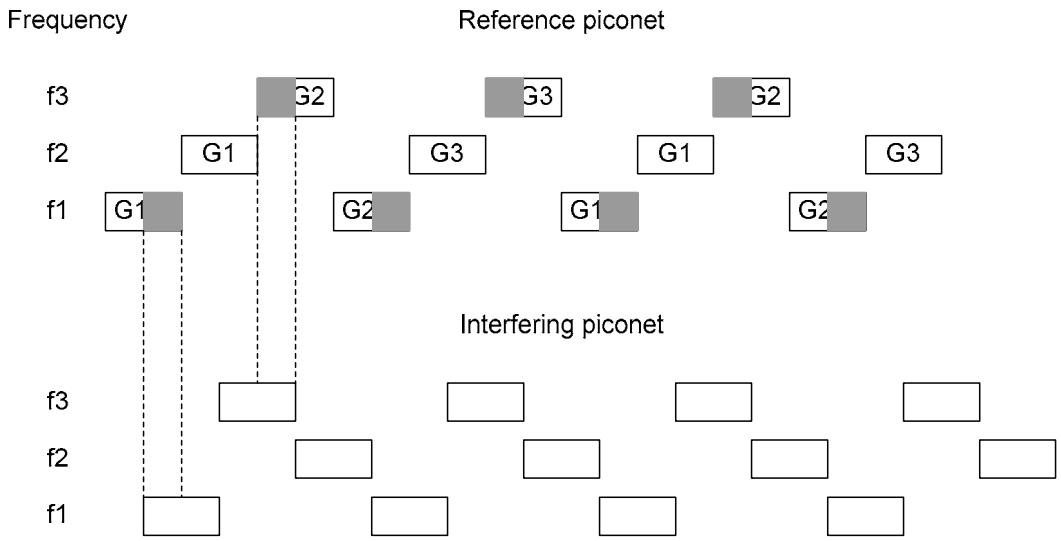

Figure 6.18 SOP Scenario – Time Spreading proposal

In should be noted that in the presence of 2 or 3 interfering piconets, it is not possible to isolate the OFDM symbols which collide since the patterns are no longer deterministic. In most cases, all of the OFDM symbols are affected by colliding symbols from interfering piconets.

An extensive simulation analysis of the proposed schemes was performed for the 110 Mbps data rates mode and the results are discussed below. Figure 6.19 shows the range results for both proposals. As seen, the half PRF scheme has slightly reduced range as compared to the time spreading scheme. The reason for this is the reduction in the frequency diversity of the system. Since a particular OFDM symbol is only transmitted once, if a particular sub-carrier is in a deep fade it becomes very difficult to recover that bit. On the other hand, in the time spreading scheme, since the same OFDM symbol is transmitted twice on two different frequency bands, even though a sub-carrier in a particular band might be in deep fade, the same sub-carrier in another frequency band might not be in deep fade. This obviously increases the frequency diversity of the system. The Half PRF scheme reduces the frequency diversity of the system by ~ 0.5 dB in terms of range performance.

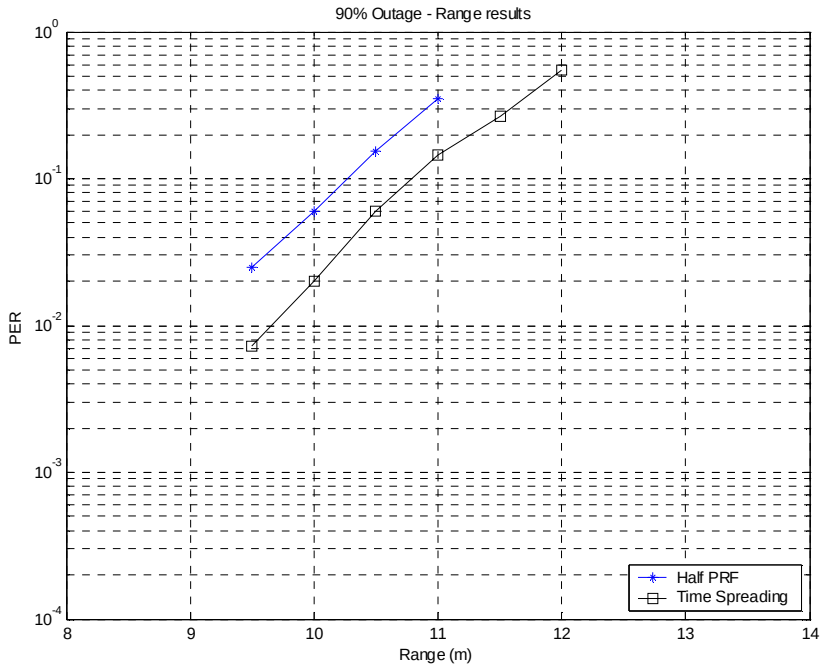

Figure 6.19 Range Comparison – Baseline, Half PRF, Time Spreading

Figure 6.20 below shows the effect of 1 un-coordinated piconet on the two systems. It is seen that the half PRF and the time spreading scheme have dissimilar performance. In the time spreading scheme, each OFDM is transmitted twice. Even though 1 OFDM symbol might have suffered a collision, the second OFDM symbol could be interference-free. This symbol is combined with the corrupted OFDM symbol, hence mitigating the effect of the interfered OFDM symbol on the decoding process. The half PRF does not provide any improvement in performance over the time spreading scheme which is quite contrary to what was expected. The reason for this could be explained with the following argument. In the Half PRF scheme, although only 1 out of 3 OFDM symbols are collided due to the presence of a single interfering piconet, each OFDM symbol is transmitted with 3 dB more power. The interfering piconet also has 3 dB more power and the collided symbols are very badly affected due to the high interference power. This combined with a reduction in the frequency diversity of

the system leads to poor SOP performance even in the presence of a single interfering piconet.

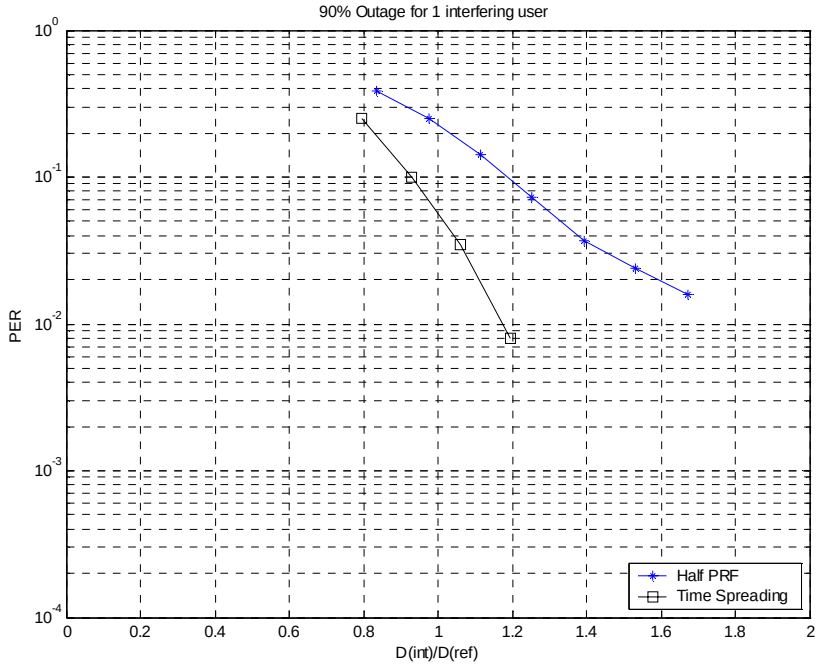

Figure 6.20 SOP Performance comparison – 1 interfering piconet

Results of the two schemes in the presence of 2 and 3 interfering piconets are shown in Figure 6.21 and Figure 6.22 below respectively. Here also it is observed that the half PRF scheme does not perform very well due to the reduction in frequency diversity and the fact that the interferer has 3 dB higher power. This leads to a large number of bit errors.

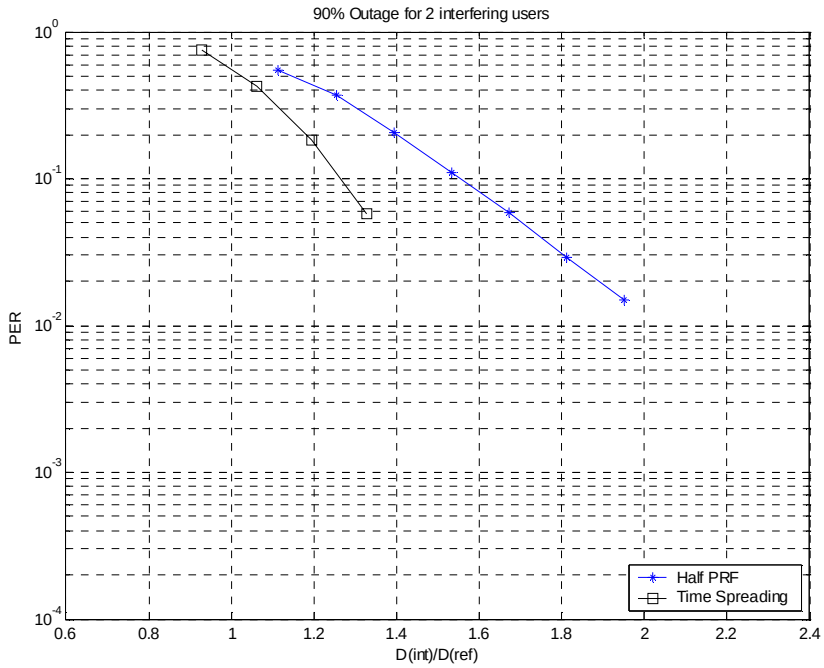

Figure 6.21 SOP performance comparison – 2 interfering piconets

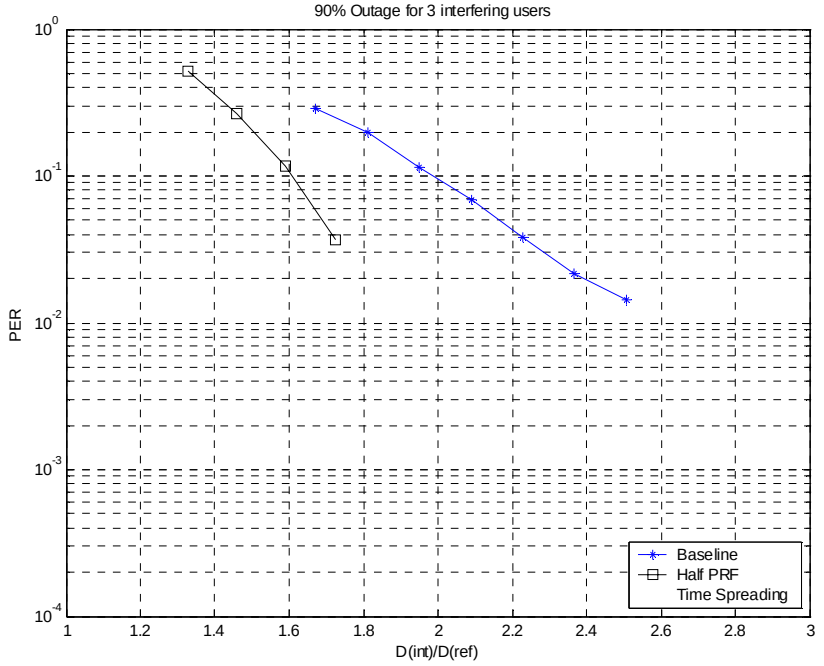

Figure 6.22 SOP performance comparison – 3 interfering piconets

A summary of the results of this section is given in Table 6.7 and Table 6.8 below. As we see, both of the proposed schemes reduce the range of the original OFDM system.

Table 6.7 Simulation Results – Range Performance comparison (Half PRF vs. Time Spreading)

Schemes	Time Spreading (Current MBOA proposal)	Half PRF
Range (8% PER, @110 Mbps)	10.7 meters	10.15 meters

Table 6.8 Simulation Results – SOP Performance (@110 Mbps)

@ 110 Mbps	1 interfering piconet (dint/dref)	2 interfering piconets (dint/dref)	3 interfering piconets (dint/dref)
Time Spreading (Current MBOA proposal)	0.9	1.24	1.6
Half PRF	1.24	1.60	2.05

6.3 Conclusions

In this chapter of the thesis, the Multiband-OFDM proposal was simulated in detail and simulations were carried to investigate/improve three different aspects of the system.

1) Firstly, the use of time interleaving was investigated. It was found that time interleaving is very important for the whole system as it increases the frequency diversity and hence increases the range of the system.

2) A novel technique was proposed which further increases the frequency diversity of the system. Extensive simulations were performed and it was shown that the frequency diversity of the system can be increased by 0.5 dB for the 110

Mbps mode. The increase in performance is expected to be higher for higher data rates.

3) Two competing schemes proposed to increase the performance of the systems in the presence of simultaneously operating piconets were simulated and their advantages/disadvantages were compared. In was shown the time spreading scheme outperforms the Half-PRF scheme in terms of range as well as interference rejection capability in the presence of 1, 2 or 3 simultaneously operating piconets.

Chapter 7

7 Conclusions and Future Work

7.1 Introduction

In this chapter, the summary of all the work presented in the prior chapters has been presented. The conclusions are based on the results obtained for the various scenarios simulated for the proposed MAC for Impulse Radio based UWB networks presented in Chapter 4 and the Multiband-OFDM based simulations the results of which were presented in Chapter 6. Furthermore, some areas for continued research have been identified and stated.

7.2 Summary and Conclusions of proposed MAC (CDMA based code-broker approach)

UWB as a technology has been defined co-exist with other users allocated services in the spectrum. Due to this UWB devices should provide minimum interference to the services already existing in their allocated bands. The power spectral density for UWB devices has been defined to be -41.3 dBm/MHz which puts a constraint on the maximum possible power transmitted from a device. This puts a basic limitation of the range achievable by any UWB device. To achieve a particular range a specified amount of energy per bit needs to be transmitted. Due to the low transmit power requirements, the only way to achieve that kind of energy per bit is by spreading the bit to be transmitted or by transmitting it multiple times. This reduces the throughput of the system and allows various other interesting options for communications as opposed to the traditional CSMA based network.

Keeping in mind the emerging new technologies (UWB networks), a new MAC layer scheme has been proposed which works on a code-broker approach and a centralized architecture. This approach is most suitable for Impulse Radio kind of implementations of UWB networks. The complete physical layer and some part of the MAC layer were simulated and the scheme was compared with traditional CSMA based networks. A comparison of the scheme was also made with the Receiver code assignment based scheme [16] and the results of both the comparisons were provided in Chapter 4. The schemes were compared in terms of latency vs. throughput, network load vs. throughput, network load vs. latency and packet error rate vs. network load.

In Chapter 3 the whole algorithm was explained and the results were presented in Chapter 4. The following conclusions can be derived from the simulation results obtained

1) If a comparison is made between both the systems using a UWB spread spectrum system i.e. each pulse being spread by a length 31 gold code, then as discussed previously, the proposed CDMA scheme outperforms the CSMA scheme completely. In other words, the proposed CDMA based code-broker approach has better throughput-delay characteristics as compared to the CSMA based network.
2) If the CSMA based network is not spread by a spreading code and a comparison of the scheme is done with the proposed system which uses spreads the signal by a length 31 code, the CSMA based scheme would outperform the proposed scheme.
3) In the comparison of the proposed scheme with the receiver code assignment based scheme, it was concluded that the proposed scheme performs slightly well than the later scheme stated above. The reason primarily being the absence of primary interferers in the channel for the proposed scheme which leads to lesser acquisition errors and hence more improvement in throughput in the system. For the receiver code assignment based scheme, primary interference is present due to imperfect

channel sensing which leads to a reduction in the throughput of the system. The latency to join the network was found out to be smaller for both the receiver based code assignment scheme as compared to the proposed scheme. This is primarily due to the fact that for the former scheme, the node does not need to associate with the code-broker in order to obtain a code.

4) When the system has a higher path loss exponent, the overall throughput of the system increases for both the schemes. The latency to join the network decreases with an increase in the path loss exponent.

7.3 Future Research Directions for the proposed code-broker scheme

Some possible methods to improve the scheme and the comparison with various other schemes have been outlined below.

1) Incorporation of more realistic packet arrival models (e.g., Poisson packet arrival rate, exponentially distributed on-off source, etc.) would give more realistic numbers of throughput/latency.
2) Intra-piconet interferences can be taken into account.
3) The whole system model of selection of a code-set could be simulated in order to se the probability of two adjacent piconets choosing the same code-set.
4) Multipath scenarios can be incorporated in the model to get more realistic scenarios. Rake receivers would have to be employed at the receiver in the case of multipath.
5) Simulations could be carried out on the basis on transmitted power instead of E_b/N_o.
6) Comparisons with the transmitted based code assignment scheme could be done to see any difference between the two schemes.

7) Since the algorithm is still in its infancy, there might still be ways to improve the algorithm and test it against various other proposed algorithms.
8) Power control kind of mechanisms could be deployed which would take care of the near-far problem.

7.4 Summary and Conclusions of Multiband-OFDM based simulations

In Chapter 5 a complete description of the 802.15.3 MAC and 802.15.3a PHY layer was provided. The specific parameters of the simulated system were provided in Chapter 6. Furthermore, in Chapter 6 three different scenarios were simulated and a methodology to increase the system performance was proposed.

1) The effect of time interleaving in the current Multiband-OFDM scheme was studied. The system performance was quantified in terms of range as well as resilience to SOP.
2) A novel bit-order reversal scheme was presented in order to increase the performance of the system by taking advantage of the frequency diversity provided by the system. The system performance was compared in terms of range as well as resilience to simultaneously operating piconets (SOP).
3) Finally, a comparison between the Half PRF (Pulse Repetition Frequency) and the Time Spreading scheme was done. Both the schemes were proposed in to decrease the effect of SOP on the system. Here also, the system performance was compared in terms of range as well as resilience to SOP.

The following conclusions can be derived from the simulation results obtained

1) Time interleaving gives an improvement in performance of the system (in terms of range) and was deemed to be important from the simulations.
2) Removal of time interleaving also affects the SOP performance of the system (i.e., reduces it).

3) Keeping both the above points in mind time interleaving across OFDM symbols is recommended to be kept in the system.
4) The bit-order reversal scheme significantly improves the performance of the present system in terms of range by taking advantage of the inherent frequency diversity provided by the system.
5) The improvement in range is greater for higher data rates as compared to lower data rates. This is due to the fact that lower data rates already take quite a lot of advantage of the frequency diversity provided by the system and hence the gains are smaller.
6) The bit-order reversal scheme does not make any difference in the performance of the system in terms of SOP.
7) The Half PRF scheme was lower range than the time spreading scheme. This is due to the fact that the Half PRF scheme has lower frequency diversity in the system.
8) The Half PRF scheme was performs were bad as compared to the time spreading scheme in terms of SOP. This is due to the fact that in Half PRF, the OFDM symbol is sent at twice the transmit power which means that the interferer is also transmitted at twice the power causing more damage to the OFDM symbol of interest. On the other hand in the time spreading scheme, the same OFDM symbol is transmitted twice which would be combined intelligently to mitigate the effect of at least 1 interfering piconet to quite some extent.

7.5 Future research directions for the MB-OFDM scheme

The MB-OFDM proposal is still under active discussion. Below some issues are outlined which if solved would increase the system performance drastically.

1) The SOP performance of the system is not very good. Consumer electronic companies would like to see a d_{int}/d_{ref} of 0.4 or less for 3 SOP. Some research effort could be put in this direction to come up with a scheme which would try to address this issue.

2) It might be possible to further increase the performance of the system by exploiting the frequency diversity inherently provided in the system.
3) Some method of ranging could be deployed in the system which would take advantage of the short symbols transmitted which in turn give very good resolution of the objects (transmitters/receivers) in the vicinity of a particular user.

Bibliography

[1] Mobile Ad-Hoc Networks, *IETF MANET Working Group.* Available: http://www.ietf.org/html.charters/manet-charter.html.

[2] A. J. GoldSmith, S. B. Wicker, "Design Challenges for Energy-Constrained Ad Hoc Wireless Networks," *IEEE Wireless Communications Magazine,* Vol. 9, No. 4, August 2002, pp. 8-27.

[3] P. Karn, "MACA: A New Channel Access Method for Packet Radio," *Proceedings of Computer Network Conference,* Sept. 1990, pp. 134-40.

[4] V. Bhargavan, "MACAW: A Media Access Protocol for Wireless LAN," *Proceedings of ACM Special Interest Group on Data Communications,* Aug. 1994, pp. 215-25.

[5] Fabrizio Talucci, Mario Gerla, "MACA-BI (MACA By Invitation) A Wireless MAC protocol for High Speed Ad Hoc Networking," *Proceedings of IEEE International Conference on Universal Personal Communications,* Vol. 2, Oct. 1997, pp. 913-917.

[6] F. A. Tobagi and L. Kleinrock, "Packet switching in radio channels: Part II - The hidden terminal problem in carrier sense multiple-access and the busy-tone solution," *IEEE Transactions on Communications,* Vol. COM-23, Dec. 1975, pp. 1417-1433.

[7] F. A. Tobagi and L. Kleinrock, "Packet switching in radio channels: Part III – Polling and (dynamic) split-channel reservation multiple access," *IEEE Transactions on Communications,* Vol. COM-24, Dec. 1976, pp. 823 -844.

[8] C. Wu and V. O. K. Li, "Receiver-initiated busy-tone multiple access in packet radio networks," *Proceedings of ACM Special Interest Group on Data Communications,* 1987, pp. 336-342.

[9] C. L. Fullmer and J. J. Garcia-Luna-Aceves, "Floor acquisition multiple access (FAMA) for packet-radio networks," *Proceedings of ACM Special Interest Group on Data Communications,* 1995, pp. 262–273.

[10] ____, "Solutions to hidden terminal problems in wireless networks," *Proceedings of ACM Special Interest Group on Data Communications,* 1997, pp. 39–49.

[11] A. C. V. Gummalla and J. O. Limb, "Design of an access mechanism for a high speed distributed wireless LAN," *IEEE Journal on Selected Areas in Communications,* Vol. 18, No. 9, Sept. 2000, pp. 1740-1750.

[12] Z. J. Haas, J. Deng, "Dual Busy Tone Multiple Access (DBTMA) – A Multiple Access Control Scheme for Ad Hoc Networks," *IEEE Transactions on Communications,* Vol. 50, No. 6, June 2002, pp. 975-985.

[13] Wireless LAN MAC and Physical Layer Specifications, IEEE 802.11, 1999. Available: http://standards.ieee.org/getieee802/802.11.html.

[14] D. J. Goodman, R. A. Valenzula, K. T. Gayliard, B. Ramamurthi, "Packet Reservation Multiple Access for Local Wireless Communications," *IEEE Transactions on Communications,* Vol. 37, No. 8, August 1989, pp. 885-890.

[15] S. Jiang, J. Rao, D. He, X. Ling, C. C. Ko, "A Simple Distributed PRMA for MANETs," *IEEE Transactions on Vehicular Technology,* Vol. 51, No. 2, March 2002, pp. 293-305.

[16] Sousa E. S., Silvester John A., "Spreading Code Protocols for Distributed Spread-Spectrum Packet Radio Networks," *IEEE Transactions on Communications,* Vol. 36, No. 3, 1973, pp. 272-281.

[17] Mario Joa-Ng, I-Tai Lu, "Spread Spectrum Medium Access Protocol with Collision Avoidance in Mobile Ad-hoc Wireless Network," *IEEE Proceedings of Eighteenth Annual Joint Conference of the Computer and Communications Societies (INFOCOM, 99),* Vol. 2, March 1999, pp. 776-783.

[18] Gand Qiang, Zegji Liu, Susumu Ushuhara, Tadanori Mizuno, "CDMA based Carrier Sense Multiple Access Protocol for Wireless LAN," *Proceedings of Vehicular Technology Conference,* IEEE VTS 53rd , Vol. 2 , May 2001, pp. 1164-1168.

[19] D. P. Gerakoulis, T. N. Saadawi and D. L. Schilling, "A Channel Access Protocol for embedding CSMA on Spread-Spectrum packet radio networks,"

IEEE International conference on Communications, Vol. 1, June 1988, pp. 199-204.

[20] Geng-Sheng Kuo, Po-Chang Ko, "A Collision-free medium access control protocol for flow-oriented Ad-Hoc wireless LAN," *Proceedings of Vehicular Technology Conference,* Vol. 1, May 1999, pp. 325-331.

[21] D. H. Davies, S. A. Gronemeyer, "Performance of slotted ALOHA random access with delay capture and randomized time of interval," *IEEE Transactions on Communications,* Vol. 28, No. 5, May 1980, pp. 703-710.

[22] D. Raychaudhuri, "Performance analysis of random-access packet switched code division multiple access channels," *IEEE Transactions on Communications,* Vol. COM-29, June 1981, pp. 895-901.

[23] F. L. Lo, Tung Sang Ng, Tony T. Yuk, "Performance Analysis of a Fully-Connected Full-Duplex CDMA ALOHA Network with Channel Sensing and Collision Detection," *IEEE Journal On Selected Areas in Communications,* Vol. 14, No. 8, December 1996, pp. 1708-1716.

[24] J. Gronkvist, A. Hansson, J. Nilsson, "A Comparison of Access Methods for Multi-Hop Ad Hoc Radio Networks," *Proceedings of Vehicular Technology Conference,* Vol. 2, May 2000, pp. 1435-1439.

[25] L. D. Nardis, Pierre Baldi, M. G. D. Benedetto, "UWB Ad – Hoc Networks," *IEEE Conference on Ultra Wideband Systems and Technologies,* May 2002, pp. 219-223.

[26] F. Cuomo, C. Martello, "MAC principles for an Ultra Wide Band wireless access," *IEEE Global Telecommunications Conference,* Vol. 6, Nov. 2001, pp. 3548-3552.

[27] Jin Ding, Li Zhao, S. R. Medidi, K. M. Sivalingam, "MAC Protocols for Ultra-Wide-Band (UWB) Wireless Networks: Impact of Channel Acquisition Time." Available: http://www.eecs.wsu.edu/~jding1/paper/ITCOM401-02/itcom401-02.pdf

[28] S. S. Kolenchery, J. K. Townsend, J. A. Freebersyser, "A Novel Impulse Radio Network for Tactical Military Wireless Communications," *Proceedings of IEEE Military Communications Conference,* Vol. 1, Oct. 1998, pp. 59-65.

[29] FCC, “Revision of Part 15 of the Commission’s Rules Regarding Ultra-Wideband Transmission Systems,” First Report and Order, ET Docket 98-153, Feb. 2002.

[30] A. Batra and al., “Proposal for IEEE 802.15.3a Alternate PHY (doc.: IEEE P802.15-02/268r3-SG3a),” Submitted to IEEE P802.15 Working Group for Wireless Personal Area Networks (WPANs), July 2003. Available: http://grouper.ieee.org/groups/802/15/pub/2003/Jul03/.

[31] R. Scholtz, “Multiple Access with Time-Hopping Impulse Modulation,” *IEEE Military Communications Conference,* Vol. 2, Oct. 1993, pp. 447-450.

[32] R. Price and P.E. Green, "A Communication Technique for Multipath Channel," *Proceedings of the IEEE,* March 1958, pp. 555-570.

[33] IEEE Standard 1394a-2000, “IEEE Standard for a High Performance Serial Bus,” *Amendment 1*. Available: http://standards.ieee.org/catalog/olis/busarch.html.

[34] F. A. Tobagi and J. S. Storey, “Improvements in throughput of a CDMA packet network due to a channel load sense access protocol,” *Proceedings of Allerton Conference.*, 1984, pp. 40–49.

[35] J. M. Musser and J. N. Daigle, “Throughput analysis of an asynchronous code division multiple access (CDMA) system," *Proceedings International Conference on Communications,* Philadelphia, 1982, pp. 2F.2.1-2F.2.7.

[36] F. A. Tobagi, “Modeling and performance analysis of multihop packet radio networks,” *Proceedings of IEEE*, Vol. 75, Jan. 1987, pp. 135-154.

[37] M. Leiner, D. L. Neilson, and F. A. Tobagi, Eds., “Special Issues on Packet Radio Networks,” *Proceedings of IEEE*, Vol. 75, No. 1, Jan. 1987, pp. 6-20.

[38] A. H. Abdelmonem, T. N. Saadawi, “Performance Analysis of Spread Spectrum Packet Radio Networks with Channel Load Sensing,” *IEEE Journal on Selected Areas in Communications*, Vol. 7, No. 1, Jan. 1989, pp. 161-166.

[39] X. H. Chen, W. X. Lu, J. Oksman, ”Use of code sensing technique in the receiver-based spreading code protocol and its performance analysis,” *IEE Proceedings-I*, Vol. 139, No. 1, February 1992, pp. 85-90.

[40] H. H. Chen, W. T. Tea, "Novel group-based spreading code protocol: hierarchy schedule sensing protocol for CDMA wireless networks," *IEE Proceedings on Communications*, Vol. 146, No. 1, Feb. 1999, pp. 15-21.

[41] Joseph Y. N. Hui, "Throughput Analysis for Code Division Multiple Accessing of the Spread Spectrum Channel," *IEEE Journal on Selected Areas in Communications*, Vol. SAC-2, No. 4, July 1984, pp. 482-486.

[42] K. W. Hung, T. S. Yum, "Efficient Spreading Code Assignment Algorithm for Packet Radio Networks," *Electronics Letters*, Vol. 28. No. 23, Nov. 1992, pp. 2193-2195.

[43] Limin Hu, "Distributed Code Assignment for CDMA Packet Radio Networks," *IEEE/ACM Transactions on Networking*, Vol. 1, No. 6, Dec. 1993, pp. 668-677.

[44] A. A. Nertossi, M. A. Bonuccelli, "Code Assignment for Hidden Terminal Interference Avoidance in Multihop Packet Radio Networks," *IEEE/ACM Transactions on Networking*, Vol. 3, No. 4, August 1995, pp. 441-449.

[45] J.J. Garcia-Luna-Aceves and Jyoti Raju, "Distributed Assignment of Codes for Multi-hop Packet Radio Networks," *Proceedings of MILCOM*, Vol. 1, Nov. 1997, pp. 450-454.

[46] B. Radunović and J.-Y. Le Boudec, "Optimal Power Control, Scheduling and Routing in UWB Networks," *Technical Report ID: IC/2003/61*. Available: http://lcawww.epfl.ch/Publications/Radunovic/IC_TECH_REPORT_200361.pdf

[47] J.-Y. Le Boudec, R. Merz, B. Radunović, J. Widmer , "A MAC protocol for UWB Very Low Power Mobile Ad-hoc Networks based on Dynamic Channel Coding with Interference Mitigation," *EPFL Technical Report ID: IC/2004/02*. Available:
http://icwww.epfl.ch/publications/documents/IC_TECH_REPORT_200402.pdf

[48] I. Cidon and M. Sidi, "Distributed Assignment algorithms for Multihop Packet-Radio Networks," *IEEE/ACM Transactions on Computers*, Vol. 38, No. 10, August 1995, pp. 1353-1361.

[49] T. Makansi, “Transmitter oriented code assignment for multihop packet radio,” *IEEE Transactions on Communications*, Vol. COM-35, Dec. 1987, pp. 1379-1382.

[50] John G. Proakis, “Digital Communications,” *Fourth Edition*, Boston: McGraw Hill, 2001.

[51] P802.15.3/D17, “(C/LM) Standard for Telecommunications and Information Exchange Between Systems - LAN/MAN Specific Requirements - Part 15.3: Wireless Medium Access Control (MAC) and Physical Layer (PHY) Specifications for High Rate Wireless Personal Area Networks”, *Feb. 2003*.

[52] R. W. Chang, “Synthesis of band-limited orthogonal signals for multi-channel data transmission,” *Bell Systems Technical Journal,* Dec. 1966, pp. 1775-1796.

[53] Richard Van Nee, Ramjee Prasad, “OFDM for Wireless Multimedia Communications,” *Artech House,* January 2000.

[54] S. S. Ghassemzadeh and V. Tarokh, "The Ultra-Wideband Indoor Path Loss Model (doc.: IEEE P802.15-02/277r0-SG3a)," Submitted to IEEE 802.15 Working Group for Wireless Personal Area Networks (WPANs), June 2002. Available: http://grouper.ieee.org/groups/802/15/pub/2002/Jul02/.

[55] M. Pendergrass and W. Beeler, “Empirically Based Statistical Ultra-Wideband Channel Model (doc.: IEEE P802.15-02/240-SG3a),” Submitted to IEEE P802.15 Working Group for Wireless Personal Area Networks (WPANs), June 2002. Available: http://grouper.ieee.org/groups/802/15/pub/2002/Jul02/.

[56] J. Foerster and Q. Li, “UWB Channel Modeling Contribution from Intel (doc.: IEEE P802.15-02/279-SG3a),” Submitted to IEEE P802.15 Working Group for Wireless Personal Area Networks (WPANs), June 2002. Available: http://grouper.ieee.org/groups/802/15/pub/2002/Jul02/.

[57] Rick Roberts, “XtremeSpectrum CFP Document (doc.: IEEE P802.15-02/154r2),” Submitted to IEEE P802.15 Working Group for Wireless Personal Area Networks (WPANs), May 2003. Available: http://grouper.ieee.org/groups/802/15/pub/2003/May03/.

[58] A. H. Muqaibel, "Characterization of Ultra Wideband Communication Channels," *Ph.D. Dissertation, Dept. of Electrical and Computer Engineering*, Virginia Tech, 2003.

Appendix A

The gold codes used in the simulation are shown in the table below.

Code Number																														
1	1	0	0	1	0	1	1	0	0	1	0	1	1	0	1	0	0	0	1	1	1	1	1	1	0	1	1	0	1	1	1
2	1	1	0	1	0	1	1	0	1	0	0	1	0	1	0	1	0	1	1	0	0	1	1	1	0	1	0	1	1	1	1
3	1	0	1	1	1	1	1	1	1	1	1	0	0	1	0	1	0	1	0	0	0	0	1	1	0	1	1	0	1	0	1
4	1	1	0	1	0	1	0	0	0	0	0	0	0	0	1	1	1	1	0	0	1	1	1	0	1	1	0	1	0	1	0
5	1	0	1	0	0	1	0	0	0	0	1	0	0	1	1	1	1	1	1	1	1	0	1	0	0	0	0	0	0	1	1
6	0	1	1	0	1	1	1	0	1	0	0	0	0	1	1	1	0	1	1	1	1	1	0	1	0	0	1	1	0	1	1
7	0	1	1	1	0	0	0	0	1	1	0	1	0	1	1	1	1	0	0	0	0	0	0	1	1	0	1	1	1	0	0
8	0	1	1	0	0	1	0	1	0	1	1	1	0	1	1	0	0	0	0	1	0	0	1	0	0	1	0	1	0	1	1
9	1	0	0	1	1	0	1	1	1	0	1	1	1	0	1	1	0	1	1	0	0	0	1	1	1	1	0	1	1	0	0
10	0	1	0	0	1	0	0	1	1	1	1	0	0	1	0	0	0	0	1	1	1	1	0	1	0	1	0	0	0	1	1
11	1	1	0	0	0	0	1	0	1	1	1	1	0	1	0	1	1	1	0	0	1	1	1	1	1	0	1	0	1	0	1
12	0	1	0	0	0	1	0	0	1	1	0	1	0	0	0	0	1	0	0	0	0	1	0	1	0	1	0	1	0	1	0
13	0	1	1	0	0	1	1	0	1	1	1	1	0	1	0	0	0	1	1	0	0	1	0	0	0	1	1	0	0	0	1
14	1	0	1	1	1	0	1	0	0	1	1	1	0	1	1	1	0	0	0	0	0	1	1	0	1	0	0	0	1	0	0
15	1	0	0	1	0	0	1	1	0	0	0	1	1	1	0	1	1	0	0	1	1	1	1	0	0	0	1	0	1	0	0
16	1	1	1	1	0	0	0	0	1	0	0	0	1	0	0	0	0	0	0	0	1	0	1	0	1	1	0	0	0	0	1
17	1	0	0	0	1	0	1	0	1	0	0	1	1	1	0	0	0	1	1	0	1	0	1	0	0	1	1	0	1	0	1
18	0	0	1	0	1	1	0	1	1	1	0	0	1	0	1	0	0	1	0	1	0	0	1	1	0	0	1	1	0	0	1
19	1	1	1	1	0	1	1	0	0	0	1	0	0	1	1	1	0	0	1	0	1	1	1	1	1	1	1	0	0	0	1
20	1	0	0	1	1	1	0	1	0	0	0	1	0	1	0	0	0	1	0	0	0	1	1	0	1	1	1	1	1	0	0
21	1	0	1	0	1	1	1	0	1	0	1	0	1	0	0	0	1	0	1	1	1	0	0	0	1	0	0	0	1	0	1
22	1	1	1	0	0	1	1	0	0	0	0	1	0	1	0	0	1	1	1	1	1	0	0	1	1	1	1	0	1	1	1
23	0	0	0	0	1	1	0	0	0	1	1	0	1	1	0	0	1	1	0	0	0	1	0	0	0	0	1	1	0	0	0

24	1	0	1	0	0	0	0	0	1	0	1	0	0	0	0	1	0	1	1	0	0	0	0	0	0	1	0	1	1	0	1
25	0	0	0	0	0	1	1	1	1	1	1	1	0	1	1	1	0	1	0	1	1	0	0	1	0	0	0	0	0	0	1
26	0	1	0	0	1	0	1	0	0	0	0	0	1	1	0	0	1	0	1	1	1	0	0	1	0	0	1	0	0	0	0
27	0	0	1	1	0	0	1	0	1	0	0	0	1	1	1	0	0	1	1	1	0	0	0	0	0	0	0	0	0	0	1
28	1	0	1	1	1	0	0	1	1	0	0	1	1	1	1	1	1	0	0	0	0	0	1	0	1	1	1	0	1	1	1
29	0	1	0	1	1	0	0	0	1	1	0	0	0	0	1	1	0	0	1	1	0	1	0	0	1	1	1	1	0	1	0
30	0	0	1	1	1	0	0	0	1	0	1	1	1	1	1	0	0	0	1	0	0	1	0	0	0	1	1	1	1	0	0
31	0	1	0	1	0	1	0	1	1	1	1	1	0	1	1	1	1	0	0	0	1	1	0	0	1	1	1	0	0	1	1
32	0	0	0	1	0	1	0	1	1	1	1	0	1	1	0	1	0	0	1	1	0	0	0	0	0	1	1	1	0	0	1
33	0	1	1	0	0	0	0	0	1	0	0	0	1	1	1	0	1	0	1	0	0	1	0	1	1	1	1	0	0	1	1

Appendix B

Hidden Node simulation

For each scenario simulated, the distance between the transmitter and the interferer is calculated. Based on the distance, the received E_b/N_o at the interferer is calculated using Equation 3.1 and Equation 3.2 for path loss exponent of 1 and 2 respectively outlined in Chapter 3. If the received E_b/N_o is more than a certain value (8 dB in our simulations, for both path loss exponent of 1 and 2), it is assumed that the interferer can listen to the transmission and hence would back-off. If the E_b/N_o is lower than the threshold, the interfering node is assumed to be hidden and would interfere with the communication between the intended transmitter and receiver. Another method to simulate hidden nodes would be to run the receiver at the interferer for each frame transmission between the transmitter and receiver but this would take a huge amount of time to simulate for all the interferers in the system. Hence the former methodology was chosen in the simulation. The threshold E_b/N_o was determined by simulating various points in the geographical area and finding the optimum distance (*i.e.*, E_b/N_o) for which the system would behave like a real world system.

Vita

Nishant Kumar was born on April 5, 1980 in New Delhi, INDIA. He received his B. E. (Bachelor of Engineering) degree in Electronics and Communications from Maharashtra Institute of Technology, Pune, INDIA in 2001. He came to Virginia Tech. in Fall of 2001 to pursue a higher education in the field of wireless communications. Since summer of 2002 Nishant has been working as a research associate in the Mobile and Portable Radio Research Group (MPRG) where he concentrated his research on the area of Ultra-Wideband Communications. He has also been working in Staccato Communications since May 2003 where he continues his work on UWB based technology. He will receive his M. S. degree in May, 2004. After graduation, Nishant will be continuing his work at Staccato Communications.